

13284

NATIONAL LIBRARY
OTTAWA



BIBLIOTHÈQUE NATIONALE
OTTAWA

NAME OF AUTHOR... MOHAMMAD IQBAL ANWAR
 TITLE OF THESIS... EFFECTS OF NON-UNIFORM MAGNETIC
 AND ELECTRIC FIELDS IN
 MAGNETO-HYDRODYNAMIC SLIDER BEARINGS
 UNIVERSITY... OF ALBERTA
 DEGREE FOR WHICH THESIS WAS PRESENTED... PH.D.
 YEAR THIS DEGREE GRANTED... 1972

Permission is hereby granted to THE NATIONAL LIBRARY
 OF CANADA to microfilm this thesis and to lend or sell copies
 of the film.

The author reserves other publication rights, and
 neither the thesis nor extensive extracts from it may be
 printed or otherwise reproduced without the author's
 written permission.

(Signed).... M. S. Cunniff..

PERMANENT ADDRESS:

...# 402, 10711 SASK/DR.
 ...Edmonton... Alberta.

DATED... 19th July... 1972

THE UNIVERSITY OF ALBERTA

EFFECTS OF NONUNIFORM MAGNETIC AND ELECTRIC FIELDS
IN MAGNETOHYDRODYNAMIC SLIDER BEARINGS

BY

© MOHAMMAD IQBAL ANWAR

A THESIS

SUBMITTED TO THE FACULTY OF GRADUATE STUDIES AND RESEARCH
IN PARTIAL FULLFILMENT OF THE REQUIREMENTS FOR THE DEGREE
OF DOCTOR OF PHILOSOPHY

DEPARTMENT OF MECHANICAL ENGINEERING
EDMONTON, ALBERTA

FALL, 1972

UNIVERSITY OF ALBERTA
FACULTY OF GRADUATE STUDIES AND RESEARCH

The undersigned certify that they have read, and recommend to the Faculty of Graduate Studies and Research for acceptance, a thesis entitled "EFFECTS OF NONUNIFORM MAGNETIC AND ELECTRIC FIELDS IN MAGNETOHYDRODYNAMIC SLIDER BEARINGS" submitted by MOHAMMAD IQBAL ANWAR in partial fulfillment of the requirements for the degree of Doctor of Philosophy.

Ch. Kollmeier
.....
Supervisor

M. J. ...
.....

David Marsden
.....

Dej. Selim ...
.....

S. H. ...
.....

T. G. ...
.....

Wm. E. Wolfe
.....
External Examiner

Date *18th July 1972*

ABSTRACT

An analytical study is made of the magnetohydrodynamic effects in a liquid-metal-lubricated slider bearing where a magnetic field is applied perpendicularly to the bearing surfaces. The analyses are carried out for an open circuit condition, and for the case when the electrical power from an external source was supplied to the bearing.

For an open circuit condition, the effects of inertia and the nonuniformly applied magnetic fields are investigated. The results indicate that the effects of inertia on load capacity decreases with the increase of Hartmann number, M , and become almost negligible at high M . The highest bearing load capacity is obtained at a given Hartmann number when the film thickness ratio is optimized. The non-uniform magnetic fields i.e., increasing magnetic field, give higher load capacity than the comparable uniform magnetic field. The influence of surface conductivity on load capacity will depend upon the distribution of the magnetic field. For uniform and increasing magnetic fields the bearing surfaces should be insulated, while for a step-type distribution the stator should be a conductor.

For the case of externally supplied electric power, a parallel plate slider bearing with uniformly applied magnetic field was analyzed. The nonuniform electric field in the bearing was created by connecting the segmented side electrodes to the power supply. The results suggest

that it would be advantageous if the electrical power is applied near the inlet portion of the bearing.

ACKNOWLEDGEMENTS

The author wishes to thank Dr. C.M. Rodkiewicz for supervising this thesis and for constant encouragement during the duration of graduate studies at the University of Alberta.

Thanks are also due to Dr. R.R. Gilpin, Dr. H.G. Schmidt-Weinmar, and Dr. M. Charles for their helpful suggestions toward the completion of this work.

The author acknowledges the National Research Council of Canada for financial support during summers of 1969-1972 through Grant NRC A-4198, and for computational charges under Grant C-0083.

The author also wishes to thank Miss Helen Wozniuk for typing this thesis.

TABLE OF CONTENTS

	<u>Page</u>
Abstract	iii
Acknowledgements	v
Table of Contents	vi
List of Figures	ix
List of Symbols	xi
CHAPTER I STATEMENT OF THE PROBLEM AND REVIEW OF RELEVANT LITERATURE	
1.1 Introduction	1
1.2 Review of the Associated Literature	4
1.3 Statement of the Problem	6
CHAPTER II THE DEVELOPMENT OF GOVERNING EQUATIONS FOR MHD LUBRICATION	
2.1 The Basic Equations	9
2.2 Simplifying Assumptions	9
2.3 The Governing Equations	11
CHAPTER III NONUNIFORM MAGNETIC FIELD EFFECTS IN MHD SLIDER BEARINGS	
3.1 Introduction	14
3.2 The Governing Equations and the Associated Boundary Conditions	14
3.3 Equations in Dimensionless Form	15
3.4 Method of Solution	21

TABLE OF CONTENTS (continued)

	<u>Page</u>
CHAPTER III continued	
3.5 Discussions and Conclusions	21
CHAPTER IV EFFECTS OF MAGNETIC FIELDS IN SLIDER BEARINGS OF ARBITRARY PROFILE	
4.1 Introduction	28
4.2 The Governing Equations and the Associated Boundary Conditions	28
4.3 Equations in Dimensionless Form	29
4.4 Method of Solution	33
4.5 Results and Conclusions	39
CHAPTER V NONUNIFORM ELECTRIC FIELD EFFECTS IN MHD SLIDER BEARINGS	
5.1 Introduction	49
5.2 The Bearing Configuration	50
5.3 The Governing Equations and the Associated Boundary Conditions	50
5.4 Solution to the Governing Equations	60
5.4.1 General Approach	60
5.4.2 Finite Difference Approximation ...	60
5.4.3 Method of Solution	62
5.5 Results and Conclusions	66
CHAPTER VI CONCLUSIONS AND SUGGESTIONS FOR FUTURE INVESTIGATIONS	
6.1 General Results and Conclusions	76
6.2 Suggestions for Future Investigation	77

TABLE OF CONTENTS (continued)

	<u>Page</u>
BIBLIOGRAPHY	79
APPENDIX A MAGNETIC FIELD DISTRIBUTION	82
APPENDIX B ELECTRIC POTENTIAL EQUATION IN FINITE-DIFFERENCE FORM	84
APPENDIX C PRESSURE EQUATION IN FINITE-DIFFERENCE FORM ...	86
APPENDIX D FINITE-DIFFERENCE FORMULAS TO OBTAIN ELECTRIC FIELD AND CURRENT DENSITY DISTRIBUTION IN THE BEARING	88
APPENDIX E CONVERGENCE PARAMETER, MESH SIZE AND ERROR INVOLVED IN COMPUTATIONS	91
APPENDIX F NUMERICAL EXAMPLE FOR EXTERNALLY SUPPLIED ELECTRIC POWER	93
APPENDIX G COMPUTER PROGRAM	95

LIST OF FIGURES

<u>Figure</u>		<u>Page</u>
2.1	MHD Slider Bearing	12
3.1	Magnetic Field Distribution	24
3.2	Change of Pressure Distribution with Magnetic Field	25
3.3	Inertia Effects on Load Capacity	26
3.4	Load Capacity for Uniform, Linearly Increasing, and Field Proportional to $(1 - \bar{x}/2)^{-1}$ Applied Magnetic Fields	27
4.1	The Transformed Domain	40
4.2	Applied Magnetic Field Distribution	41
4.3	Maximum Load Capacity for Uniformly Applied Magnetic Field	42
4.4	Flow Rate for Uniformly Applied Magnetic Field ...	43
4.5	Frictional Force and Friction Factor for Uniformly Applied Magnetic Field	44
4.6	Maximum Load Capacity for Linearly Increasing Applied Magnetic Field	45
4.7	Frictional Force and Friction Factor for Linearly Increasing Magnetic Field	46
4.8	Maximum Load Capacity for Step-Type Applied Magnetic Field	47

LIST OF FIGURES (continued)

<u>Figure</u>		<u>Page</u>
4.9	Frictional Force and Friction Factor for Step-Type Applied Magnetic Field	48
5.1	MHD Finite Width Parallel Plate Slider Bearing ...	51
5.2	Finite-Difference Network for Potential Equation .	61
5.3	Finite-Difference Network for Pressure Equation ..	63
5.4	Potential Lines for the Applied Potential to Side Electrodes	71
5.5	Current Streamlines for the Applied Potential to Side Electrodes	72
5.6	Pressure Distribution in the Parallel Plate Slider Bearing	73
5.7	Load Capacity for the Parallel Plate Slider Bearing	74
5.8	Frictional Force for the Parallel Plate Slider Bearing	75

LIST OF SYMBOLS

a's	coefficients in equation (5.33)
A	cross-sectional area of bearing (in xy plane)
b	coefficients in equation (5.34)
\vec{B}	magnetic induction field
B_y	applied magnetic field
\bar{B}_y	$B_y/B_{y,inlet}$, defined in equation (3.6)
\bar{B}_y	$B_y/B_{y,reference}$, defined in equation (4.5)
C_f	friction factor, \bar{F}/\bar{W}
C_n	constants in equations (3.14), (5.12), and (5.13)
D	width of the bearing (z-direction)
D_n	constants in equation (3.13)
\vec{E}	electric field
E_x	electric field in x-direction
\bar{E}_x	dimensionless electric field, $(E_x h/U) \sqrt{\sigma/\mu}$
E_z	electric field in z-direction
\bar{E}_z	dimensionless electric field, $(E_z h_i/U) \sqrt{\sigma/\mu}$
\bar{E}_z	dimensionless electric field, $(E_z h_0/U) \sqrt{\sigma/\mu}$
\bar{E}_z	dimensionless electric field, $(E_z h/U) \sqrt{\sigma/\mu}$
f	functional relation to the stream function by $\bar{\psi} = K \sum_{n=0}^{\infty} f_n(\eta) \delta^n$

F	frictional force defined by equation (4.17), and (5.30)
\bar{F}	dimensionless frictional force, $Fh_0/\mu UL$
\bar{F}	dimensionless frictional force, $Fh/\mu UDL$
h	film thickness
h_i	h at inlet
h_0	h at outlet
\bar{h}	h/h_0
h_r	film thickness ratio, h_i/h_0
h'	dh/dx
h	step size in numerical method ($\sim \Delta h$)
\vec{H}	magnetic field
I	total current
\bar{I}	dimensional current, $I/LU \sqrt{\mu\sigma}$
\vec{J}	current density
J_x	current density in x-direction
\bar{J}_x	dimensionless current density, $(J_x h/U) 1/\sqrt{\mu\sigma}$
J_z	current density in z-direction
\bar{J}_z	dimensionless current density, $(J_z h/U) 1/\sqrt{\mu\sigma}$
k	may take values 0,1,2 ... in equation (3.20)
K	constant, h_i/Lh'
L	length of the bearing
L_1	magnetic field step location in Fig. 4.2
L_1	length of the side electrode in Fig. 5.1
m	may take values 0,1,2 ... in equation (3.20)
M	an integer in numerical method

M	Hartmann number, $(h_i \sqrt{\sigma/\mu}) B_{y,inlet}$, defined in equation (3.6)
M	Hartmann number, $(h_0 \sqrt{\sigma/\mu}) B_{y,reference}$, defined in equation (4.5)
M_R	M_{outlet}/M
n	may take values 0,1,2 ...
N	an integer in numerical method
p	gauge pressure
\bar{p}	dimensionless pressure, $ph_i^2/L\mu U$, and $ph_0^2/L\mu U$
\bar{p}	dimensionless pressure, $ph^2/L\mu U$
p	may take values 0,1,2 ... in equation (3.20)
Q	flow rate per unit width $\int_0^h u dy$
\bar{Q}	Q/Uh_i
\bar{Q}	Q/Uh_0
Q_x	flow rate defined by equation (5.16)
\bar{Q}_x	Q_x/Uh
Q_z	flow rate defined in equation (5.18)
\bar{Q}_z	Q_z/Uh
Re^*	modified Reynolds number, $(UL/\nu)(h_i/L)^2$
Rm	magnetic Reynolds number, $UL \sigma\mu_0$
S	L/L_1
S'	$dB_y/d\bar{x}$
u	velocity in x-direction
\bar{u}	u/U
U	velocity of the slider
v	velocity in y-direction

\bar{v}	dimensionless velocity, vL/Uh_i
\bar{v}	dimensionless velocity, vL/Uh_0
\vec{V}	velocity of fluid
w	velocity in z-direction
\bar{W}	dimensionless load capacity, $Wh_i^2/L^2\mu U$
\bar{W}_0	dimensionless load capacity when $M = 0$
\bar{W}	dimensionless load capacity, $Wh_0^2/L^2\mu U$
\bar{W}	dimensionless load capacity $Wh^2/\mu UDL^2$
x	coordinate along the slider
\bar{x}	x/L
y	coordinate normal to the slider
\bar{y}	y/h_i
\bar{y}	y/h
z	coordinate normal to xy plane
z_0	width of the bearing
\bar{z}	z/z_0
\bar{z}	z/D
α	defined by equation (4.21)
β	defined by equation (4.22)
δ	h/h_i
η	$h_i\bar{y}/h$
μ	fluid dynamic viscosity
μ_0	permeability
ρ	fluid density

ν	fluid kinematic viscosity
σ	fluid electrical conductivity
ϕ	electrical potential defined as $\vec{E} = \nabla\phi$
$\bar{\phi}$	dimensionless electrical potential, $(\phi h/UD) \sqrt{\sigma/\mu}$
$\bar{\phi}_a$	dimensionless applied electrical potential to the side electrode
Φ_t	terminal potential
$\bar{\psi}$	dimensionless stream function defined by equation (3.11)
$\underline{\psi}$	dimensionless stream function defined by equation (4.9)
ω	relaxation factor defined in equation (5.35)

Subscript

i, j space subscripts of grid point in x and z direction

Superscript

' differentiation with respect to independent variable

CHAPTER I
STATEMENT OF THE PROBLEM AND
REVIEW OF RELEVANT LITERATURE

1.1 Introduction

In view of the increasing use of liquid metals in engineering and industry, considerable attention is being paid to various magneto-hydrodynamic machines and devices, including MHD bearings. The design of bearings employing ordinary lubricants for units where the interior cavities are filled with liquid metal presents considerable difficulty. The major difficulties are due to the limitations of ordinary lubricants and the need for complicated seals. In such cases, the use of the working fluid itself as the lubricant, will introduce a significant simplification. From hydrodynamic and thermodynamic viewpoints, liquid metals offer several advantages over conventional lubricants. An important advantage is the possibility of operation at high temperatures. In addition, the high thermal conductivity of liquid metals enables the heat generated by viscous action to be readily conducted away from the source of generation. The resulting effect is a tendency toward uniformity of temperature and viscosity within the lubricant film. The properties of liquid metals which can effect the performance of bearings adversely are low viscosity and corrosivity.

In evaluating the possible merits of various types of bearings

for liquid-metal applications, it is necessary to consider the characteristics of each type of bearing in relation to the fluid properties. It is shown by Bisson and Anderson [1] that one important requirement of rolling-element bearings is an absolute compatibility of the race and the rolling-element materials with the lubricant. This requirement for absolute material compatibility with the lubricating fluid, makes it impractical to use the highly corrosive liquid metals as lubricants in rolling-element bearings.

However, the hydrodynamic and hydrostatic type of bearings can tolerate some corrosion and surface damage while still maintaining their function. Thus, the requirements for material compatibility are not as rigorous as those for rolling-element bearings. In hydrodynamic and hydrostatic bearings, a continuous film maintains separation of the surfaces in relative motion, and the pressure required to support the load is either supplied from an external source (hydrostatic bearing) or is generated within the bearing itself (hydrodynamic). The hydrostatic bearing is most suitable for supporting loads with no rotation or with low angular speeds. It has the advantage that for a fixed pressure, the load capacity is independent of the lubricant viscosity. Therefore, the performance of liquid-metal lubricated hydrostatic bearings is neither seriously affected by the high corrosivity nor the low viscosity of liquid metals.

On the other hand, viscosity is the most important property of a lubricant in hydrodynamic bearings. The load capacity of an hydrodynamic bearing is dependent on the viscosity of the lubricant,

i.e., the higher the viscosity of the lubricant, the larger the load capacity. The viscosities of the proposed liquid metals are approximately one to two orders of magnitude less than those of ordinary lubricating oils at the same temperature. Therefore, the reductions in load capacity of the same order can be expected when these metals are used as lubricants. To overcome the problem of reduced load capacity the application of magnetic fields has been proposed. This has motivated the study of magnetohydrodynamics in lubrication.

Magnetohydrodynamics is the study of the motion of an electrically conducting fluid in the presence of a magnetic field. Electric currents induced in the fluid as a result of its motion modify the field. At the same time, the flow in the magnetic field produces mechanical forces which modify the motion. The current engineering interest in electromagnetic fluid interaction phenomena has been mainly due to the concept of MHD power generation. Other engineering devices such as the MHD pump and meter, MHD coupler and bearing, etc., have been the outcome of the application of the theory.

In general, the bearing configurations possible in hydrodynamic lubrication may also be considered for the MHD bearings. However, the combination of electromagnetic and hydrodynamic effects will further increase the number of possible arrangements available for study. Therefore, in the present study the analysis will be confined to a plane slider bearing.

1.2 Review of the Associated Literature

The magnetohydrodynamic effects were first demonstrated by Hartmann and Lazarus [2] in their experiments in 1937. They showed that for a typical set of data using mercury flowing in a channel, the electromagnetic pressure gradient may be as high as ten times the hydrodynamic pressure gradient at the same flow rate. Later, Synder [3] in his theoretical analysis showed that the effects noted by Hartmann may be utilized to increase the load carrying capacity of a bearing operating with an electrically conducting lubricant. This created the interest of other authors to study the magnetic effects in the field of lubrication. Hence, the analyses were extended toward optimizing the design variables which will result in the maximum load capacity.

Osterle and Young [4] considered a step-type slider bearing with a uniformly applied magnetic field. They concluded that for maximum load capacity of the bearing, the film thickness should be a step-function, while the bearing surfaces should be insulators.

Hughes [5] analyzed an inclined slider bearing under general electrical loading conditions. The magnetic field was applied normal to the bearing surfaces which were assumed to be perfect insulators. He found that significant increase in load capacity can be achieved even at low Hartmann numbers if the power is supplied to the bearing system from an external source. Hughes [6] also extended his analysis to finite width step-type slider bearing.

Kuzma [7] considered a parallel plate slider bearing with

stator as a perfect conductor and slider as an insulator. He showed that this bearing, with nonuniform applied magnetic field, has a greater load capacity than a step-type bearing subject to uniform magnetic field. Shukla [8] pointed out that the advantages noted by Kuzma are more dependent on the nonuniform conductivity of bearing surfaces than on the nonuniformly applied magnetic field. He showed that the uniform magnetic field is more advantageous provided that the conductivity of a bearing surface is a step-type function. His results for such a case indicate that for a maximum load capacity the bearing film thickness should be a step-function for Hartmann number, $M \leq 5.5$, and parallel for $M > 5.5$.

Prakash [9] carried out the analysis of a composite slider bearing in the presence of an applied magnetic field. He concluded that an MHD composite bearing does not always give an increase in load capacity as compared to an equivalent inclined slider bearing.

The review of literature further reveals that there has been very few experimental attempts to verify the theoretical results of MHD bearings. This may be attributed to the complications involved in designing the apparatus and in the difficulty of measuring the dependent variables.

Maki, Kuzma and Donnelly [10] carried out the investigation for a step-type hydrodynamic thrust bearing theoretically and experimentally. The magnetic field was applied normal to the bearing surfaces and at the same time the side electrodes were connected to an external power supply such that there was a radial flow of the current. Using

mercury, the pressure and voltage distributions, and the torque at the slider were measured. The authors obtained good agreement between the theory and the experimental results. It should be pointed out, however, that the data were obtained for low speed and very low Hartmann numbers. Nevertheless, the experiment revealed that the increase in pressure due to magnetic and electric effects is possible.

Other cited experiments have been performed for a MHD hydrostatic bearing [11], and a journal bearing [12].

1.3 Statement of The Problem

The review of literature indicates that the MHD bearing analyses have been primarily confined to bearings where the applied magnetic field has been assumed uniform in part or full length of the bearing. Secondly, where the external power was also applied to the bearing to further improve the load capacity, it was assumed that the electric field was uniform throughout the length of the bearing.

For the above cases where the magnetic and electric fields were assumed uniform, the problem was simplified from the mathematical viewpoint. Therefore, in most of the cases an analytical solution was possible.

From hydrodynamic theory of lubrication it may be recalled that the pressure rise in the bearing is due to the change in the film thickness. This change, in practice, is brought about by the geometry of the bearing. Therefore a number of bearing configurations are possible. Typical examples of bearings in use are plane tapered, step-type, journal, and composite bearings. However, when a magnetic field

is applied to such a bearing, and if the lubricant is an electrically conducting fluid, then there results an electromagnetic body force, in addition to the hydrodynamic forces in the fluid film. The combination of these effects i.e., hydrodynamic and magnetic, changes the flow in the bearing, thereby causing modifications in the pressure distribution. Such effects may be utilized to increase the load capacity of the bearing.

In general, the magnitude and the distribution of the body force produced in a particular type of bearing depends upon:

- (i) the applied magnetic field,
- (ii) the bearing surface properties,
- (iii) the external circuit conditions.

The effects of bearing shapes and the properties of bearing surfaces have been investigated to some extent, but the effects of the applied magnetic, and applied electric fields have been confined only to uniformly applied fields. Therefore, it is considered important to investigate the effects of nonuniformly applied magnetic and electric fields.

From the literature it is noted that the inertia terms in the equations of motion have been neglected. However, in the case of a bearing operating at high speeds and utilizing a lower viscosity lubricant such as liquid metals, the contribution of inertia terms may become significant.

In summary the present study concerns:

- (i) Nonuniform magnetic field effects in MHD slider bearings.

- (ii) Inertia effects on load capacity of MHD bearings.
- (iii) Nonuniform electric field effects in MHD slider bearings.

The outline of the present study stated above shall be presented in the following format.

The governing equations for the study of MHD lubrication are developed in Chapter II. These equations are then simplified for the particular case under consideration in the subsequent chapters.

In Chapter III, the effects of nonuniformly applied magnetic fields and inertia effects are described. The analysis of nonuniformly applied magnetic fields for an arbitrary bearing profile are presented in Chapter IV. Chapter V is devoted to studying the effects of step-type applied electric field. The conclusions and suggestions for future investigations are discussed in Chapter VI.

CHAPTER II
THE DEVELOPMENT OF GOVERNING
EQUATIONS FOR MHD LUBRICATION

2.1 The Basic Equations

The theory of magnetohydrodynamic lubrication is the same as conventional hydrodynamic lubrication, except that the interaction between the conducting fluid and the electromagnetic fields must be included. As a result the number of equations to be dealt with increases. This interaction phenomena couples the electromagnetic and fluid variables, thus creating additional difficulties for the solution of the problem.

The basic equations for the study of magnetohydrodynamics are fluid equations, Maxwell's equations, Ohm's law, and constitutive equations.

2.2 Simplifying Assumptions

Prior to the formulation of the problem in MHD lubrication, several assumptions are made in order to simplify the basic equations. The assumptions to simplify the fluid mechanic equations are:

- (1) The fluid is Newtonian.
- (2) The flow is laminar.
- (3) The lubricant is incompressible.

- (4) The lubricant viscosity is constant.
- (5) Elastic distortions are negligible.
- (6) Temperature variations in the fluid film are neglected.
- (7) Steady state has been reached.

In addition to the fluid mechanic assumptions other assumptions of electromagnetic nature are made. These assumptions include:

- (8) The conductivity of the liquid metal is constant.
- (9) There is no charge accumulation.
- (10) The liquid metal is homogeneous and non-magnetic.
- (11) Displacement currents are negligible with respect to conduction currents.
- (12) All velocities are very small compared to the velocity of light.
- (13) Magnetostatic forces are negligible. This is justified since liquid metals are non-magnetic.

Considering the assumptions above the equations of magneto-hydrodynamic may be written in a general form such as:

Navier-Stokes Equations

$$\rho[(\vec{V} \cdot \nabla)\vec{V}] = -\nabla p + \mu\nabla^2\vec{V} + \vec{J} \times \vec{B} \quad (2.1)$$

Continuity Equation

$$\nabla \cdot \vec{V} = 0 \quad (2.2)$$

Maxwell's field equation

$$\begin{aligned} \nabla \cdot \vec{B} = 0, \quad \nabla \times \vec{E} = 0 \\ \nabla \times \vec{H} = \vec{J}, \quad \nabla \cdot \vec{J} = 0 \end{aligned} \quad (2.3)$$

Ohm's Law

$$\vec{J} = \sigma(\vec{E} + \vec{V} \times \vec{B}) \quad (2.4)$$

and constitutive equation

$$\vec{B} = \mu_0 \vec{H} \quad (2.5)$$

The above set of equations, in general, describe the action of magnetohydrodynamic effects in liquid-metal lubricated hydrodynamic bearings. To analyze a given lubrication problem, equations (2.1) through (2.4) must be solved simultaneously subject to a given set of fluid mechanic and electromagnetic boundary conditions. In this general form, however, these equations are not tractable and additional simplification must be made for any particular bearing configuration.

2.3 The Governing Equations

The bearing considered in present work is shown in Fig. 2.1. The coordinate system is fixed with respect to the stationary surface of the bearing. The magnetic field is applied perpendicularly to the bearing surfaces, and it is assumed to have an arbitrary distribution along the length of bearing. The slider is assumed to be made of insulating material while the stator may be of insulating or perfectly conducting material.

For the bearing under consideration it is now possible to make further simplifying assumptions. These are as follows:

- (1) Lubricating film is very thin, $\frac{h}{L} \leq 1$.

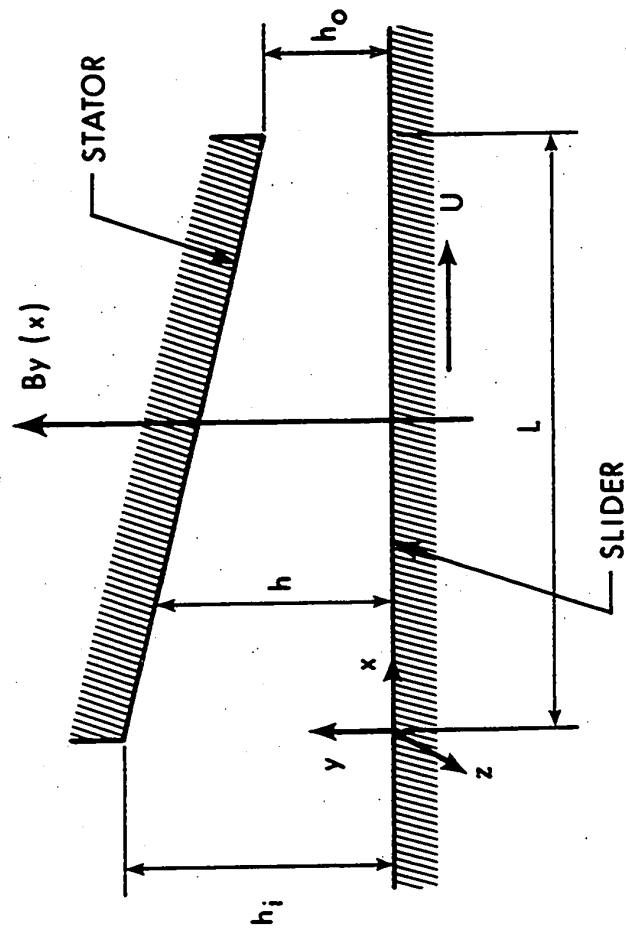


FIG. 2.1 MHD SLIDER BEARING

(2) Order of magnitude consideration may be used to simplify the equations.

(3) The magnetic field induced by currents is assumed to be negligible with respect to the applied magnetic field. ($R_m \ll 1$).

Under these assumptions equations (2.1) through (2.5) reduce to:

$$\rho(u \frac{\partial u}{\partial x} + v \frac{\partial u}{\partial y} + w \frac{\partial u}{\partial z}) = - \frac{\partial p}{\partial x} + \mu \frac{\partial^2 u}{\partial y^2} - J_z B_y \quad (2.6)$$

$$0 = \frac{\partial p}{\partial y} \quad (2.7)$$

$$\rho(u \frac{\partial w}{\partial x} + v \frac{\partial w}{\partial y} + w \frac{\partial w}{\partial z}) = - \frac{\partial p}{\partial z} + \mu \frac{\partial^2 w}{\partial y^2} + J_x B_y \quad (2.8)$$

$$\frac{\partial u}{\partial x} + \frac{\partial v}{\partial y} + \frac{\partial w}{\partial z} = 0 \quad (2.9)$$

$$J_x = \sigma(E_x - w B_y) \quad (2.10)$$

$$J_z = \sigma(E_z + u B_y) \quad (2.11)$$

The above magnetohydrodynamic equations have been simplified to a great extent, however, the equations are difficult to solve. In the following Chapters III through V, these equations will be further simplified by making additional assumptions for the particular model under consideration. The boundary conditions shall be specified and the solution will be presented.

CHAPTER III
NONUNIFORM MAGNETIC FIELD EFFECTS
IN MHD SLIDER BEARINGS*

3.1 Introduction

In this chapter, the effects of the nonuniformly applied magnetic fields are investigated. In addition, the inertia effects are also analyzed. In the analysis the bearing is assumed to be infinitely long in z-direction.

3.2 The Governing Equations and the Associated Boundary Conditions

For infinite bearing model, the equations (2.6) through (2.11) are further simplified under the following assumptions:

- (1) No fluid flow in z-direction.
- (2) The bearing and the slider surfaces are made of perfectly insulating material.
- (3) The side electrodes to be perfect conductors.

Hence the governing equations may be reduced to the following form:

$$\rho(u \frac{\partial u}{\partial x} + v \frac{\partial u}{\partial y}) = - \frac{dp}{dx} + \mu \frac{\partial^2 u}{\partial y^2} - \sigma(E_z + uB_y)B_y \quad (3.1)$$

* A portion of this chapter was presented in the ASLE/ASME Lubrication Conference, Pittsburgh, Pennsylvania, October 5-7, 1971. Later published in Journal of Lubrication Technology, Trans. ASME, Series F, Vol. 94, No. 1, Jan. 1972.

$$\frac{\partial u}{\partial x} + \frac{\partial v}{\partial y} = 0 \quad (3.2)$$

$$J_z = \sigma(E_z + u B_y) \quad (3.3)$$

with the following boundary conditions

$$u(x,0) = U$$

$$u(x,h) = v(x,0) = v(x,h) = 0 \quad (3.4)$$

$$p(0) = p(L) = 0$$

As the electrodes are assumed to be very good conductors compared to the fluid, we have from, $\nabla \times \vec{E} = 0$, that E_z is a constant (as the variation in z direction has been neglected) which will be determined later.

Now since $\nabla \times \vec{E} = 0$, a terminal potential can be defined as:

$$\phi_t = - \int_0^{z_0} E_z dz \quad (3.5)$$

3.3 Equations in Dimensionless Form

The governing equations may be written in dimensionless form by introducing the following dimensionless quantities.

$$\begin{aligned}\bar{x} &= \frac{x}{L}, \quad \bar{u} = \frac{u}{U}, \quad \bar{E}_z = \left(E_z \frac{h_i}{U}\right) \sqrt{\frac{\sigma}{\mu}} \\ \bar{y} &= \frac{y}{h_i}, \quad \bar{v} = \frac{vL}{Uh_i}, \quad \bar{B}_y = \frac{B_y}{B_{y,\text{inlet}}} \\ \bar{z} &= \frac{z}{z_0}, \quad \bar{p} = \frac{\rho h_i^2}{L\mu U}, \quad \bar{Q} = \frac{Q}{Uh_i}\end{aligned}\quad (3.6)$$

$$Re = \frac{UL}{\nu} \left(\frac{h_i}{L}\right)^2$$

$$M = \left(h_i \sqrt{\frac{\sigma}{\mu}}\right) B_{y,\text{inlet}}$$

Equation (3.1) and (3.2) then become

$$Re \left(\bar{u} \frac{\partial \bar{u}}{\partial \bar{x}} + \bar{v} \frac{\partial \bar{u}}{\partial \bar{y}} \right) = - \frac{d\bar{p}}{d\bar{x}} + \frac{\partial^2 \bar{u}}{\partial \bar{y}^2} - M^2 \bar{u} \bar{B}_y^2 - M \bar{B}_y \bar{E}_z \quad (3.7)$$

$$\frac{\partial \bar{u}}{\partial \bar{x}} + \frac{\partial \bar{v}}{\partial \bar{y}} = 0 \quad (3.8)$$

The boundary conditions:

$$\bar{u}(\bar{x}, 0) = 1$$

$$\bar{u}(\bar{x}, \bar{y}_h) = \bar{v}(\bar{x}, \bar{y}_h) = \bar{v}(\bar{x}, 0) = 0 \quad (3.9)$$

$$\bar{p}(0) = \bar{p}(1) = 0$$

Defining the stream function such that

$$\bar{u} = \frac{\partial \bar{\psi}}{\partial y}, \quad \bar{v} = -\frac{\partial \bar{\psi}}{\partial x}$$

Equation (3.7) becomes

$$\text{Re}^* \left(\frac{\partial \bar{\psi}}{\partial y} \frac{\partial^2 \bar{\psi}}{\partial x \partial y} - \frac{\partial \bar{\psi}}{\partial x} \frac{\partial^2 \bar{\psi}}{\partial y^2} \right) = -\frac{d\bar{p}}{dx} + \frac{\partial^3 \bar{\psi}}{\partial y^3} - M^2 \bar{B}_y^2 \frac{\partial \bar{\psi}}{\partial y} - M \bar{B}_y \bar{E}_z \quad (3.10)$$

The stream function may be expanded, after Synder [13]

$$\bar{\psi} = K \sum_{n=0}^{\infty} f_n(\eta) \delta^n \quad (3.11)$$

where $\eta = h_i \bar{y}/h$, $\delta = h/h_i$. Substituting (3.11) into (3.10) with $K = h_i/Lh'$ and $h' = dh/dx = \text{constant}$, the equation (3.10) may be written

$$\begin{aligned} & \text{Re}^* \left[\left(\sum_{n=0}^{\infty} f_n' \delta^n \right) \left(\sum_{n=0}^{\infty} (n-1) f_n' \delta^n \right) - \left(\sum_{n=0}^{\infty} n f_n \delta^n \right) \left(\sum_{n=0}^{\infty} f_n'' \delta^n \right) \right] \\ & = \sum_{n=0}^{\infty} f_n''' \delta^n - \left(\frac{h}{h_i} \right)^2 M^2 \bar{B}_y^2 \sum_{n=0}^{\infty} f_n' \delta^n \\ & \quad - \left(\frac{h}{h_i} \right)^3 \frac{1}{K} \left[\frac{d\bar{p}}{dx} + M \bar{B}_y \bar{E}_z \right] \end{aligned} \quad (3.12)$$

Inspection of last term in Eq. (3.12) and in view of [14] it seems appropriate to express it as

$$\left(\frac{h}{h_i}\right)^3 \frac{1}{K} \left[\frac{d\bar{p}}{dx} + M \bar{B}_y \bar{E}_z \right] = \sum_{n=0}^{\infty} D_n \delta^n \quad (3.13)$$

The magnetic field may be assumed to have the following form:

$$\left(\frac{h}{h_i}\right) [\bar{B}_y] = \sum_{n=0}^{\infty} C_n \delta^n \quad (3.14)$$

Substituting (3.13) and (3.14) into (3.12) we obtain

$$\begin{aligned} & \text{Re}^* \left[\left(\sum_{n=0}^{\infty} f_n' \delta^n \right) \left(\sum_{n=0}^{\infty} (n-1) f_n' \delta^n \right) - \left(\sum_{n=0}^{\infty} n f_n \delta^n \right) \left(\sum_{n=0}^{\infty} f_n'' \delta^n \right) \right] \\ & = \sum_{n=0}^{\infty} f_n''' \delta^n - M^2 \left(\sum_{n=0}^{\infty} C_n \delta^n \right)^2 \left(\sum_{n=0}^{\infty} f_n' \delta^n \right) \\ & \quad - \sum_{n=0}^{\infty} D_n \delta^n \end{aligned} \quad (3.15)$$

On expansion of (3.15) the following set of differential equations are obtained

$$\delta^0: f_0''' + \text{Re}^* f_0' f_0' - M^2 (C_0^2 f_0') = D_0 \quad (3.16)$$

$$\delta^1: f_1''' + \text{Re}^* (f_0'' f_1 + f_0' f_1') - M^2 (C_0^2 f_1' + 2C_0 C_1 f_0') = D_1 \quad (3.17)$$

$$\begin{aligned} \delta^2: f_2''' + \text{Re}^* (2f_0'' f_2 + f_1 f_1'') - M^2 (C_0^2 f_2' + 2C_0 C_1 f_1' \\ + C_1^2 f_0' + 2C_0 C_2 f_0') = D_2 \end{aligned} \quad (3.18)$$

$$\delta^3: f_3'''' + \operatorname{Re}^*(3f_0''f_3 + 2f_1''f_2 + f_2''f_1 - f_0'f_3' - f_1'f_2') \\ - M^2(C_0^2 f_3' + 2C_0 C_1 f_2' + C_1^2 f_1' + 2C_0 C_2 f_1' + 2C_1 C_2 f_0' + 2C_0 C_3 f_0') = D_3 \quad (3.19)$$

.....

$$\delta^n: f_n'''' + \operatorname{Re}^* \sum_{m=n}^0 \{m f_{n-m}'' f_m' - (n-m-1) f_m' f_{n-m}'\} \\ - M^2 \sum_{k=0}^n \left(\sum_{p=0}^k C_p C_{k-p} \right) f_{n-k}' = D_n \quad (3.20)$$

From the boundary conditions (3.9) and the equation (3.11) the following set of conditions for function f are obtained.

$$f_0(0) = f_0'(0) = f_0'(1) = 0, \quad f_0(1) = \frac{\bar{\psi}}{K} \quad (3.21)$$

$$f_1(0) = f_1(1) = f_1'(1) = 0, \quad f_1'(0) = \frac{1}{K} \quad (3.22)$$

and

$$f_n(0) = f_n(1) = f_n'(0) = f_n'(1) = 0 \quad (3.23)$$

where $n = 2, 3, \dots$

External Circuit Conditions:

The unknown \bar{E}_z in equation (3.13) may be obtained by considering the external circuit conditions of the bearing. If the bearing surfaces are insulators the total current flowing out of the bearing may be expressed as

$$I = \int_A J_z \, dx dy = \sigma \int_A E_z \, dx dy + \sigma \int_0^L \int_0^h u B_y \, dy dx \quad (3.24)$$

In terms of nondimensional parameters it gives

$$\bar{I} = \frac{I}{LU\sqrt{\mu\sigma}} = \bar{E}_z \int_A d\bar{x}d\bar{y} + M\bar{Q} \int_0^1 \left(\frac{C_0}{\delta} + C_1 + C_2\delta^1 + \dots \right) d\bar{x} \quad (3.25)$$

For the open circuit case $\bar{I} = 0$ and equation (3.25) reduces to

$$-\bar{E}_z \int_A d\bar{x}d\bar{y} = M\bar{Q} \int_0^1 \left(\frac{C_0}{\delta} + C_1 + C_2\delta^1 + \dots \right) d\bar{x} \quad (3.26)$$

Load Capacity:

The bearing load capacity is found by integrating the pressure distribution. In terms of dimensionless variables the load capacity per unit width of the bearing is

$$\bar{W} = \frac{Wh_i^2}{L^2\mu U} = \int_0^1 \bar{p} \, d\bar{x} \quad (3.27)$$

3.4 Method of Solution

The equations (3.16) through (3.20) are ordinary differential equations of third order and linear except equation (3.16). These equations and the boundary conditions (3.21) through (3.23) are similar to the set of equations solved by Rodkiewicz and Anwar [14], except there are additional terms due to the magnetic effects. However, the same numerical methods can be successfully adopted.

In order to obtain the solution to the problem, the distribution of the applied magnetic field has to be assumed. In the present analysis, we shall consider three cases, Fig. 3.1, namely:

- (A) uniform field,
- (B) linearly increasing field, and
- (C) field proportional to $(1 - \frac{\bar{x}}{2})^{-1}$.

Knowing the distribution of the magnetic field we can find the C's from equation (3.14), (see Appendix A) which are then substituted in equations (3.16) through (3.20) and (3.26). The solution of these equations give the constants D's. The pressure distribution is then obtained from expression (3.13). The load capacity of the bearing is given by equation (3.27).

3.5 Discussion and Conclusions

The pressure distribution curves for uniform and linearly increasing field are shown in Fig. 3.2. The M=0 curve, the case of no magnetic field, is also shown for comparison. It is noted that the position of maximum pressure changes slightly due to the presence of

magnetic field. It is evident from the figure that there is an increase in pressure distribution when the constant magnetic field is applied. Further increase is obtained when the applied field is made nonuniform. Consequently, the integration of the various pressure distribution curves results in the functional dependence of the load capacity on the magnetic field distribution and the Hartmann number. These results are presented in Figs. 3.3 and 3.4.

Figure 3.3 presents the relationship between the load capacity and the Hartmann number for neglected and included inertia terms. It is noted that the increase in load capacity due to the inertia effects decreases with the increase of Hartmann number. The no inertia terms results compare favourably with the low Hartmann number solution of Prakash [9], which extends only up to $M = 1.2$. The solution of the present work covers the range $0 \leq M \leq 5$.

In Fig. 3.4 the functional dependence of the ratio of MHD load capacity to the ordinary hydrodynamic load capacity is given. It is evident that the load capacity ratio for the nonuniform field is higher than for the uniform field for a given inlet Hartmann number. This increase depends upon the distribution function and the outlet Hartmann number.

To show that the nonuniform field is more advantageous than the uniform field, we consider the case of uniformly increasing field of Hartmann number M . For such an applied field the average Hartmann number ratio $M_{\bar{x}}/M$, which will be different than one, may be estimated. It is found that the load capacity ratio for this averaged Hartmann

number, applied throughout the bearing, is smaller than the load capacity ratio for the original linearly increasing field.

For case C the distribution function is given by $C_0 \left(1 - \frac{x}{2}\right)^{-1}$. In the present analysis, C_0 was made equal to 1 giving $M_{\text{outlet}} = 2M$. The corresponding load capacity curve is also shown in Fig. 3.4.

From the load capacity curves it is noted that the curves for case B were terminated at lower Hartmann numbers than for the other cases. This was due to the convergence difficulties.

The convergence of the power series (3.11), without the magnetic effects, was discussed by Rodkiewicz and Anwar [14]. It is noted that when the magnetic effects are included the convergence depends upon Hartmann number and distribution of the magnetic field.

For case A and C, it was found that for Hartmann number up to 5, the series can be approximated by the first eight terms of (3.11). The contribution of the 9th and the higher terms were found negligible.

It was noted that the convergence for case B, depended upon the gradient of the applied field and the Hartmann number. With the increase of these quantities it was found that more terms had to be taken into consideration in order to obtain the required convergence. For example, for $M_R = 2$ and $M = 1.5$, it was necessary to include up to fifteen terms to obtain reasonably accurate solution.

Since the inertia effects on load capacity are noted to be small it is proposed that the inertia terms may be neglected. In Chapter IV the analysis will be considered without the inertia terms.

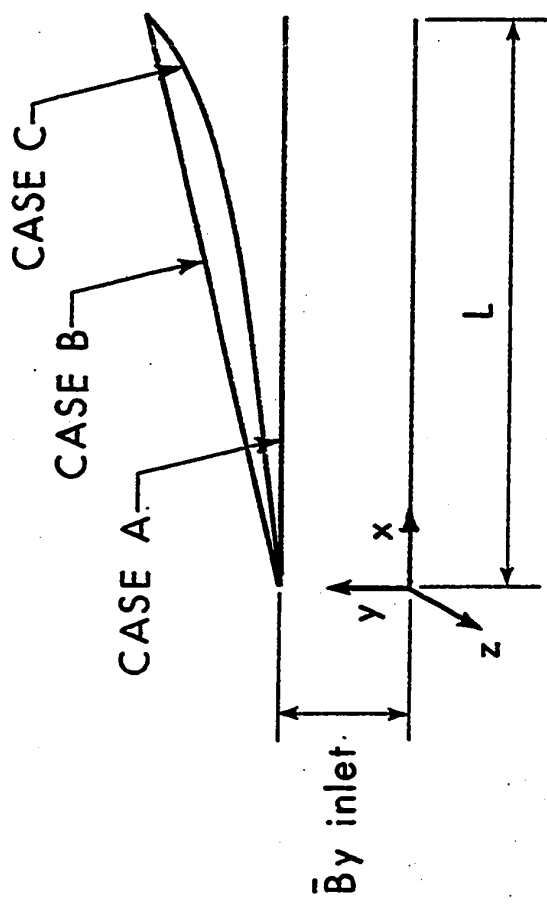


FIG. 3.1 MAGNETIC FIELD DISTRIBUTION

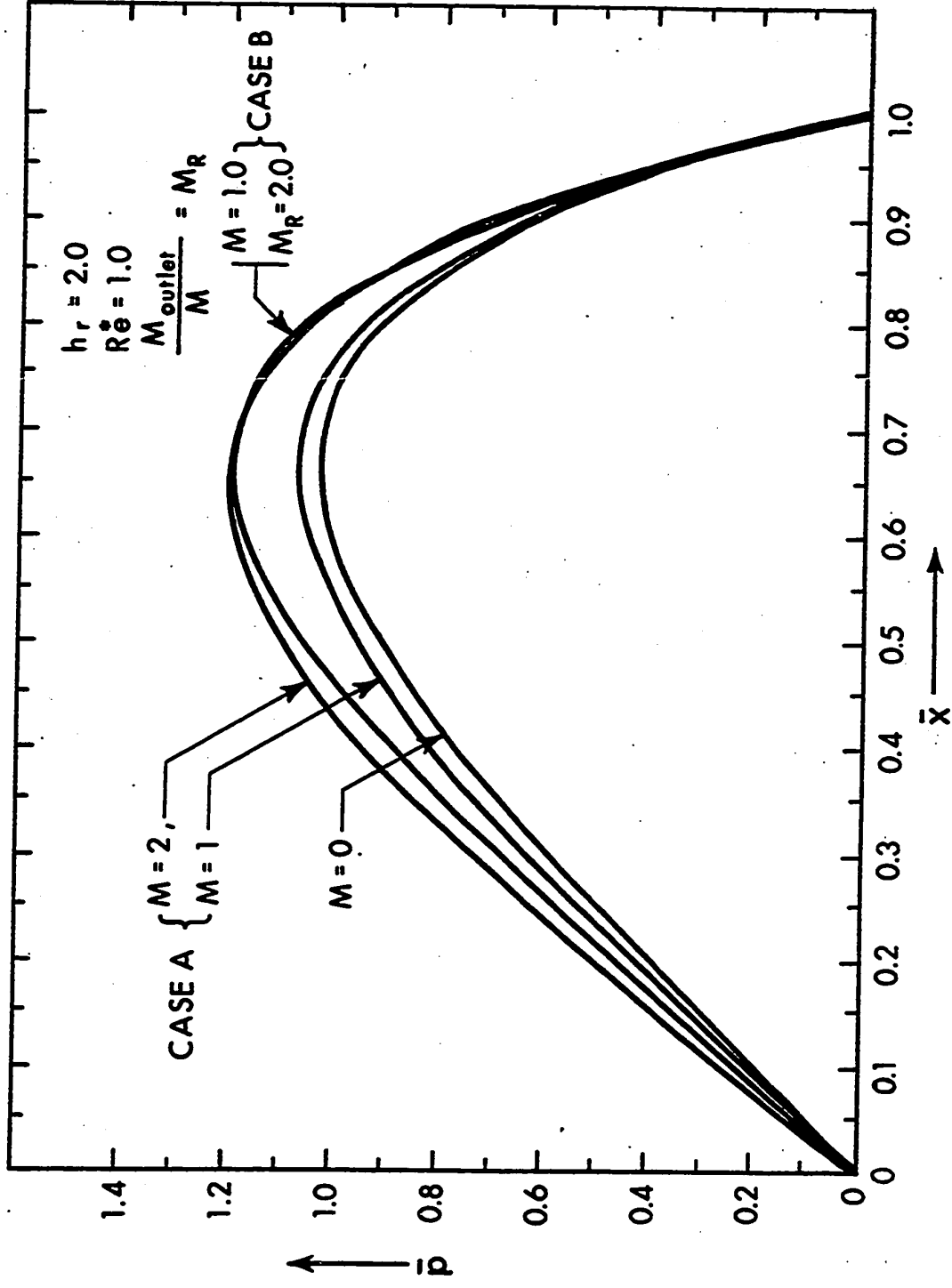


FIG. 3.2 CHANGE OF PRESSURE DISTRIBUTION WITH MAGNETIC FIELD (Open Circuit Condition)

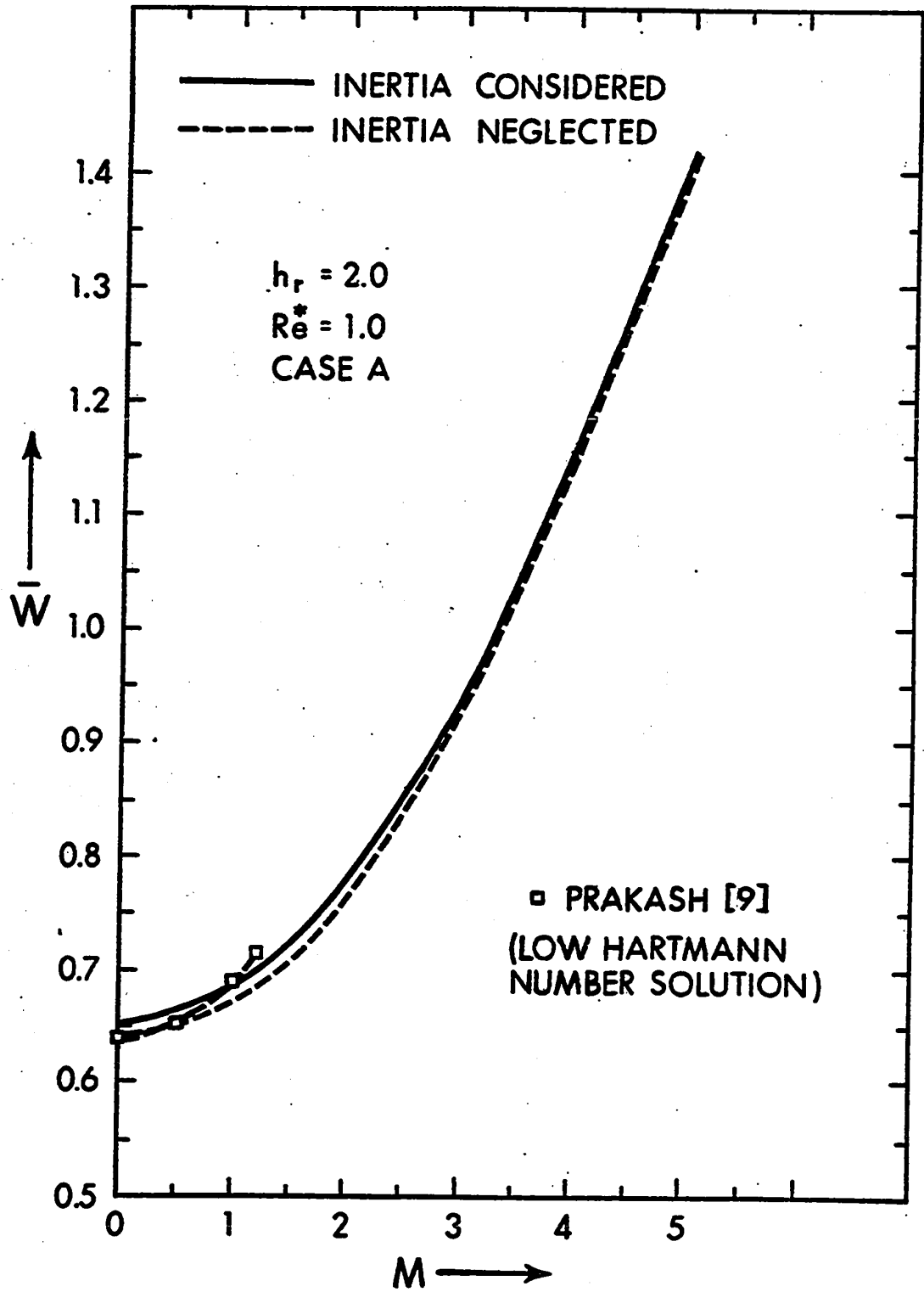


FIG. 3.3 INERTIA EFFECTS ON LOAD CAPACITY
(Open Circuit Condition)

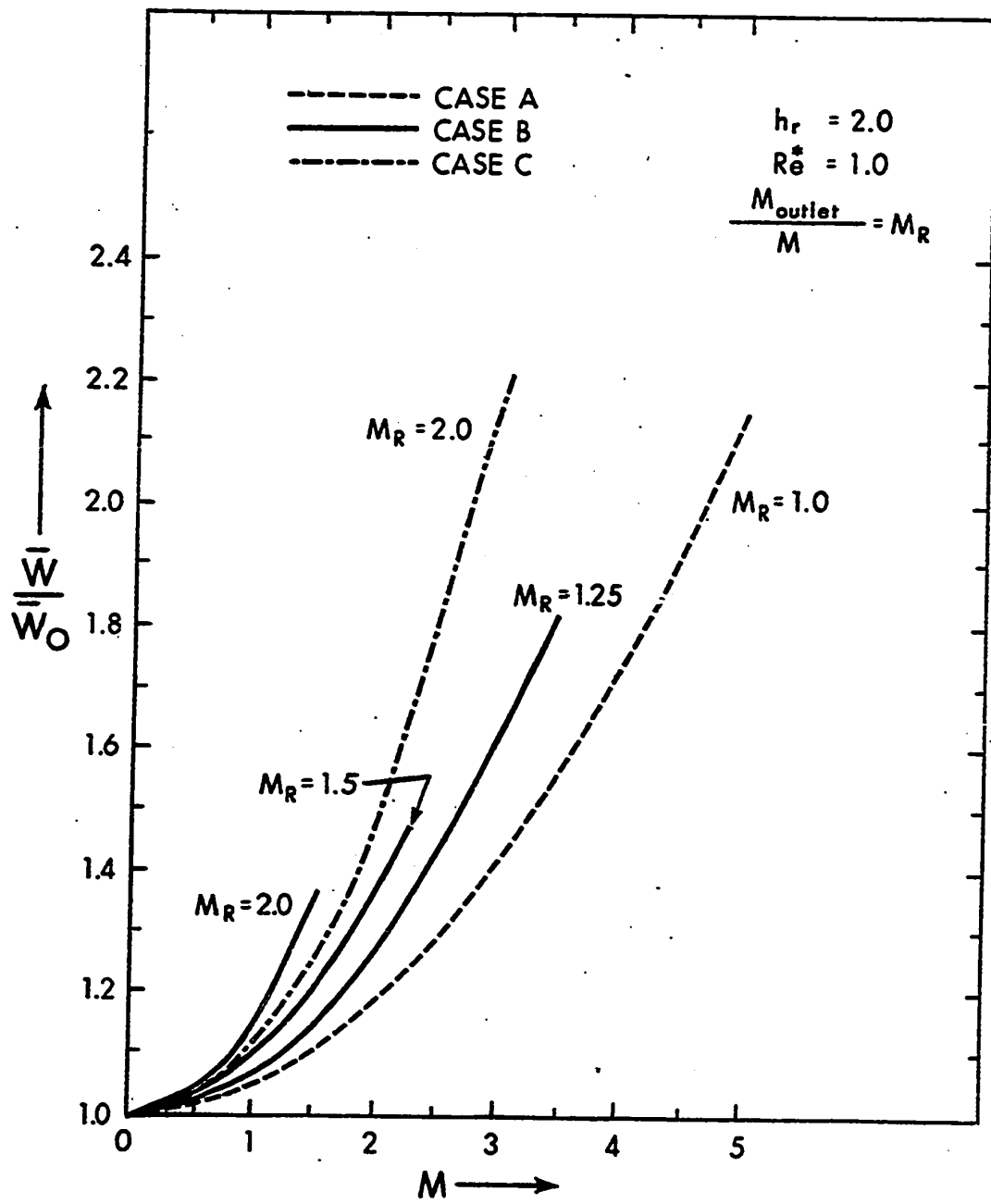


FIG. 3.4 LOAD CAPACITY FOR CASE A, B AND C
(Open Circuit Condition)

CHAPTER IV
EFFECTS OF MAGNETIC FIELDS IN SLIDER
BEARINGS OF ARBITRARY PROFILE*

4.1 Introduction

In the previous chapter, the solution of an MHD bearing with nonuniformly applied magnetic fields was presented. In the analysis the inertia terms were retained and the resulting nonlinear partial differential equation was solved by a power series method. The solution was limited to low Hartmann numbers due to the slow convergence of the proposed power series for the stream function. In the present chapter the inertia terms are neglected and the solution for the resulting equations are presented.

4.2 The Governing Equations and the Associated Boundary Conditions

Since the inertia terms are neglected the governing equations (3.1) through (3.3) yield

$$0 = -\frac{dp}{dx} + \mu\left(\frac{\partial^2 u}{\partial y^2}\right) - \sigma(E_z + u B_y) B_y \quad (4.1)$$

* A portion of this Chapter has been accepted for publication and will appear in the Journal of Lubrication Technology, ASME. July, 1972. And another portion has been accepted for publication in Wear, an International Journal on the Science and Technology of Friction, Lubrication and Wear. (Forthcoming)

$$\frac{\partial u}{\partial x} + \frac{\partial v}{\partial y} = 0 \quad (4.2)$$

$$J_z = \sigma(E_z + u B_y) \quad (4.3)$$

with the following associated boundary conditions:

$$u(x,0) = U$$

$$u(x,h) = v(x,0) = v(x,h) = 0 \quad (4.4)$$

$$p(0) = p(L) = 0$$

4.3 Equations in Dimensionless Form

The above equations may be nondimensionalized by letting:

$$\begin{aligned} \bar{x} &= \frac{x}{L}, \quad \bar{u} = \frac{u}{U}, \quad \bar{E}_z = \left(\frac{E_z h_0}{U} \right) \sqrt{\frac{\sigma}{\mu}} \\ \bar{y} &= \frac{y}{h}, \quad \bar{v} = \frac{vL}{Uh_0}, \quad \bar{B}_y = \frac{B_y}{B_{y,\text{reference}}} \\ \bar{h} &= \frac{h}{h_0}, \quad \bar{p} = \frac{\rho h_0^2}{L\mu U}, \quad \bar{Q} = \frac{Q}{Uh_0} \end{aligned} \quad (4.5)$$

$$M = \left(h_0 \sqrt{\frac{\sigma}{\mu}} \right) B_{y,\text{reference}}, \quad S = \frac{L_1}{L}$$

The nondimensionalization will transfer the original fluid field into the square field as shown in Fig. 4.1. Equation (4.1) and (4.2) become:

$$\frac{\partial^2 \bar{u}}{\partial \bar{y}^2} - \bar{h}^2 M^2 \bar{B}_y^2 \bar{u} - \bar{h}^2 M \bar{B}_y \bar{E}_z - \bar{h}^2 \frac{d\bar{p}}{d\bar{x}} = 0 \quad (4.6)$$

$$\frac{\partial \bar{u}}{\partial \bar{x}} + \frac{1}{\bar{h}} \frac{\partial \bar{v}}{\partial \bar{y}} = 0 \quad (4.7)$$

The boundary conditions:

$$\bar{u}(\bar{x}, 0) = 1$$

$$\bar{u}(\bar{x}, 1) = \bar{v}(\bar{x}, 0) = \bar{v}(\bar{x}, 1) = 0 \quad (4.8)$$

$$\bar{p}(0) = \bar{p}(1) = 0$$

Defining the stream function such that

$$\bar{u} = \frac{\partial \bar{\psi}}{\partial \bar{y}}, \quad \bar{v} = -\bar{h} \frac{\partial \bar{\psi}}{\partial \bar{x}} \quad (4.9)$$

Equation (4.6) becomes

$$\frac{\partial^3 \bar{\psi}}{\partial \bar{y}^3} - \bar{h}^2 M^2 \bar{B}_y^2 \frac{\partial \bar{\psi}}{\partial \bar{y}} - \bar{h}^2 M \bar{B}_y \bar{E}_z - \bar{h}^2 \frac{d\bar{p}}{d\bar{x}} = 0 \quad (4.10)$$

With the following boundary conditions on $\bar{\psi}$:

$$\bar{y} = 0, \quad \bar{\psi} = 0, \quad \frac{\partial \bar{\psi}}{\partial \bar{y}} = 1 \quad (4.11)$$

$$\bar{y} = 1, \quad \bar{\psi} = \frac{\bar{Q}}{h}, \quad \frac{\partial \bar{\psi}}{\partial \bar{y}} = 0$$

External circuit conditions:

To determine the unknown \bar{E}_z in equation (4.10) it will be necessary to consider the external circuit of the bearing system. It is noted that when one of the bearing surfaces is a conductor it is a short circuited case which gives

$$\bar{E}_z = 0 \quad (4.12)$$

when the bearing surfaces are insulated and the end plates are perfect conductors we have from equation (4.3)

$$I = \int_A \sigma(E_z + u B_y) dx dy \quad (4.13)$$

or in terms of dimensionless parameters

$$\bar{I} = \frac{I}{LU \sqrt{\mu\sigma}} = \bar{E}_z \int_0^1 \int_0^1 \bar{h}(\bar{x}) d\bar{x} d\bar{y} + M\bar{Q} \int_0^1 \bar{B}_y d\bar{x} \quad (4.14)$$

For the open circuit case $\bar{I} = 0$ and equation (4.14) reduces to

$$-\bar{E}_z \int_0^1 \int_0^1 \bar{h}(x) \, d\bar{x} \, d\bar{y} = M\bar{Q} \int_0^1 \bar{B}_y \, d\bar{x} \quad (4.15)$$

Load Capacity:

The load capacity may be found by integrating the pressure over the length of the slider. In terms of dimensionless variables, the load capacity per unit width of the bearing is

$$\bar{W} = \frac{Wh_0^2}{L^2\mu U} = \int_0^1 \bar{p} \, d\bar{x} \quad (4.16)$$

Frictional force:

The frictional force at the slider is given by

$$F = - \int_0^L \mu \left(\frac{\partial u}{\partial y} \right)_{y=0} \, dx \quad (4.17)$$

In terms of dimensionless variables the frictional force per unit width of bearing is

$$\bar{F} = \frac{Fh_0}{\mu UL} = - \int_0^1 \frac{1}{\bar{h}} \left(\frac{\partial \bar{u}}{\partial \bar{y}} \right)_{\bar{y}=0} \, d\bar{x} \quad (4.18)$$

The friction factor C_f is given by

$$C_f = \frac{\bar{F}}{\bar{W}} \quad (4.19)$$

4.4 Method of Solution

The equation (4.10) is a linear differential equation of third order in which the coefficients are function of x . The equation is difficult to integrate directly in its present form. However, the solution to the problem can be obtained by considering the differential equation (4.10) at each section along the length of the bearing. At any particular section the general solution may be written as

$$\bar{\psi} = C_1 + C_2 e^{\sqrt{\alpha} \bar{y}} + C_3 e^{-\sqrt{\alpha} \bar{y}} - \frac{\beta}{\alpha} \bar{y} \quad (4.20)$$

where

$$\alpha(\bar{x}) = \bar{h}^2 M^2 \bar{B}_y^2 \quad (4.21)$$

and

$$\beta(\bar{x}) = \bar{h}^2 M \bar{B}_y \bar{E}_z + \bar{h}^2 \frac{d\bar{p}}{d\bar{x}} \quad (4.22)$$

using the boundary conditions (4.11) in (4.20) and eliminating the integration constants we obtain

$$\beta(\bar{x}) = \frac{-\bar{Q} \alpha^{3/2} (1 - e^{2\sqrt{\alpha}}) - \bar{h} \alpha (1 + e^{2\sqrt{\alpha}} - 2e^{\sqrt{\alpha}})}{\bar{h} (2 + 2e^{2\sqrt{\alpha}} - 4e^{\sqrt{\alpha}} - \sqrt{\alpha} e^{2\sqrt{\alpha}} + \sqrt{\alpha})} \quad (4.23)$$

The foregoing values of $\beta(\bar{x})$ may be calculated if we know $\bar{h}(\bar{x})$ and \bar{Q} . The values of $\bar{h}(x)$ are prescribed by the bearing profile while the value of \bar{Q} is assumed in order to start the computations. Rearranging equation (4.22) we have

$$\frac{d\bar{p}}{dx} = \frac{\beta(\bar{x})}{h^2} - M \bar{B}_y \bar{E}_z \quad (4.24)$$

This equation (4.24) may be integrated numerically as the right-hand side is known at each point of the grid shown in Fig. 4.1. The numerically obtained value of pressure at the outlet is compared with the boundary condition (4.8) and if these two values agree within the specified limit then we have obtained the solution to the problem. In case of disagreement, a new assumption of \bar{Q} is made and the above procedure is repeated.

Once the pressure distribution in the bearing is obtained, the bearing load capacity and frictional force are obtained by numerical integration of equations (4.16) and (4.18) respectively.

4.5 Results and Conclusions

The foregoing analysis and the method of solution may be applied to obtain the load capacity of a slider bearing of an arbitrary geometry where the distribution of transversely applied magnetic field may take any form of distribution along the length of bearing. However, in this presentation a plane tapered type slider bearing is considered in the presence of an applied magnetic field which may have the following distribution (See Fig. 4.2):

- (A) uniform
- (B) linearly increasing
- (C) step-type.

The results of these three cases are summarized below.

(A) Uniformly Applied Magnetic Field

As pointed out in [3,4], for uniformly applied magnetic fields, the greatest increase in load capacity occurs if the bearing surfaces are perfect electrical insulators. Thus, the same properties are assumed here. For any Hartmann number the load capacity may be obtained by fixing the ratio of film thickness at inlet to outlet h_r . However, it is noted that for a given Hartmann number there is an optimum value of h_r for which the load capacity obtained is the greatest. Hence, the calculations were carried out using various values of h_r , for any Hartmann number, until the optimum h_r was found. The values of the load capacity and the optimum h_r are plotted against M in Fig. 4.3. The corresponding plot of the flow rate through the bearing \bar{Q} vs M is shown in Fig. 4.4. It can be seen that the optimum h_r increases with the increase of M at low Hartmann numbers and reaches its maximum at $M = 3$. Any further increase in M results in the decrease of optimum h_r . The optimized load capacity increases with the increase of M .

In order to show the influence of optimum h_r and conductivity of the bearing surfaces the results of Shukla [8] are also shown in Figs. 4.3 and 4.4. It is noted that the load capacity obtained in the present analysis is slightly less than obtained by Shukla at low M , but are higher for large Hartmann numbers. Therefore Shukla's arrangement may be considered slightly advantageous. At higher Hartmann numbers, however, the present configuration with insulated surfaces gives better results when the film thickness is optimized. Thus the stator surface need not possess variable conductivity (which might be difficult to achieve from the practical point of view) in order to

obtain the greatest increase in load capacity. Figure 4.4 shows that for $M > 2$, \bar{Q} decreases with the increase of M in both analyses. However, there is a considerable difference between the two values at any Hartmann number although the minimum film thickness is the same. This difference may be explained by observing that both bearings form two different systems for the induced currents. As a result the effects of body force on flow are different for each of the cases. For Shukla's arrangement the effects of this force is to retard the flow near the outlet of the bearing. In the present system an accelerating force is generated near the inlet and retarding force near the outlet. This arrangement reduces \bar{Q} , but the overall effects are not as dominant as in Shukla's analysis.

In Fig. 4.5 the relation of the frictional force and the friction factor, to the Hartmann numbers is indicated for the same optimum conditions as Fig. 4.4. It can be seen that the frictional force increases with the increase of M while the friction factor decreases.

(B) Linearly Increasing Applied Magnetic Field

Increasing applied magnetic field, along the length of the bearing, may take any form i.e., linearly increasing, parabolic distribution etc. In the present analysis the calculations are presented for the linearly increasing field in order to show the application of the present method to nonuniform magnetic fields. The slider bearing considered is assumed to have insulated surfaces. The distribution of the linearly applied magnetic field is assumed such that the intensity of the magnetic field at outlet is twice that at the inlet of the

bearing. This gives the ratio of $M_{\text{outlet}}/M_{\text{inlet}} = M_R = 2$. In obtaining the solution for any Hartmann number the ratio h_r is optimized, as described in Case A, in order to obtain the greatest load capacity. A plot of the optimized h_r and the load capacity versus M is presented in Fig. 4.6. It is observed that h_r decreases with the increase of $M(M>1)$ while the load capacity increases. The load capacity obtained for the uniformly applied field, Case A, is also shown in the same figure. From Chapter III and the present results, it is noted that nonuniform applied magnetic fields give higher load capacity than comparable uniform magnetic fields.

A plot of frictional force and friction factor against M is shown in Fig. 4.7. It can be seen that the trends of these curves are similar to these noted for Case A.

The difficulty in obtaining the solution for high Hartmann numbers which was reported in Chapter III has been eliminated with the present method by ignoring the inertia terms.

(C) Step-type Applied Magnetic Field

For a step-type case the magnetic field of uniform strength is applied in the downstream part of the bearing. The stator of the bearing is assumed of conducting material while the bearing is an insulator. It is noted [7] that a bearing of such an arrangement generates load carrying capacity even when the two surfaces are parallel. The load capacity depends upon the Hartmann number, applied magnetic field step location S , and the ratio of the film thickness at inlet to outlet, h_r . However, it is noted that for a given Hartmann number

there is an optimum value of h_r and S for which the load capacity is the highest. Hence the calculations were carried out using various values of h_r and S , for any Hartmann number, until the optimum h_r and S were found. The optimized h_r and the corresponding load capacity are plotted against M in Fig. 4.8. It can be seen that the optimum h_r decreases with the increase of M . It becomes equal to one when $M = 4$. This is the case of the parallel slider bearing. When $M > 4$ the bearing film becomes divergent. The optimum step location is fairly constant ($S = .65$) when $M < 3$. Further increase in M decreases the step location until $M = 5$, and thereafter it becomes practically constant again ($S = 0.55$). The results of Kuzma [7] are also shown in the same figure. It can be seen that when the ratio h_r is optimized the maximum load capacity is higher than for the parallel slider bearing. This difference becomes quite significant at large M . It is interesting to note that when $M = 4$ and $S = 0.6$, the parallel slider bearing gives the highest load capacity.

Figure 4.9 shows a plot of the frictional force and the friction factor, for maximum load conditions, as function of M . It can be seen that the frictional force increases with the increase of Hartmann number while the friction factor decreases. For comparison the plot indicates the results of Kuzma [7]. It is noted that the values of frictional force obtained, for $M > 5$, are higher than those of a parallel slider bearing. However, the friction factor values are reasonably in agreement.

Conclusions:

A simple method of calculating the load capacity for an MHD slider bearing has been described in this chapter. The transversely applied magnetic field may have any form of distribution along the length of the bearing. The method may be conveniently applied to slider bearings of a general profile where the bearing surfaces may be insulators, conductors, or possess variable conductivity in x-direction. From the results the following conclusions are drawn:

(1) For uniformly applied magnetic fields the load capacity obtained is the highest if the ratio of film thickness at the inlet to that at the outlet is optimized and the bearing surfaces are insulated.

(2) For step-type applied magnetic fields one obtains an increase in load capacity if the stator is a conductor. However, to obtain the maximum increase the ratio of film thickness at the inlet to that at the outlet has to be optimized.

(3) For linearly increasing applied magnetic fields the highest load capacity is obtained if the ratio of film thickness at the inlet to that at the outlet is optimized and the bearing surfaces are insulated. The results indicate that the nonuniform magnetic fields give higher load capacity than the comparable uniform magnetic fields.

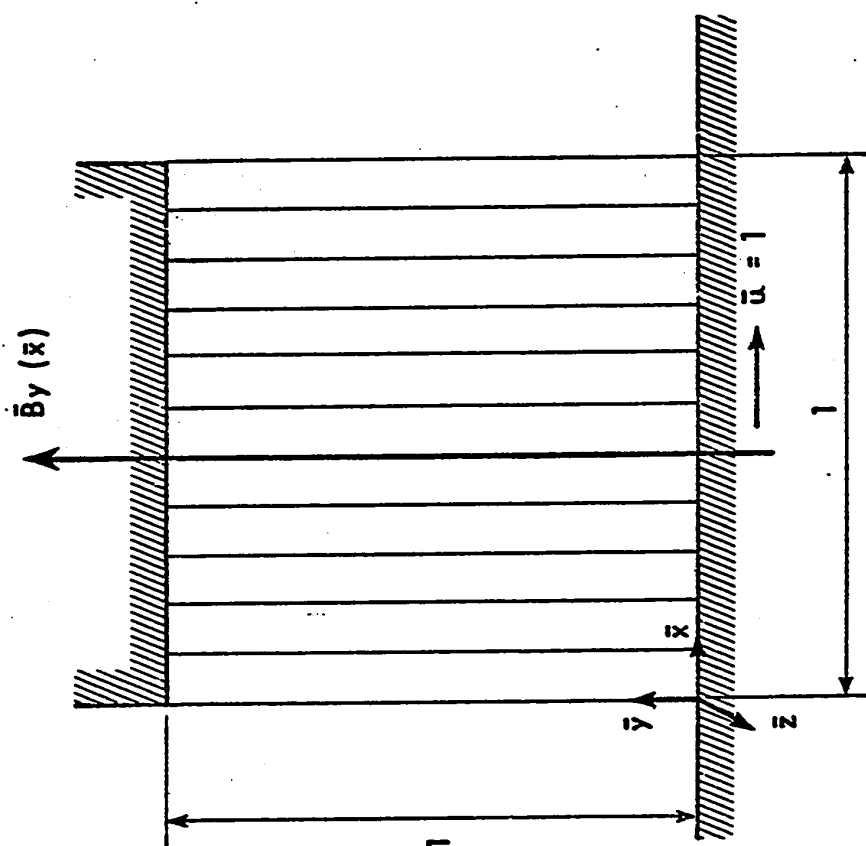


FIG.4.1 THE TRANSFORMED DOMAIN

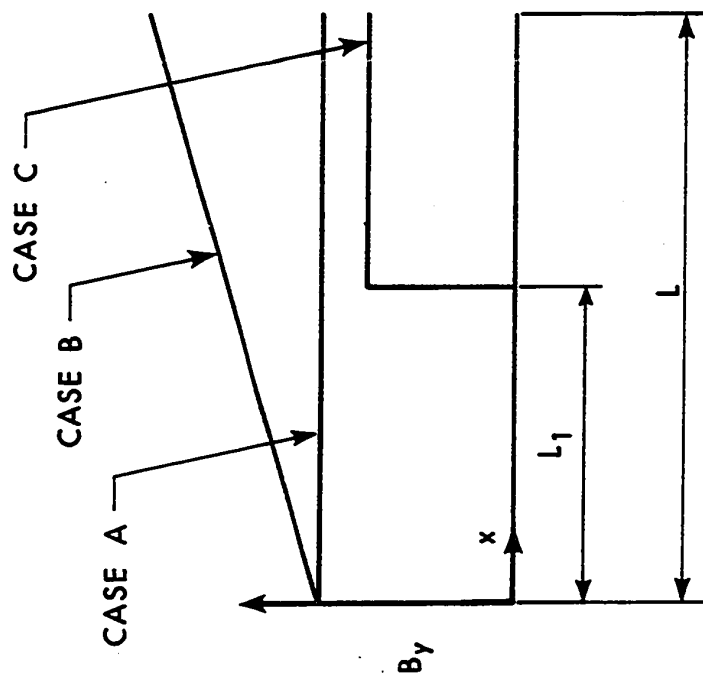


FIG. 4.2 APPLIED MAGNETIC FIELD DISTRIBUTION

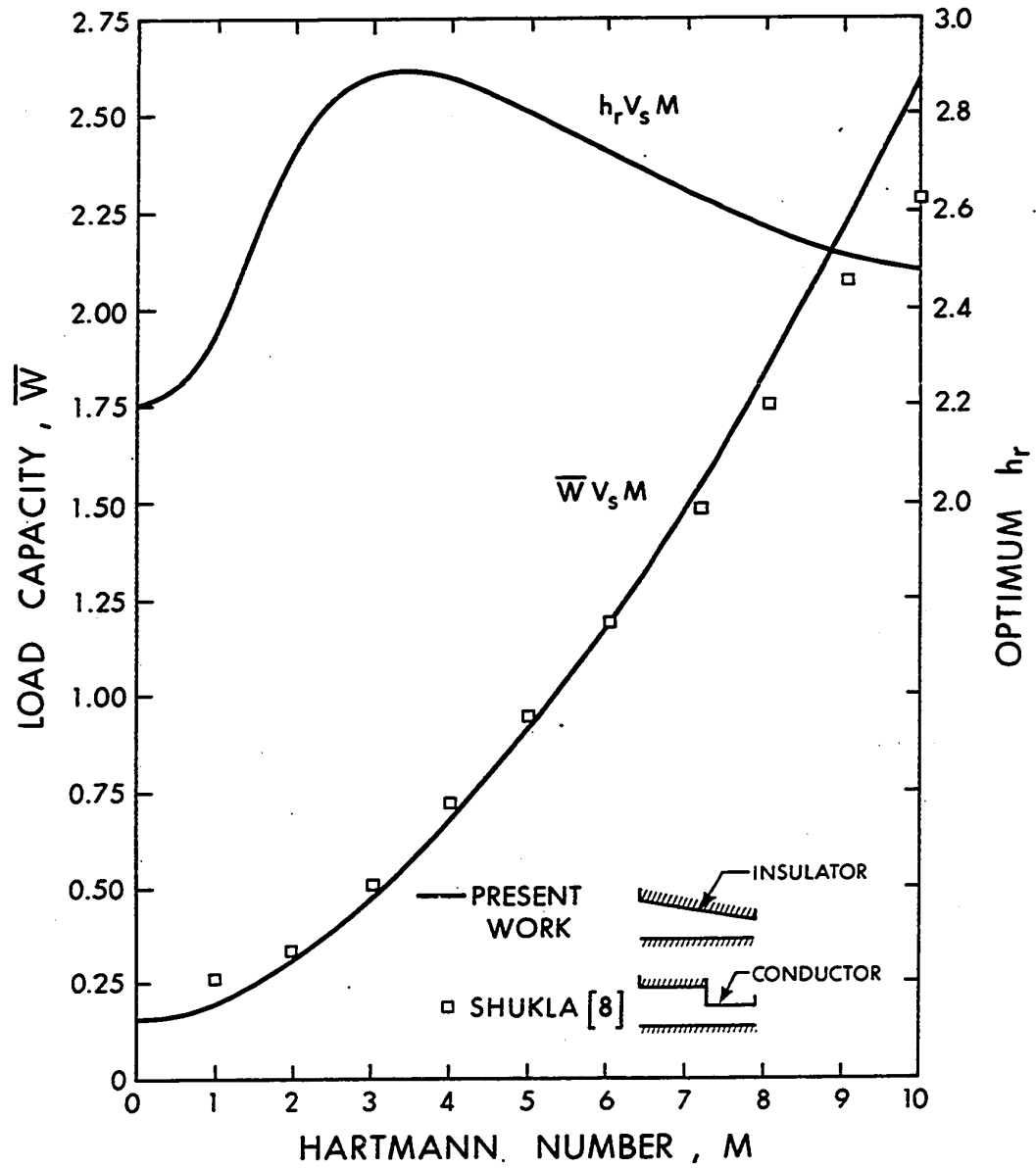


FIG. 4.3 MAXIMUM LOAD CAPACITY FOR CASE A
(Uniformly Applied Magnetic Field)

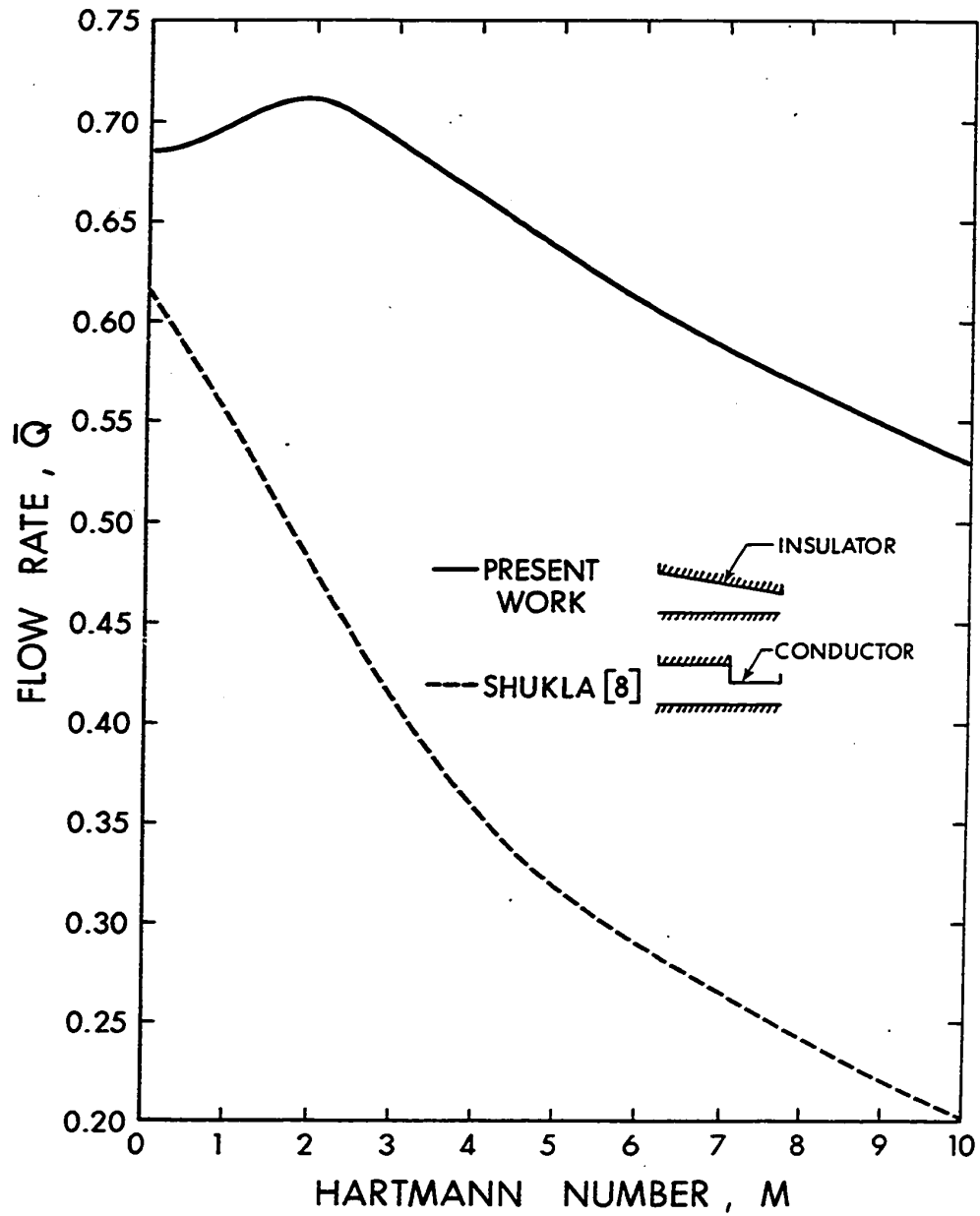


FIG. 4.4 FLOW RATE FOR CASE A

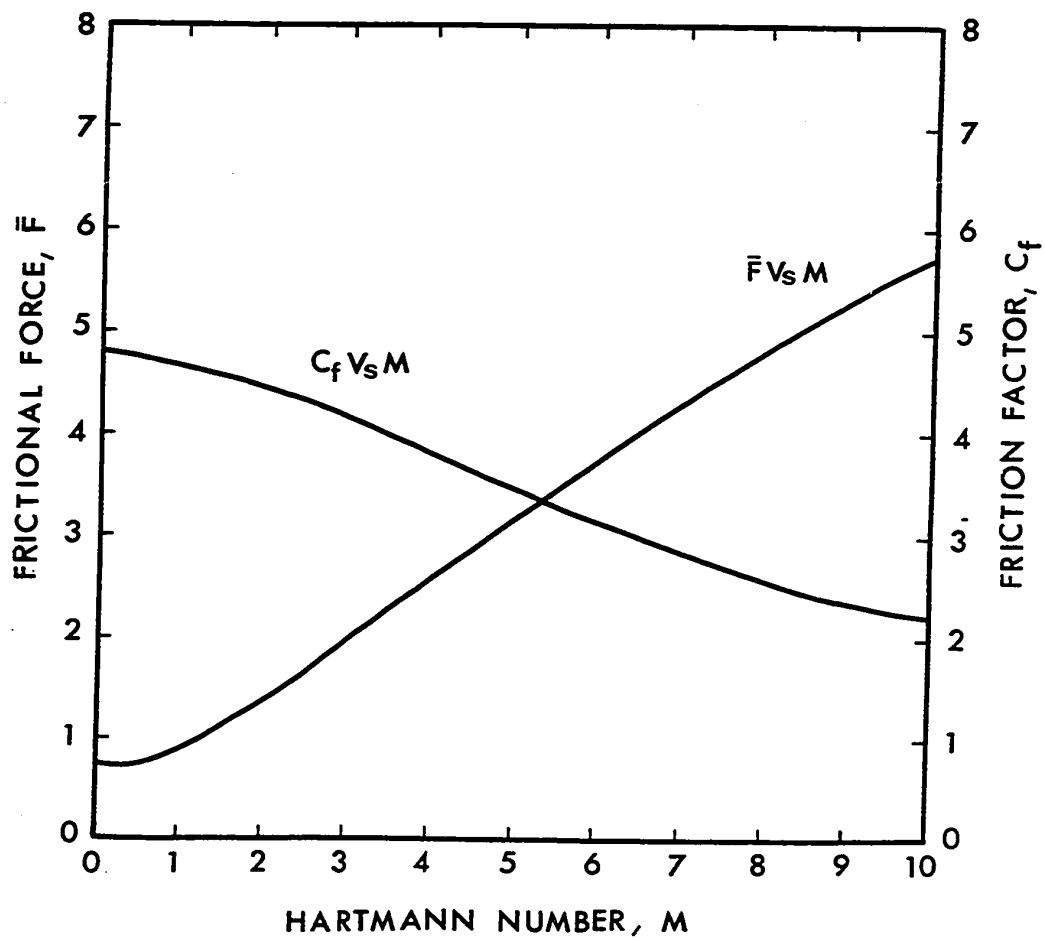


FIG. 4.5 FRICTIONAL FORCE AND FRICTION FACTOR FOR CASE A

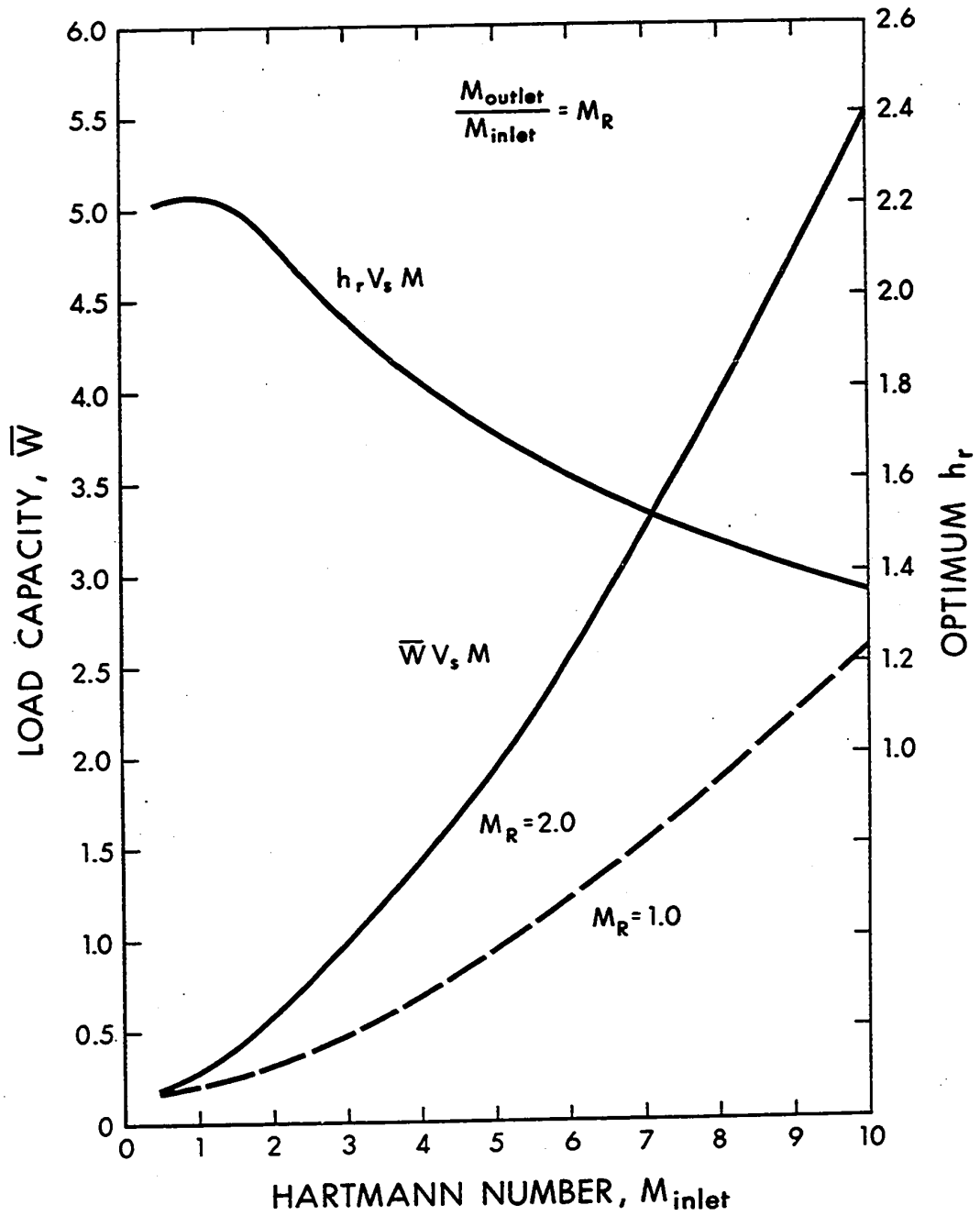


FIG. 4.6 MAXIMUM LOAD CAPACITY FOR CASE B
(Linearly Increasing Applied Magnetic Field)

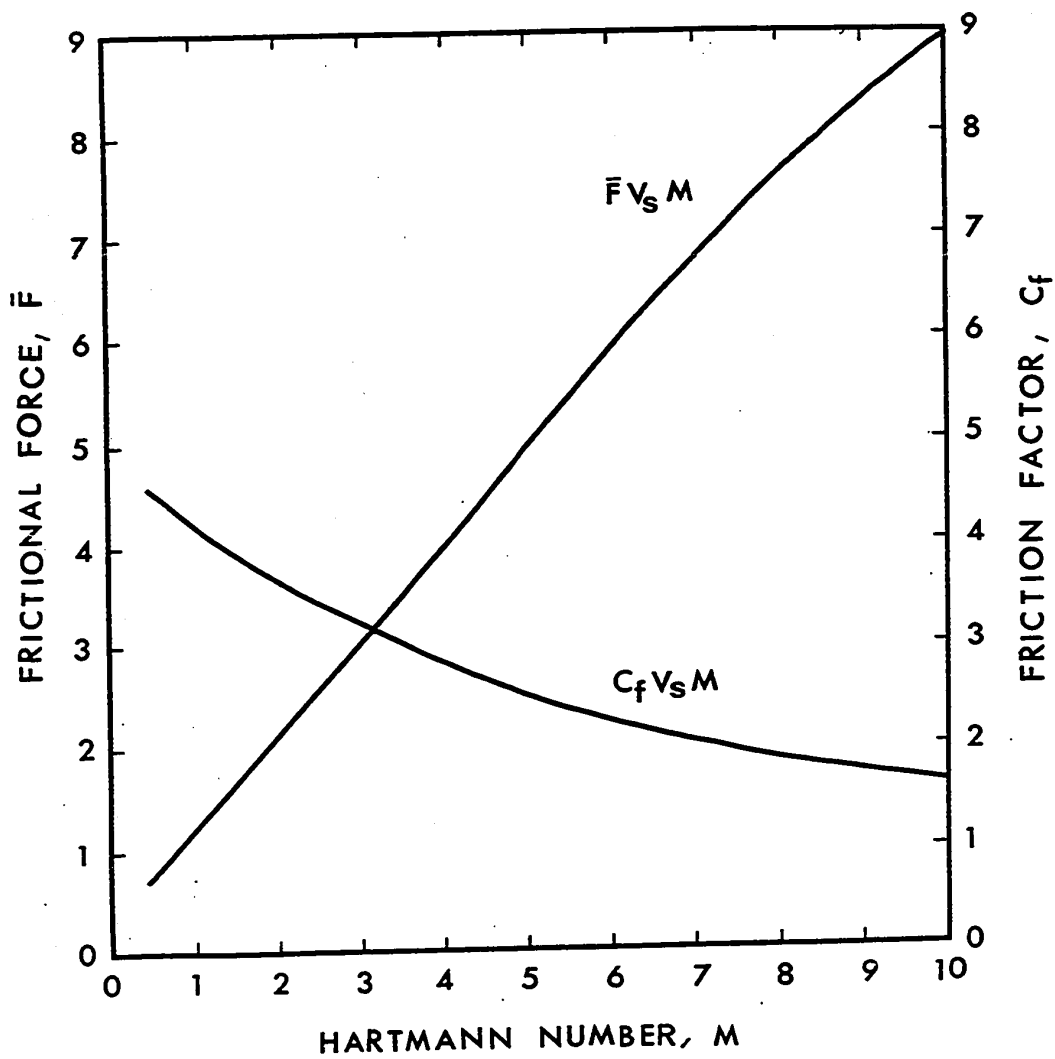


FIG. 4.7 FRICTIONAL FORCE AND FRICTION FACTOR FOR CASE B

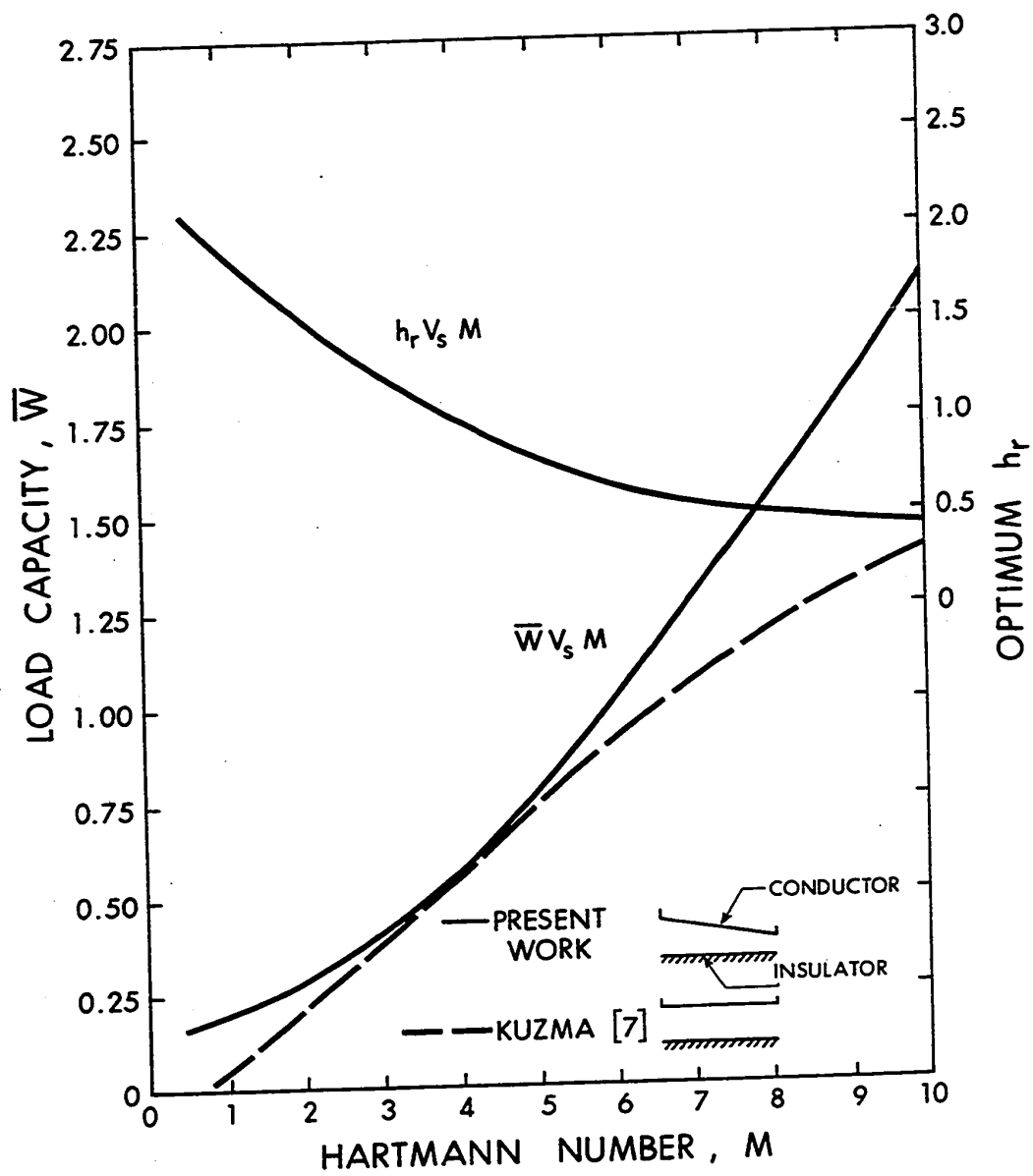


FIG. 4.8 MAXIMUM LOAD CAPACITY FOR CASE C
(Step-type Applied Magnetic Field)

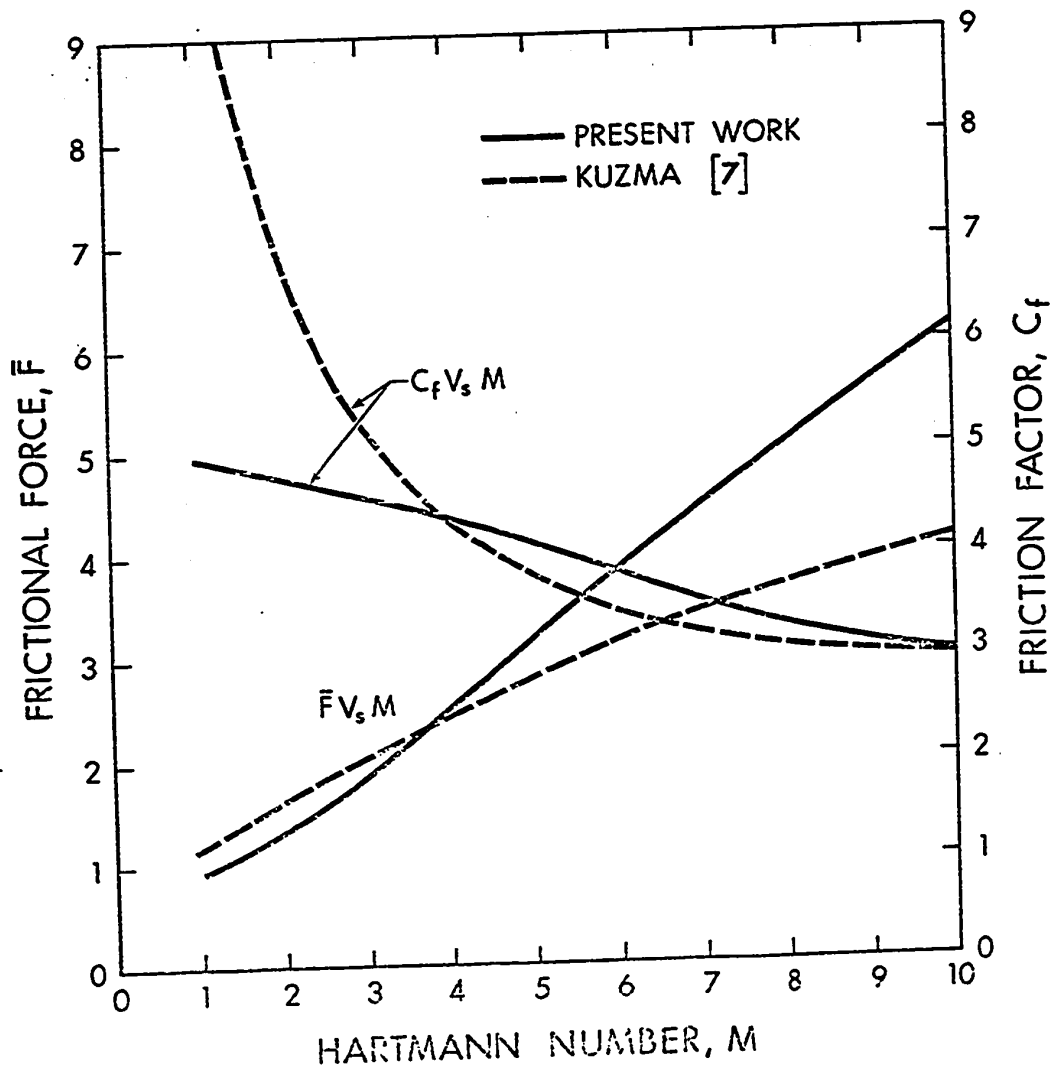


FIG. 4.9 FRICTIONAL FORCE AND FRICTION FACTOR

CHAPTER V
NONUNIFORM ELECTRIC FIELD EFFECTS
IN MHD SLIDER BEARINGS

5.1 Introduction

The review of literature and the results presented in the previous chapters indicate that at small Hartmann numbers only a slight increase in load capacity is obtained under open circuit condition. However, a significant increase may be obtained when Hartmann numbers are very large. Thus, to substantially increase the load capacity a very high strength magnetic field would be required. Consequently, this would necessitate a very large magnet which would be impractical.

In order to improve the load capacity at low M the supply of electrical power to the bearing, by connecting the side electrodes to the external source, has been proposed [5,6,9,10]. This arrangement has substantially improved the bearing load capacity even at very low Hartmann numbers.

However, in these analyses it was assumed that since the electrodes were perfect conductors, and the bearings were assumed infinitely wide, then from equations (2.3) E_z was essentially a constant. Therefore, any variation of E_z in the bearing and near the edges was neglected.

It was concluded in Chapters III and IV, that the nonuniformly

applied magnetic fields improve the average load bearing capacity. This intuitively suggests that if the applied electric field from a certain part of the bearing is removed, then further improvement in the load capacity can be expected. This may be achieved by segmenting the side plates into the conductor and insulated parts. The external power is then only supplied to the conductor part.

The purpose of this Chapter is to investigate the effects on load capacity of such a bearing configuration.

5.2 The Bearing Configuration

The finite width parallel plate bearing with a uniform magnetic field applied perpendicularly to the bearing surfaces is shown in Fig. 5.1. The bearing surfaces are made of insulating material. Each of the side plates is segmented into two parts; the electrode, and the insulated. The electrode part is a perfect conductor, while the latter part is an insulator. The electrode part may be connected to the external generator such that the current can be supplied to the bearing.

5.3 The Governing Equations and the Associated Boundary Conditions

The general equations developed and simplified in Chapter II, remain valid for the present model. However, when the external potential is applied to the bearing system shown in Fig. 5.1, it becomes necessary to consider the Maxwell's curl equations as well. Thus, to obtain the solution all these equations have to be solved simultaneously subject to the appropriate boundary conditions on the fluid and electric fields.

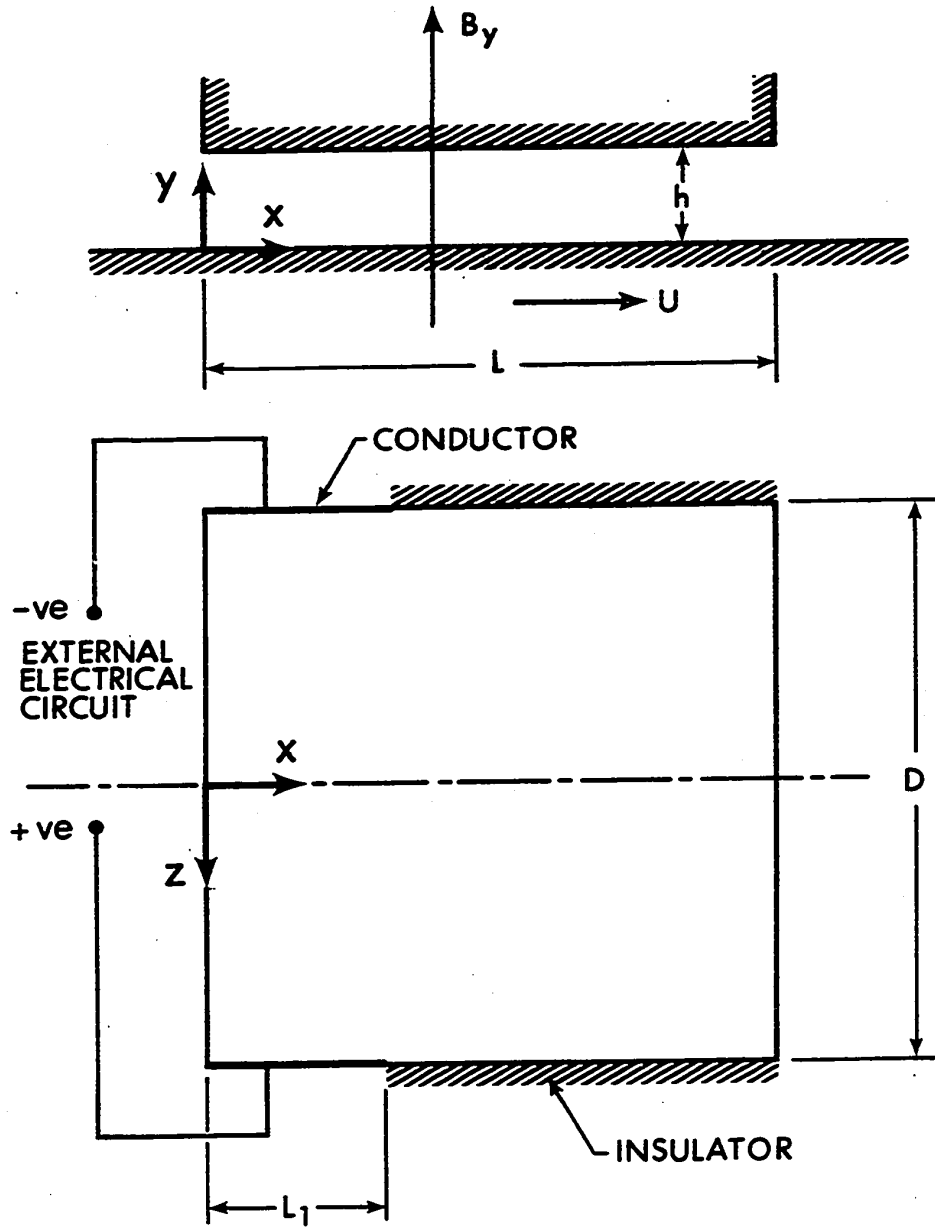


FIG. 5.1 MHD FINITE WIDTH PARALLEL PLATE SLIDER BEARING

This indeed, is a difficult task and at this stage we make some further assumptions to put the problem in a manageable form. These assumptions are:

(1) It may be recalled that the coupling of the fluid equations and Maxwell's equations are through Ohm's Law, stated in Chapter II as:

$$\vec{J} = \sigma(\vec{E} + \vec{V} \times \vec{B}) \quad (2.4)$$

In the present analysis consideration is essentially on the MHD where the applied magnetic field is not high, and the velocity of the slider is not large. Therefore, it would be reasonable to assume that the induced voltage, $\vec{V} \times \vec{B}$ is much smaller than the applied voltage. Hence, for such a case the second term may be neglected compared to the first term in equation (2.4), and the equation may be written in the following form:

$$\vec{J} = \sigma(\vec{E}) \quad (5.1)$$

By making the above assumptions, the fluid equations have been uncoupled from Maxwell's equations. Therefore, each set of equations can be solved independently with the appropriate boundary conditions.

(2) For the bearing under consideration \vec{E} and \vec{J} may be assumed to be functions of x and z .

(3) As indicated in the results of Chapter III, the inertia terms are neglected.

From assumptions (1) and (2) and equation (2.3) the following results:

$$\nabla \cdot \vec{E} = 0 \quad (5.2)$$

Defining $\vec{E} = -\nabla\phi$, and combining this definition with the above equation, the Laplace's equation for the two dimensional domain (x,z) is obtained.

$$\frac{\partial^2 \phi}{\partial x^2} + \frac{\partial^2 \phi}{\partial z^2} = 0 \quad (5.3)$$

The solution of this equation with the appropriate boundary conditions will give the ϕ distribution, and hence the electric field in the bearing.

In order to solve equation (5.3) it is necessary to specify the boundary conditions on the four sides of the domain xz. From Fig. 5.1, it is apparent that the electric potential is applied to the electrode parts of the side plates, while the remaining parts of the side plates are insulators. The boundary conditions, however, at inlet and outlet of the bearing are difficult to prescribe due to the continuous flow of the lubricant. Since the slider bearing essentially represents a portion of the thrust bearing arrangement, it may be noted that at the end of each thrust pad the grooves of small width for entry and discharge of the lubricant are provided. It may be pointed out that this arrangement can be modified so that near the inlet and the outlet the insulated walls may be provided. However, in the present

analysis, the arrangement is approximated by assuming that the insulated walls are located at the inlet and outlet of the bearing. The boundary conditions for such an arrangement may be written as

$$\frac{\partial \phi}{\partial x} (0, z) = \frac{\partial \phi}{\partial x} (L, z) = 0$$

$$\frac{\partial \phi}{\partial z} (x, \pm \frac{D}{2}) = 0 \quad \text{when } x \geq L_1 \quad (5.4)$$

$$\phi(x, \pm \frac{D}{2}) = \pm \phi_a \quad \text{when } x \leq L_1$$

Under the assumptions (1) through (3), the governing equations (2.6) through (2.11) now take the following form

$$0 = -\frac{\partial p}{\partial x} + \mu \left(\frac{\partial^2 u}{\partial y^2} \right) - J_z B_y \quad (5.5)$$

$$0 = -\frac{\partial p}{\partial z} + \mu \left(\frac{\partial^2 w}{\partial y^2} \right) + J_x B_y \quad (5.6)$$

$$\frac{\partial u}{\partial x} + \frac{\partial v}{\partial y} + \frac{\partial w}{\partial z} = 0 \quad (5.7)$$

$$J_x = \sigma(E_x) \quad (5.8)$$

$$J_z = \sigma(E_z) \quad (5.9)$$

The boundary conditions are

$$u = U, v = w = 0 \text{ at } y = 0 \quad (5.10)$$

$$u = v = w = 0 \text{ at } y = h$$

$$p = 0 \text{ for } x = 0, L \quad (5.11)$$

$$p = 0 \text{ for } z = \pm \frac{D}{2}$$

From equations (5.5), (5.6) and (5.7) when combined with the boundary conditions (5.10), the magnetohydrodynamic form of Reynold's equation may be obtained by employing the following procedure.

Since J_x and J_z are assumed to be functions of x and z only, equations (5.5) and (5.6) may be integrated directly to yield

$$u = \frac{1}{2\mu} \left(\frac{\partial p}{\partial x} + J_z B_y \right) y^2 + C_1 y + C_2 \quad (5.12)$$

$$w = \frac{1}{2\mu} \left(\frac{\partial p}{\partial z} + J_x B_y \right) y^2 + C_3 y + C_4 \quad (5.13)$$

where C 's are constants of integration. When these are evaluated with the use of boundary conditions (5.10) then

$$u = \frac{1}{2\mu} \left(\frac{\partial p}{\partial x} + J_z B_y \right) (y^2 - yh) + U \left(1 - \frac{y}{h} \right) \quad (5.14)$$

$$w = \frac{1}{2\mu} \left(\frac{\partial p}{\partial z} - J_x B_y \right) (y^2 - yh) \quad (5.15)$$

The x-component of the fluid flow rate per unit width, Q_x can now be expressed as

$$Q_x = \int_0^h u dy \quad (5.16)$$

Combining (5.14) and (5.16), the following is obtained

$$Q_x = -\frac{h^3}{12\mu} \left(\frac{\partial p}{\partial x} + J_z B_y \right) + \frac{Uh}{2} \quad (5.17)$$

Similarly, the z-component of fluid flow rate per unit length is expressed as

$$Q_z = \int_0^h w dy \quad (5.18)$$

which, when combined with equation (5.15) yields

$$Q_z = -\frac{h^3}{12\mu} \left(\frac{\partial p}{\partial z} - J_x B_y \right) \quad (5.19)$$

At this stage the continuity equation (5.7), may be integrated with respect to y . Using boundary conditions (5.10), the following is obtained.

$$\frac{\partial}{\partial x} \int_0^h u dy + \frac{\partial}{\partial z} \int_0^h w dy = 0 \quad (5.20)$$

From equations (5.16) and (5.18) the above equation becomes

$$\frac{\partial Q_x}{\partial x} + \frac{\partial Q_z}{\partial z} = 0 \quad (5.21)$$

Substituting equations (5.17) and (5.19) into equation (5.21) yields

$$\frac{\partial}{\partial x} \left[\frac{h^3}{12\mu} \left(\frac{\partial p}{\partial x} + J_z B_y \right) + \frac{Uh}{2} \right] + \frac{\partial}{\partial z} \left[\frac{h^3}{12\mu} \left(\frac{\partial p}{\partial z} - J_x B_y \right) \right] = 0 \quad (5.22)$$

When h is not a function of x as is the present case, the above equation reduces to

$$\frac{\partial^2 p}{\partial x^2} + \frac{\partial^2 p}{\partial z^2} = B_y \left(\frac{\partial J_x}{\partial z} - \frac{\partial J_z}{\partial x} \right) \quad (5.23)$$

It is interesting to note that the above pressure equation is independent of the viscosity of the lubricant. At this point it is convenient to put the governing equations into dimensionless form by using the characteristics quantities usually employed in MHD lubrication. These are:

$$\begin{aligned} \bar{x} &= \frac{x}{L}, \quad \bar{u} = \frac{u}{U}, \quad \bar{B}_y = \frac{B_y}{B_{y,\text{applied}}} \\ \bar{y} &= \frac{y}{h}, \quad \bar{p} = \frac{\rho h^2}{\mu U L}, \quad M = (h\sqrt{\frac{\sigma}{\mu}}) B_{y,\text{applied}} \\ \bar{z} &= \frac{z}{D}, \quad \bar{J}_x = \left(\frac{J_x h}{U} \right) \frac{1}{\sqrt{\sigma \mu}}, \quad \bar{J}_z = \left(\frac{J_z h}{U} \right) \frac{1}{\sqrt{\sigma \mu}} \\ \bar{E}_x &= \left(\frac{E_x h}{U} \right) \sqrt{\frac{\sigma}{\mu}}, \quad \bar{E}_z = \left(\frac{E_z h}{U} \right) \sqrt{\frac{\sigma}{\mu}}, \quad \bar{\phi} = \left(\frac{\phi h}{D} \right) \sqrt{\frac{\sigma}{\mu}} \\ \bar{Q}_x &= \frac{Q_x}{Uh}, \quad \bar{Q}_z = \frac{Q_z}{Uh}, \quad S = \frac{L_1}{L} \end{aligned} \quad (5.24)$$

In dimensionless form the potential equation (5.3) becomes

$$\frac{\partial^2 \bar{\phi}}{\partial \bar{x}^2} + \left(\frac{L}{D}\right)^2 \frac{\partial^2 \bar{\phi}}{\partial \bar{z}^2} = 0 \quad (5.25)$$

With the following boundary conditions

$$\frac{\partial \bar{\phi}}{\partial \bar{x}}(0, \bar{z}) = \frac{\partial \bar{\phi}}{\partial \bar{x}}(1, \bar{z}) = 0$$

$$\frac{\partial \bar{\phi}}{\partial \bar{z}}(\bar{x}, \pm \frac{1}{2}) = 0 \quad \text{when } \bar{x} \geq S \quad (5.26)$$

$$\bar{\phi}(\bar{x}, \pm \frac{1}{2}) = \pm \bar{\phi}_a \quad \text{when } \bar{x} \leq S$$

While the pressure equation (5.23) reduces to

$$\frac{\partial^2 \bar{p}}{\partial \bar{x}^2} + \left(\frac{L}{D}\right)^2 \frac{\partial^2 \bar{p}}{\partial \bar{z}^2} = M \left(\frac{L}{D} \frac{\partial \bar{J}_x}{\partial \bar{z}} - \frac{\partial \bar{J}_z}{\partial \bar{x}} \right) \quad (5.27)$$

with the following boundary conditions

$$\bar{p} = 0, \quad \bar{x} = 0, 1 \quad (5.28)$$

$$\bar{p} = 0, \quad \bar{z} = \pm \frac{1}{2}$$

Load Capacity:

The integration of the pressure over the bearing area yields the load capacity. In terms of dimensionless variables it may be written as

$$\bar{W} = \frac{Wh^2}{\mu UDL^2} = \int_{-1/2}^{1/2} \int_0^1 \bar{p} \, d\bar{x} \, d\bar{z} \quad (5.29)$$

Frictional Force:

The frictional force on the slider is given by

$$F = - \int_{-D/2}^{D/2} \int_0^L \mu \left(\frac{\partial u}{\partial y} \right)_{y=0} \, dx \, dz \quad (5.30)$$

From equation (5.15) the above equation becomes

$$F = \int_{-D/2}^{D/2} \int_0^L \left[\frac{h}{2} \left(\frac{\partial p}{\partial x} + B_y J_z \right) + \frac{\mu U}{h} \right] \, dx \, dz \quad (5.31)$$

which when simplified gives

$$\bar{F} = \frac{Fh}{\mu UDL} = 1 + \frac{M}{2} \int_{-1/2}^{1/2} \int_0^1 \bar{J}_z \, d\bar{x} \, d\bar{z} \quad (5.32)$$

5.4 Solution to the Governing Equations

5.4.1 General Approach

The problem formulated in section 5.2, requires the solution of equations (5.25) and (5.27) with the corresponding boundary conditions (5.26) and (5.28) respectively. These equations are difficult to solve analytically and hence a numerical approach is adopted.

In the present study, the method of finite-difference will be used [12,15-17]. The resulting equations will be solved using the point successive-overrelaxation method [17].

5.4.2 Finite-Difference Approximation

Considering a 5-point molecule shown in Fig. 5.2, the partial differential equation (5.25) is transformed into a finite-difference form (see Appendix B). After rearranging, the equation for any point (i,j) in the grid may be written for $\Delta x = \Delta y$, in the following form

$$\bar{\phi}_{i,j} = a_1 \bar{\phi}_{i+1,j} + a_2 \bar{\phi}_{i-1,j} + a_3 \bar{\phi}_{i,j+1} + a_4 \bar{\phi}_{i,j-1} \quad (5.33)$$

where

$$a_1 = a_2 = \frac{1}{2} \left(\frac{1}{1 + \frac{L^2}{D^2}} \right)$$

$$a_3 = a_4 = \frac{1}{2} \left(\frac{1}{1 + \frac{D^2}{L^2}} \right)$$

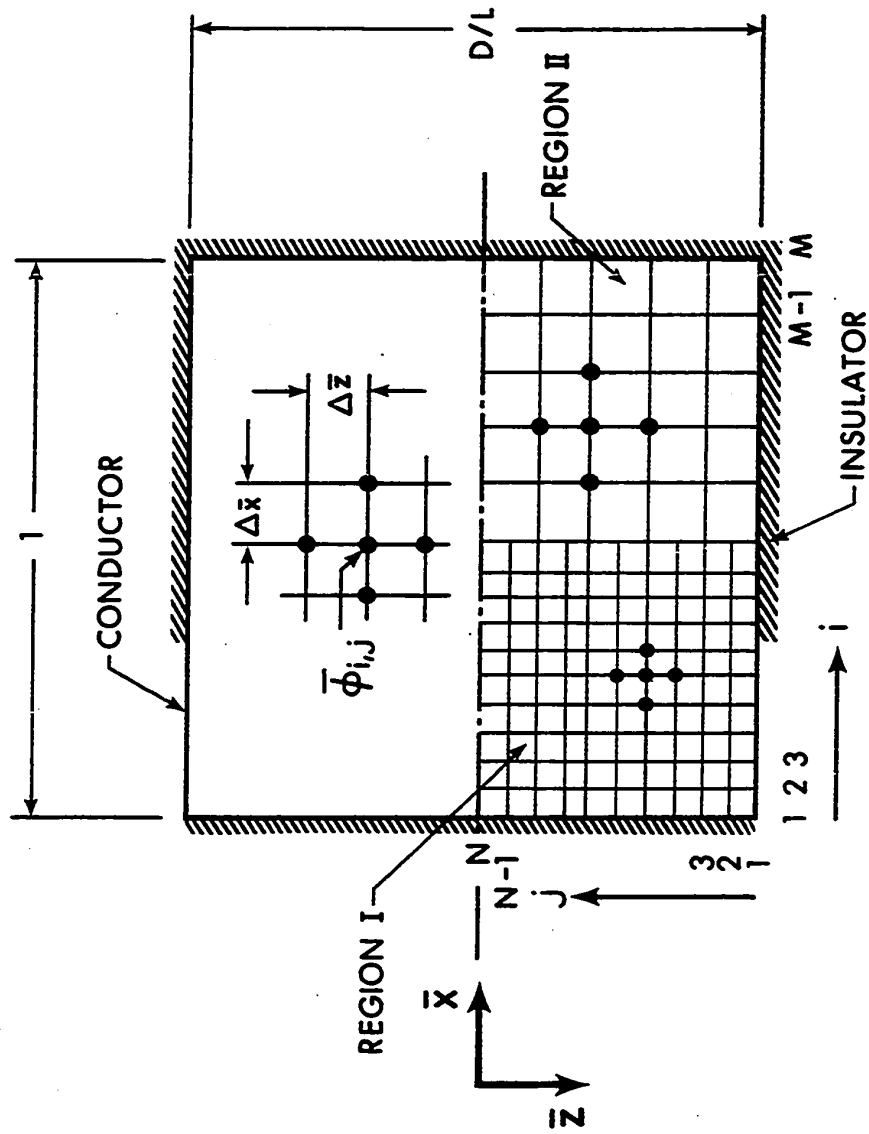


FIG. 5.2 FINITE-DIFFERENCE NETWORK
FOR POTENTIAL EQUATION (5.25)

Similarly using the 5-point molecule shown in Fig. 5.3, equation (5.27) for $\Delta x = \Delta y = \Delta h$, becomes (see Appendix C)

$$\bar{p}_{i,j} = b_1 \bar{p}_{i+1,j} + b_2 \bar{p}_{i-1,j} + b_3 \bar{p}_{i,j+1} + b_4 \bar{p}_{i,j-1} + b_5 \bar{E}_{i,j} \quad (5.34)$$

where

$$b_1 = b_2 = \frac{1}{2} \left(\frac{1}{1 + \frac{L^2}{D^2}} \right)$$

$$b_3 = b_4 = \frac{1}{2} \left(\frac{1}{1 + \frac{D^2}{L^2}} \right)$$

$$b_5 = -\frac{1}{2} \left(\frac{\Delta^2 h}{1 + \frac{L^2}{D^2}} \right)$$

and

$$\bar{E}_{i,j} = M \left(\frac{L}{D} \frac{\partial \bar{J}}{\partial z} - \frac{\partial \bar{J}}{\partial x} \right)$$

5.4.3 Method of Solution

The finite-difference approximation at each of the grid points has essentially reduced the problem to solving a set of ordinary linear equations.

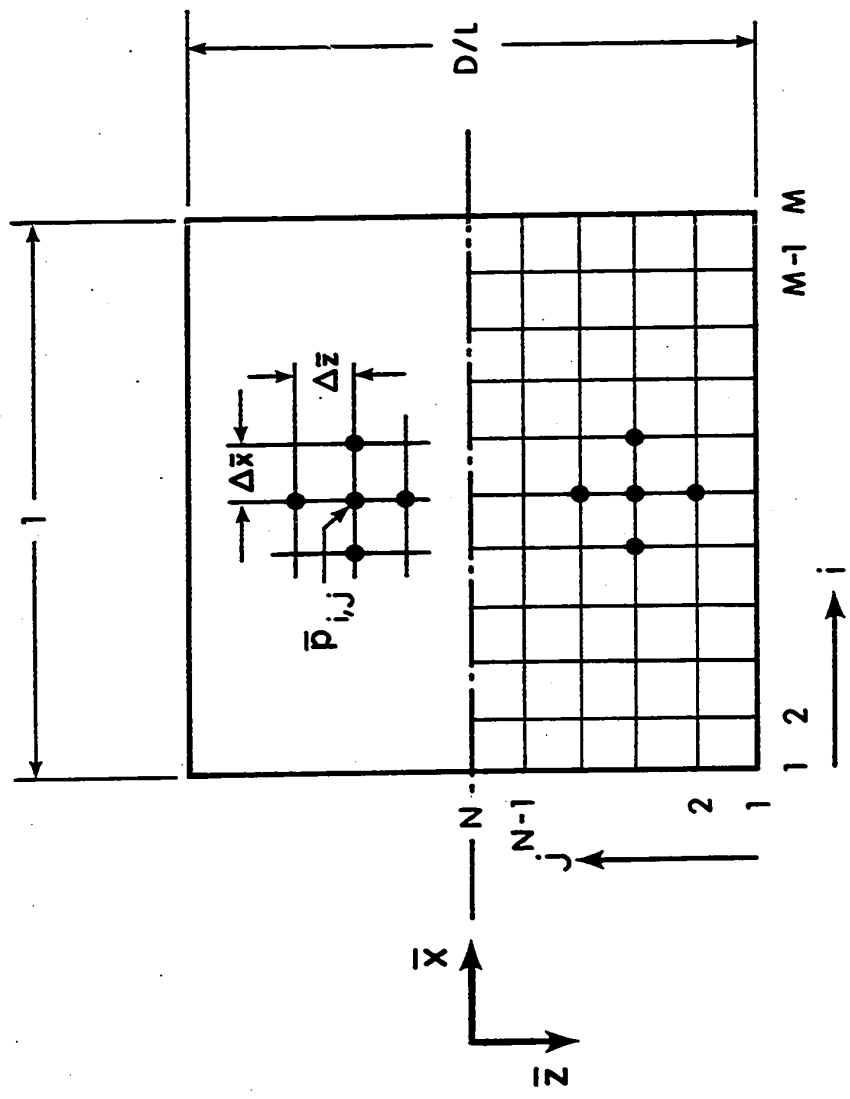


FIG. 5.3 FINITE-DIFFERENCE NETWORK
FOR PRESSURE EQUATION (5.27)

From Fig. 5.2, it is clear that due to symmetry about the middle line only one half of the domain may be considered for computations.

(a) Solution for Electric Potential Equation

Since the equation is uncoupled, the solution to this equation (5.25) with boundary conditions (5.26) is obtained first.

Due to unusual boundary conditions on $\bar{\phi}$ the half domain was further divided into two regions; close to the electrode and far away from it. In region I, close to the electrode it was divided into a finer mesh as compared to the far away region. This was primarily to overcome the difficulties in computations due to the steep gradient of $\bar{\phi}$ near the electrode plate and especially the corner.

The application of equation (5.25) at each of the grid points gives a set of linear equations. These equations are then solved by the successive-overrelaxation procedure [17] by a digital computer, IBM 360/67.

If the number of iterations performed is denoted by K, the procedure can be defined with:

$$\begin{aligned} \bar{\phi}_{i,j}^{(K)} = & \bar{\phi}_{i,j}^{(K-1)} + \omega (a_1 \bar{\phi}_{i+1,j}^{(K-1)} + a_2 \bar{\phi}_{i-1,j}^{(K-1)} + a_3 \bar{\phi}_{i,j+1}^{(K-1)} \\ & + a_4 \bar{\phi}_{i,j-1}^{(K-1)} - \bar{\phi}_{i,j}^{(K-1)}) \end{aligned} \quad (5.35)$$

where ω is a parameter known as a relaxation factor, the choice of which determines the rate of convergence. The iteration procedure is terminated when the following convergence condition is satisfied.

$$\max \frac{|\bar{\phi}_{i,j}^{(K)} - \bar{\phi}_{i,j}^{(K-1)}|}{\bar{\phi}_{i,j}^{(K)}} \leq 10^{-5} \quad (5.36)$$

Once the potential distributing in the bearing is obtained, \bar{E}_x , \bar{E}_z , \bar{J}_x , \bar{J}_z , $\partial\bar{J}_x/\partial\bar{z}$ and $\partial\bar{J}_z/\partial\bar{x}$ may be approximated at each of the grid points by the finite-difference formulas given in Appendix D. The total current through the bearing for the applied potential $\bar{\phi}_a$ is then obtained by carrying out the numerical integration of \bar{J}_z distribution at the center line. The area to be considered for the total current will be in the \bar{xy} plane.

(b) Solution for Pressure Equation

Knowing the electric field and the current distribution in the bearing, the pressure equation (5.27) may be solved. A uniform grid size shown in Fig. 5.3, is used in calculations. The procedure of solving the finite-difference equations is the same as described above. Equations (5.35) and (5.36) may be written in terms of pressure as

$$\begin{aligned} \bar{p}_{i,j}^{(K)} = & \bar{p}_{i,j}^{(K-1)} + \omega(b_1\bar{p}_{i+1,j}^{(K-1)} + b_2\bar{p}_{i-1,j}^{(K-1)} + b_3\bar{p}_{i,j+1}^{(K-1)} + b_4\bar{p}_{i,j-1}^{(K-1)} \\ & + b_5\bar{E}_{i,j} - \bar{p}_{i,j}^{(K-1)}) \end{aligned} \quad (5.37)$$

and

$$\max \frac{|\bar{p}_{i,j}^{(K)} - \bar{p}_{i,j}^{(K-1)}|}{\bar{p}_{i,j}^{(K)}} \leq 10^{-5} \quad (5.38)$$

Once the solution to the pressure equation is obtained, the load capacity and the frictional force on the slider are found by integrating the equations (5.29) and (5.32) respectively. The method employed for integration was Simpson's Integration Rule.

The optimum values of relaxation factor ω , and the mesh size employed in the computations is given in Appendix E. The error involved in the numerical solution is also briefly discussed in this Appendix.

5.5 Results and Conclusions

As shown in Fig. 5.1, the electrical power is supplied to the bearing by connecting the side electrodes to the external source. For an applied potential to the electrodes, $\bar{\phi}_a$, the electrical current flowing through the bearing system will depend on the electrode length S . In order to study the effects of nonuniform electric field on the bearing load capacity, the current flowing through the bearing is kept constant, while the electrode length S is varied. The constant flow of current can be achieved by adjusting the value of the applied potential $\bar{\phi}_a$. The results of such a bearing arrangement with $L/D = 1.0$ are discussed below for $M = 0.1$ to 1.0 .

The solution of equation (5.25) gives the potential distribution in the bearing. The current density in the bearing is then obtained by using the formulas given in Appendix D. Knowing the current density distribution, the current streamlines are obtained by integrating the current density distribution. The potential lines for $\bar{\phi}_a = 2.02$ and $S = 0.4$ are shown in Fig. 5.4. For the same conditions,

Fig. 5.5 shows the current streamlines in the bearing. The tendency of concentration of electric currents near the corner of the electrode is exhibited in this figure. It was noted that with the increase of the electrode length, this concentration of current decreased.

The solution of the pressure equation (5.27) presented in Fig. 5.6 indicates that there is a pressure buildup in the bearing when an electric potential is applied to the electrode parts of the side plates. The results further reveal that for a given hydrodynamic condition and for a fixed current flow through the bearing, the pressure distribution depends upon the electrode length S , and the Hartmann number. The pressure buildup in the parallel plate bearing with segmented side electrodes may be explained as follows.

From the current streamlines diagram (Fig. 5.5) it can be seen that when the electric potential is applied to the side electrodes, there is a net current flow in the negative direction of z -axis. The interaction between the current passing through the fluid and the applied magnetic field results in an electromagnetic body force in the fluid film. In the present analysis, the important components of the electromagnetic force as shown in equation (5.5) and (5.6) are: $J_z \times B_y$ in x -direction, and $J_x \times B_y$ in z -direction. The distribution of the body force in the bearing for uniformly applied magnetic field therefore will depend on the distribution of the current density. In order to illustrate the role of the electromagnetic body force on the flow more clearly, let us consider the situation at the center of the bearing. As the bearing is symmetrical about the middle line, J_x

will be zero at the center. Therefore, the only component of the body force at the center will be the x-component. If one visualizes the direction of this body force, it can be seen that the effects of the electromagnetic force is to accelerate the fluid between the bearing surfaces in the same direction as the motion of the slider, thus resulting in an increase in pressure. However, if the electromagnetic force is distributed uniformly, then there is no pressure buildup in the parallel plate bearing. Mathematically, this can be easily seen from equation (5.27) and the boundary conditions (5.28). For a uniform electric field, the right hand side of the equation is zero, so that $\bar{p} = 0$ throughout the bearing. However, for a nonuniform electric field, the right hand side is nonzero resulting in a nonzero pressure distribution.

The physical reasoning of the pressure rise in the bearing may be explained if the MHD parallel plate bearing is visualized as consisting of two parts. For simplicity, let us assume that the resulting electric field is uniform and is only confined to the electrode part of the bearing. Then, the bearing may be divided into two distinct parts; the upper part where the fluid is being pumped by the electromagnetic body force, and the lower part which essentially represents an ordinarily couette flow superimposed by a forced flow. In order that the couette part sustains the extra fluid which is being pumped through the bearing, a definite pressure drop will be required. Therefore, a positive pressure gradient develops in the pumping part of the bearing. However, this increase in pressure will depend on the con-

ditions in the lower part. The situation may be viewed as somewhat similar to a step-type hydrodynamic bearing. As will be seen later, that the pressure developed in the bearing becomes smaller, if the couette part is made smaller by increasing the length of the side electrodes. Finally, the pressure reduces to zero when the side electrodes are extended to the full length of the bearing. Then, the bearing configuration simply represents an MHD couette arrangement.

Figure 5.6 shows the pressure distribution along the length of the bearing for $\bar{I} = 2.5$, $S = 0.1$, and $M = 1.0$. The curves are plotted for the center of the bearing ($\bar{z} = 0$), and $\bar{z} = 0.25$ and 0.375 . It is noted that the maximum pressure distribution occurs at the center of the bearing indicating the location of the maximum electromagnetic body force in x-direction in the bearing. The curves further show that the position of maximum pressure moves towards the inlet of the bearing as \bar{z} increases from the centerline. The reason for this shift may be attributed to the concentration of current near the electrode.

The load capacity of the bearing against M for various values of S is shown in Fig. 5.7. It is noted that for a fixed S , the load capacity increases with the increase of M . The effect of electrode length S on load capacity is clearly indicated in this figure. It can be seen that as S is increased, the pressure developed in the bearing becomes smaller. Finally, for $S = 1.0$, the pressure reduces to zero, and the bearing has no load carrying capacity.

Figure 5.8 shows a plot of frictional force on the slider against M . It is noted that the frictional force increases with the

increase of M . However, it may be pointed out that the frictional force is independent of the electrode length S . Finally, the frictional force as shown in equation (5.32), depends on the total current through the bearing for a given Hartmann number.

The foregoing results of MHD parallel plate slider bearing suggest that if the electrical power is supplied to the bearing to improve the load carrying capacity, it would be advantageous to apply this power near the inlet portion of the bearing.

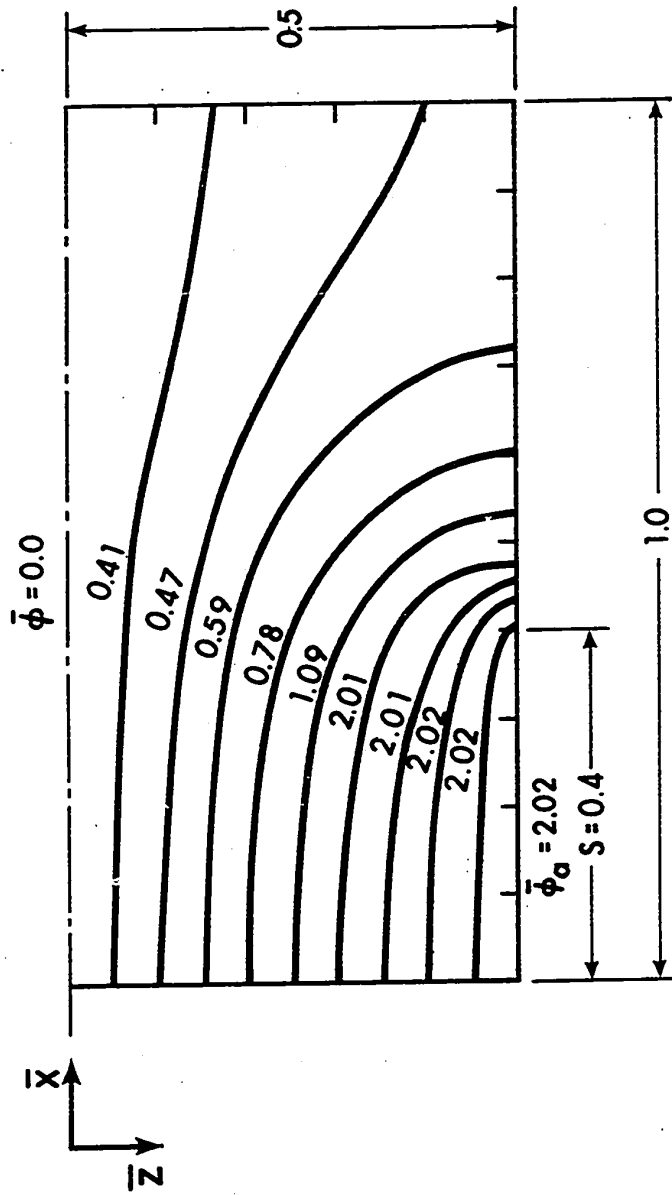


FIG. 5.4 POTENTIAL LINES FOR THE APPLIED
POTENTIAL TO SIDE ELECTRODE

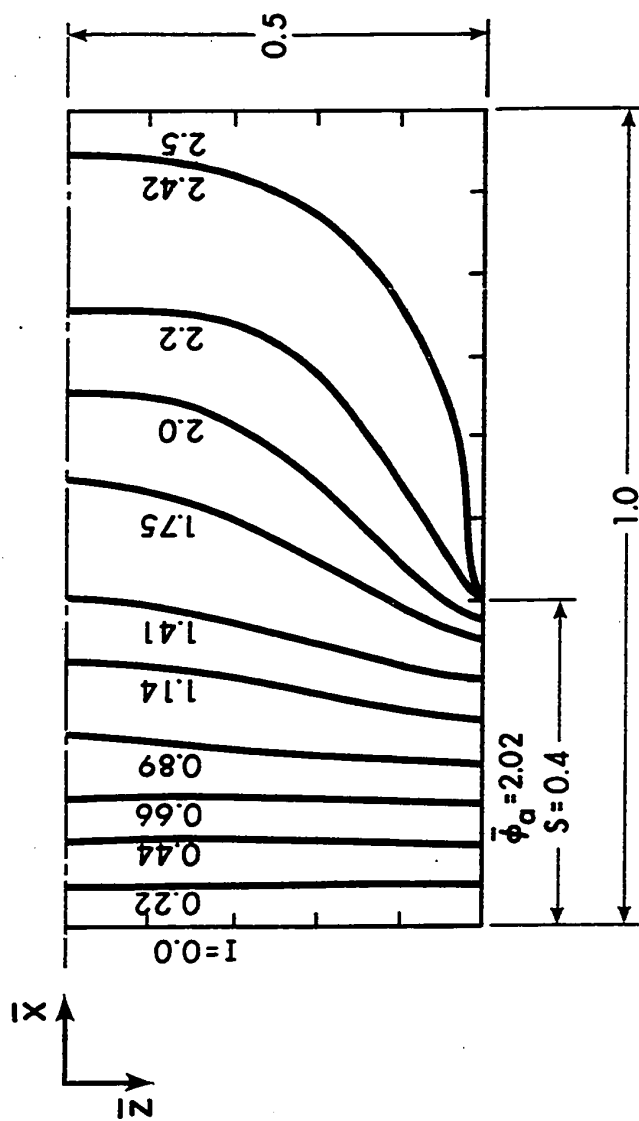


FIG. 5.5 CURRENT STREAMLINES FOR THE APPLIED POTENTIAL TO SIDE ELECTRODE

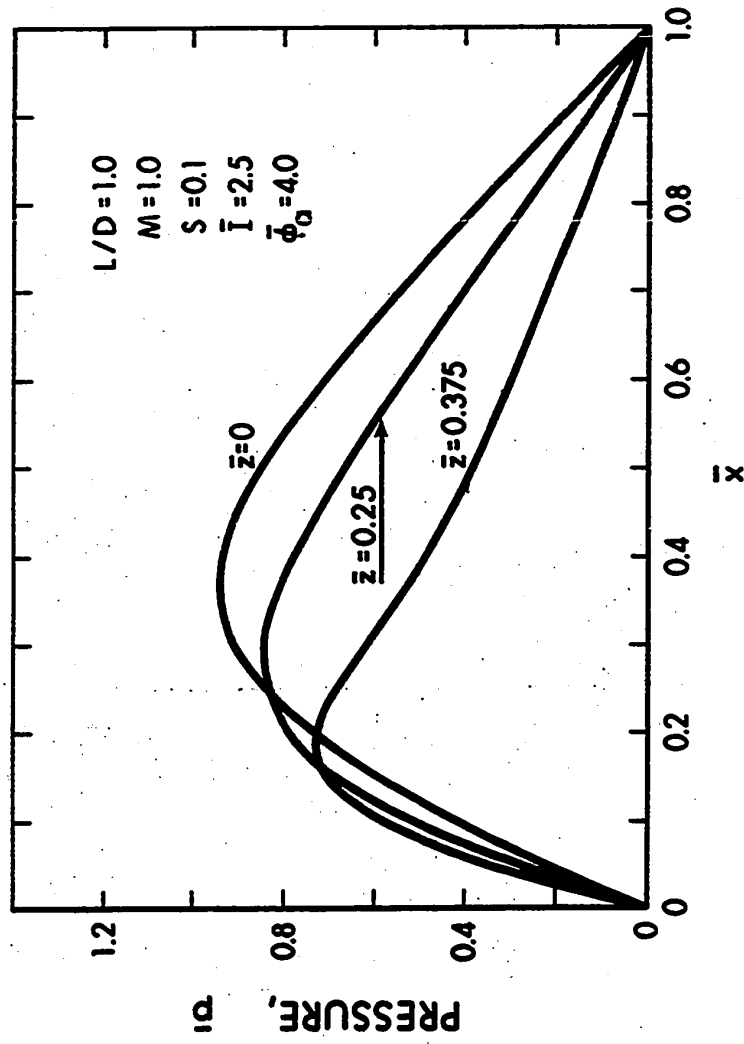


FIG. 5.6 PRESSURE DISTRIBUTION IN
THE PARALLEL PLATE BEARING

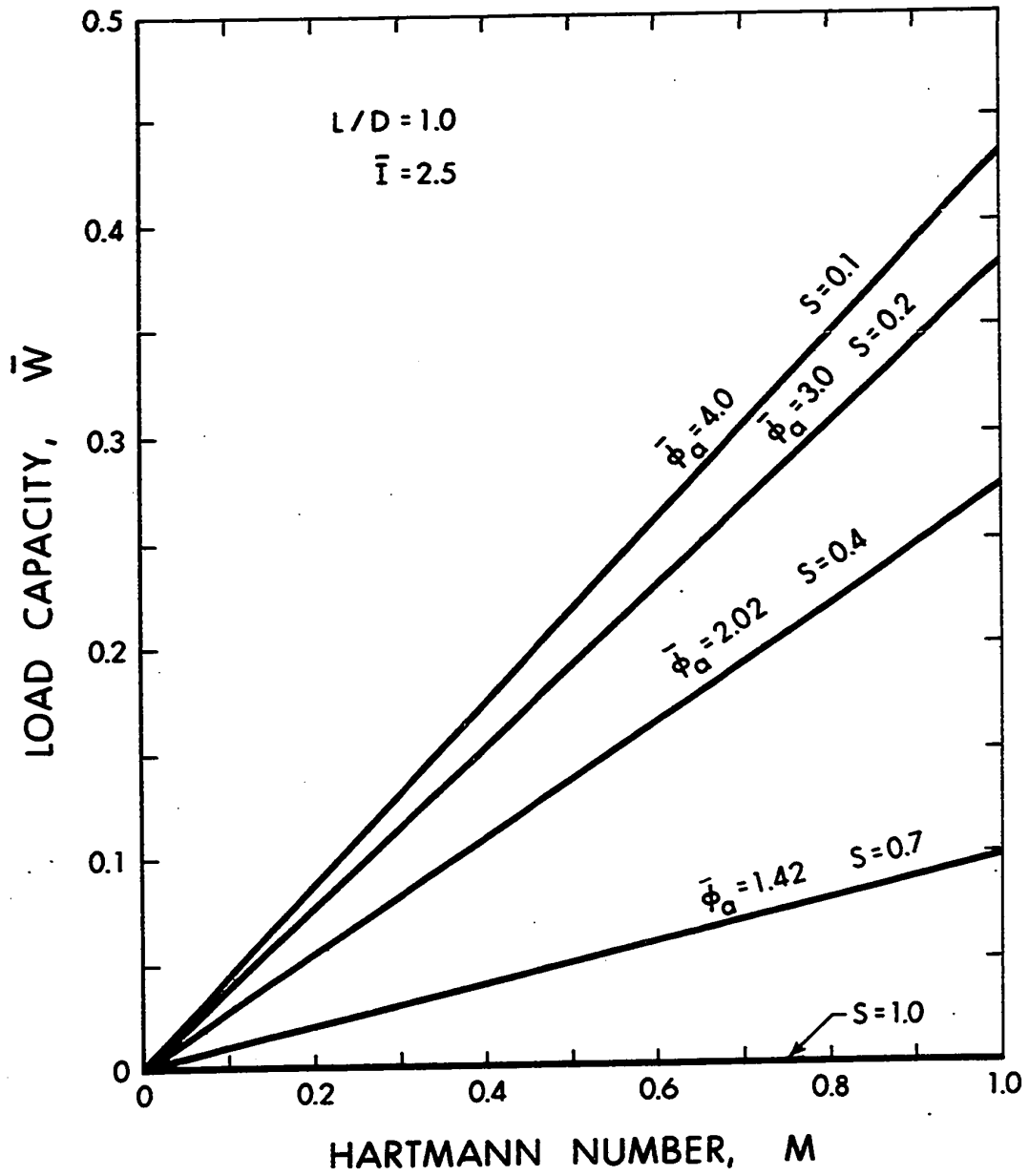


FIG. 5.7 LOAD CAPACITY FOR THE PARALLEL PLATE BEARING

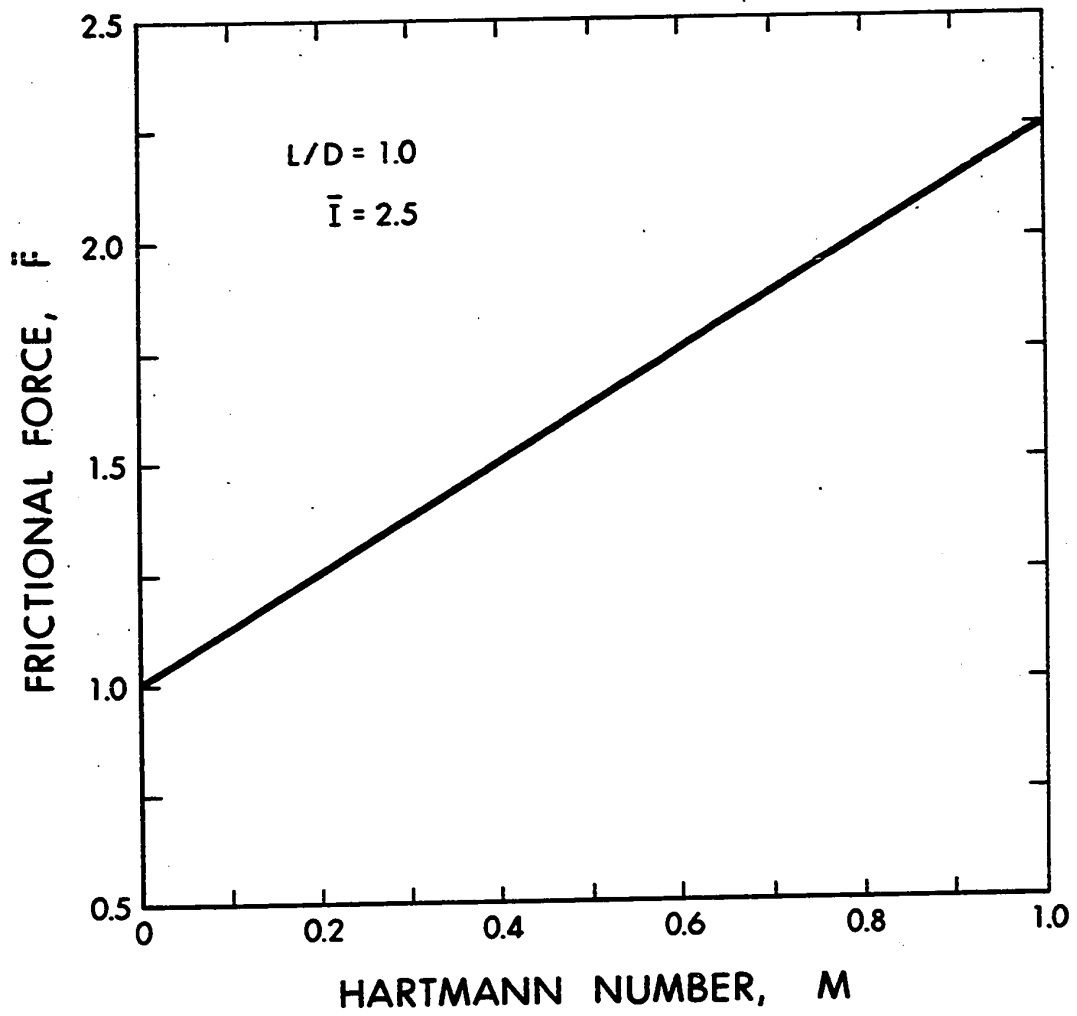


FIG. 5.8 FRICTIONAL FORCE FOR
THE PARALLEL PLATE BEARING

CHAPTER VI

CONCLUSIONS AND SUGGESTIONS FOR FUTURE INVESTIGATION

6.1 General Results and Conclusions

A theoretical study was made of the effects of electromagnetic interactions on the fluid film of a liquid-metal-lubricated slider bearing where the magnetic field was applied perpendicularly to the bearing surfaces. The analyses were carried out for an open circuit condition, and for the case where the electrical power from an external source was supplied to the bearing. The main results are summarized below.

For an open circuit condition the applied magnetic fields were assumed to have uniform, increasing, and step-type distribution. The effects of inertia on load capacity were analysed. The results indicate that the contribution of inertia terms decreases with the increase of Hartmann numbers, and it becomes negligible at high M . Therefore, the inertia terms were neglected and the solution was presented for uniform, linearly increasing and step-type applied magnetic fields. It is noted that for each type of magnetic fields, the maximum load capacity of bearings is obtained when the ratio of film thickness at the inlet to that at the outlet is optimized. The bearing surfaces have to be insulators for uniform and increasing magnetic fields, while the stator have to be a conductor for a step-type magnetic

field. The results also indicate that nonuniform magnetic fields i.e., increasing type, give higher load capacity than the comparable uniform magnetic field. However, the improvement obtained in load capacity by applying a nonuniform magnetic field is only moderate. For step-type applied magnetic field the load capacity obtained is less as compared to the uniformly applied magnetic field. It is interesting to note that for such a case, when $M > 4$ the maximum load capacity is obtained when the fluid film is divergent. The method of solution developed in Chapter IV may be employed in analyzing bearings having complicated profiles, e.g., multisteped and composite bearings.

For the case of externally supplied electric current, a parallel plate slider bearing was analyzed. The magnetic field was applied perpendicularly to the bearing surfaces. The segmented side electrodes were connected to the electrical power source, thus giving a nonuniform electric field distribution in the bearing. The results indicate that a parallel plate bearing with such an arrangement have load carrying capacity. The results suggest that if the electrical power is supplied to the bearing to improve the load capacity, it would be advantageous to apply the power near the inlet portion of the bearing.

6.2 Suggestions for Future Investigation

In the present work the effects of nonuniformly applied magnetic and electric fields were analyzed for a simple slider bearing. The analyses may be extended for bearings with complicated profiles.

For nonuniformly applied electric fields considered in Chapter V, the fluid equations were uncoupled from Maxwell's equations by making certain assumptions. It is suggested that these equations may be solved in the coupled form and the results compared with those presented here.

Another possible aspect of further investigation in magneto-hydrodynamic lubrication is attempting to design a bearing having automatic electrical adjustments in order to compensate for transient loads.

The present investigation and the results of other authors as discussed in review of literature, have shown the possibility of MHD slider bearing. In order to develop it into a practical device, it is suggested that a series of experiments should be carried out.

BIBLIOGRAPHY

1. Bisson, E.E. and Anderson, W.J., "Advanced Bearing Technology", NASA SP-38, National Aeronautics and Space Administration, Washington, D.C.
2. Hartmann, J. and Lazarus, F., "Hg-Dynamics II - Experimental Investigations on the Flow of Mercury in a Homogeneous Magnetic Field", Kgl. Danske Videnskab. Selskab, Mat.-Fys. Medd. 14, No. 7, Copenhagen (1937).
3. Snyder, W.T., "The Magnetohydrodynamic Slider Bearing", Journal of Basic Engineering, Trans. ASME, Series D, Vol. 84, No. 1, Mar. 1962, pp. 197-204.
4. Osterle, J.F. and Young, J.F., "On the Load Capacity of Hydro-magnetically Lubricated Slider Bearing", Wear, Vol. 5, 1962, pp. 227-234.
5. Hughes, W.F., "The Magnetohydrodynamic of Inclined Slider Bearing with a Transverse Magnetic Field", Wear, Vol. 6, 1963, pp. 315-324.
6. Hughes, W.F., "The Magnetohydrodynamic Finite Step Slider Bearing", Journal of Basic Engineering, Trans. ASME Series D, Vol. 85, No. 1, March 1963, pp. 129-136.
7. Kuzma, D.C., "The Magnetohydrodynamic Parallel Plate Slider Bearing", Journal of Basic Engineering, Trans. ASME, Series D, Vol. 87, No. 3, Sept. 1965, pp. 778-780.

8. Shukla, J.B., "The Optimum One-Dimensional Magnetohydrodynamic Slider Bearing", *Journal of Lubrication Technology, Trans. ASME, Series F, Vol. 92, No. 3, July 1970, pp. 530-534.*
9. Prakash, J., "Magnetohydrodynamic Effects in Composite Bearings", *Journal of Lubrication Technology, Trans. ASME, Series F, Vol. 89, No. 3, July 1967, pp. 323-328.*
10. Maki, E.R., Kuzma, D.C., and Donnelly, R.J., "The Magnetohydrodynamic Thrust Bearing", *Journal of Fluid Mech. 1967, Vol. 30, Part 1, pp. 83-95.*
11. Kreiger, R.J., Day, H.J. and Hughes, W.F., "The MHD Hydrostatic Thrust Bearing-Theory and Experiments", *Journal of Lubrication Technology, Trans. ASME, Series F, Vol. 89, No. 3, July 1967, pp. 307-313.*
12. Dudzinsky, S.J., Young, F.J. and Hughes, W.F., "On the Load Capacity of the MHD Journal Bearing", *Journal of Lubrication Technology, Trans. ASME, Series F, Vol. 90, No. 1, Jan. 1968, pp. 139-143.*
13. Snyder, W.T., "The Nonlinear Hydrodynamic Slider Bearing", *Journal of Basic Engineering, Trans. ASME Series D, Vol. 85, No. 3, Sept. 1963, pp. 429-434.*
14. Rodkiewicz, C.M. and Anwar, M.I., "Inertia and Convective Effects in Hydrodynamic Lubrication for a Slider Bearing", *Trans. ASME Series F, Vol. 93, No. 2, Apr. 1971, pp. 313-315.*

15. Raimondi, A.A. and Boyd, J., "A Solution for the Finite Journal Bearing and its Application to Analysis and Design: III", Trans. ASLE, Vol. 1, No. 2, 1958, pp. 194-203.
16. Hays, D.F., "Plane Slider of Finite Width", Trans. ASLE, Vol. 1, No. 2, 1958, pp. 233-
17. Young, D., "The Numerical Solution of Elliptic and Parabolic Partial Differential Equation", Survey of Numerical Analysis, TODD, J., ed., McGraw-Hill, New York, 1962.
18. Varga, R.S., "Matrix Iterative Analysis", Prentice-Hall,
19. Lapidus, L., "Digital Computation for Chemical Engineers" McGraw-Hill, 1962.
20. Hughes, W.F. and Young, F.J., "The Electromagnetodynamics of Fluids", John Wiley and Sons Inc., 1966.
21. Sutton, G.W., and Sherman, A., "Engineering Magnetohydrodynamics", McGraw-Hill, 1965.
22. Pinkus, O. and Sternlicht, B., "Theory of Hydrodynamic Lubrication", McGraw-Hill, 1961.

APPENDIX A
MAGNETIC FIELD DISTRIBUTION

The expression for the magnetic field, equation (3.14), may be written

$$\bar{B}_y = \frac{C_0}{\delta} + C_1 + C_2\delta + C_3\delta^2 + \dots \quad (\text{A.1})$$

For Case A

$$C_1 = 1, C_0 = C_2 = C_3 \dots = 0 \quad (\text{A.2})$$

For Case B

$$C_1 = 1 + 2S', C_2 = -2S' \quad (\text{A.3})$$

$$C_0 = C_3 = C_4 \dots = 0$$

where

$$S' = \frac{d\bar{B}_y}{dx}$$

and for Case C

$$C_1 = C_2 = C_3 \dots = 0$$

and

$$\bar{B}_y = C_0 \delta^{-1} \quad (\text{A.4})$$

When $C_0 = 1$

$$\bar{B}_y = \delta^{-1} = \left(1 - \frac{\bar{x}}{2}\right)^{-1} \quad (\text{A.5})$$

APPENDIX B
ELECTRIC POTENTIAL EQUATION IN
FINITE-DIFFERENCE FORM

The potential equation (5.25) may be written for convenience as

$$\frac{\partial^2 \bar{\phi}}{\partial x^2} + \left(\frac{L}{D}\right)^2 \frac{\partial^2 \bar{\phi}}{\partial z^2} = 0 \quad (5.25)$$

Considering the five-point molecule shown in Fig. 5.2, the following may be written [19]

$$\frac{\partial^2 \bar{\phi}}{\partial x^2} = \frac{\bar{\phi}_{i+1,j} - 2\bar{\phi}_{i,j} + \bar{\phi}_{i-1,j}}{\Delta x^2} + 0 \quad (\Delta x^2) \quad (B.1)$$

$$\frac{\partial^2 \bar{\phi}}{\partial z^2} = \frac{\bar{\phi}_{i,j+1} - 2\bar{\phi}_{i,j} + \bar{\phi}_{i,j-1}}{\Delta z^2} + 0 \quad (\Delta z^2) \quad (B.2)$$

Substituting (B.1) and (B.2) into equation (5.25), the following is obtained

$$\begin{aligned} \bar{\phi}_{i,j} = & \frac{1}{2} \left(\frac{D^2 \Delta z^2}{D^2 \Delta z^2 + L^2 \Delta x^2} \right) (\bar{\phi}_{i+1,j} + \bar{\phi}_{i-1,j}) \\ & + \frac{1}{2} \left(\frac{L^2 \Delta x^2}{D^2 \Delta z^2 + L^2 \Delta x^2} \right) (\bar{\phi}_{i,j+1} + \bar{\phi}_{i,j-1}) \end{aligned} \quad (B.3)$$

When $\Delta\bar{x} = \Delta\bar{z} = \Delta h$, the above equation becomes

$$\bar{\phi}_{i,j} = a_1 \bar{\phi}_{i+1,j} + a_2 \bar{\phi}_{i-1,j} + a_3 \bar{\phi}_{i,j+1} + a_4 \bar{\phi}_{i,j-1} \quad (\text{B.4})$$

where

$$a_1 = a_2 = \frac{1}{2} \left(\frac{1}{1+L^2/D^2} \right)$$

$$a_3 = a_4 = \frac{1}{2} \left(\frac{1}{D^2/L^2+1} \right)$$

APPENDIX C

PRESSURE EQUATION IN FINITE-DIFFERENCE FORM

Rewriting the pressure equation (5.27) from Chapter V as

$$\frac{\partial^2 \bar{p}}{\partial \bar{x}^2} + \left(\frac{L}{D}\right)^2 \frac{\partial^2 \bar{p}}{\partial \bar{z}^2} - M \left(\frac{L}{D}\right) \frac{\partial \bar{J}_z}{\partial \bar{x}} - \frac{\partial \bar{J}_x}{\partial \bar{z}} = 0 \quad (5.27)$$

Using the five-point molecule shown in Fig. 5.2, we may write [19]

$$\frac{\partial^2 \bar{p}}{\partial \bar{x}^2} = \frac{\bar{p}_{i+1,j} - 2\bar{p}_{i,j} + \bar{p}_{i-1,j}}{\Delta \bar{x}^2} + O(\Delta \bar{x}^2) \quad (C.1)$$

$$\frac{\partial^2 \bar{p}}{\partial \bar{z}^2} = \frac{\bar{p}_{i,j+1} - 2\bar{p}_{i,j} + \bar{p}_{i,j-1}}{\Delta \bar{z}^2} + O(\Delta \bar{x}^2) \quad (C.2)$$

Substituting (C.1) and (C.2) into equation (5.27) yields

$$\begin{aligned} \bar{p}_{i,j} = & \frac{1}{2} \left(\frac{D^2 \Delta \bar{z}^2}{D^2 \Delta \bar{z}^2 + L^2 \Delta \bar{x}^2} \right) \bar{p}_{i+1,j} + \frac{1}{2} \left(\frac{D^2 \Delta \bar{z}^2}{D^2 \Delta \bar{z}^2 + L^2 \Delta \bar{x}^2} \right) \bar{p}_{i-1,j} \\ & + \frac{1}{2} \left(\frac{L^2 \Delta \bar{x}^2}{D^2 \Delta \bar{z}^2 + L^2 \Delta \bar{x}^2} \right) \bar{p}_{i,j-1} + \frac{1}{2} \left(\frac{L^2 \Delta \bar{x}^2}{D^2 \Delta \bar{z}^2 + L^2 \Delta \bar{x}^2} \right) \bar{p}_{i,j+1} \\ & - \frac{1}{2} \left(\frac{D^2 \Delta \bar{x}^2 \Delta \bar{z}^2}{D^2 \Delta \bar{z}^2 + L^2 \Delta \bar{x}^2} \right) \bar{E}_{i,j} \end{aligned} \quad (C.3)$$

For $\Delta\bar{x} = \Delta\bar{z} = \Delta h$, the above equation may be written as

$$\bar{p}_{i,j} = b_1 \bar{p}_{i+1,j} + b_2 \bar{p}_{i-1,j} + b_3 \bar{p}_{i,j+1} + b_4 \bar{p}_{i,j-1} + b_5 E_{i,j} \quad (C.4)$$

where

$$b_1 = b_2 = \frac{1}{2} \left(\frac{1}{1+L^2/D^2} \right)$$

$$b_3 = b_4 = \frac{1}{2} \left(\frac{1}{D^2/L^2+1} \right)$$

$$b_5 = \frac{1}{2} \left(\frac{1}{1+L^2/D^2} \right)$$

and

$$E_{i,j} = -M \left(\frac{1}{D} \frac{\partial \bar{J}_x}{\partial \bar{z}} - \frac{\partial \bar{J}_z}{\partial \bar{x}} \right)$$

APPENDIX D

FINITE-DIFFERENCE FORMULAS TO OBTAIN ELECTRIC FIELD
AND CURRENT DENSITY DISTRIBUTION IN THE BEARING

Using the 5-point molecule shown in Fig. D.1 the following finite-difference formulas may be written:

$$\bar{E}_x(1,j) = \bar{J}_x(1,j) = - (-6\bar{\phi}_{5,j} + 32\bar{\phi}_{4,j} - 72\bar{\phi}_{3,j} - 96\bar{\phi}_{2,j} - 50\bar{\phi}_{1,j}) / (24\Delta x) \quad (D.1)$$

$$\bar{E}_x(2,j) = \bar{J}_x(2,j) = - (\bar{\phi}_{5,j} - 6\bar{\phi}_{4,j} + 18\bar{\phi}_{3,j} - 18\bar{\phi}_{2,j} - 3\bar{\phi}_{1,j}) / (12\Delta x) \quad (D.2)$$

$$\bar{E}_x(i,j) = \bar{J}_x(i,j) = - (-\bar{\phi}_{i+2,j} + 8\bar{\phi}_{i+1,j} - 8\bar{\phi}_{i-1,j} + \bar{\phi}_{i-2,j}) / (12\Delta x) \quad (D.3)$$

$$\begin{aligned} \bar{E}_x(M-1,j) = \bar{J}_x(M-1,j) = & (-3\bar{\phi}_{M,j} - 10\bar{\phi}_{M-1,j} + 18\bar{\phi}_{M-2,j} \\ & - 6\bar{\phi}_{M-3,j} + \bar{\phi}_{M-4,j}) / (12\Delta x) \end{aligned} \quad (D.4)$$

$$\begin{aligned} \bar{E}_x(M,j) = \bar{J}_x(M,j) = & (50\bar{\phi}_{M,j} - 96\bar{\phi}_{M-1,j} + 72\bar{\phi}_{M-2,j} \\ & - 32\bar{\phi}_{M-3,j} + 6\bar{\phi}_{M-4,j}) / (-24\Delta x) \end{aligned} \quad (D.5)$$

$$\begin{aligned} \bar{E}_z(i,1) = \bar{J}_z(i-1) = & - (-6\bar{\phi}_{i,5} + 32\bar{\phi}_{i,4} - 72\bar{\phi}_{i,3} \\ & - 96\bar{\phi}_{i,2} - 50\bar{\phi}_{i-1}) / (24\Delta z) \end{aligned} \quad (D.6)$$

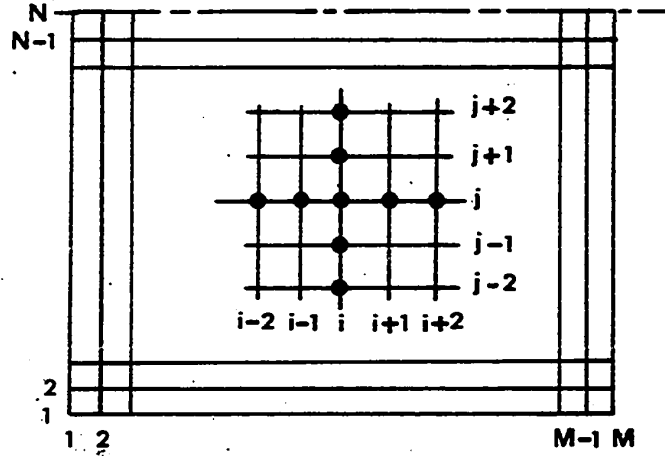


FIG. D.1 5-POINT MOLECULE

$$\bar{E}_Z(i,2) = \bar{J}_Z(i,2) = -(\bar{\phi}_{i,5} - 6\bar{\phi}_{i,4} + 18\bar{\phi}_{i,3} - 10\bar{\phi}_{i,2} - 3\bar{\phi}_{i,1}) / (12\Delta Z) \quad (D.7)$$

$$\bar{E}_Z(i,j) = \bar{J}_Z(i,j) = -(-\bar{\phi}_{i,j+2} + 8\bar{\phi}_{i,j+1} - 8\bar{\phi}_{i,j-1} + \bar{\phi}_{i,j-2}) / (12\Delta Z) \quad (D.8)$$

$$\begin{aligned} \bar{E}_Z(i,N-1) = \bar{J}_Z(i,N-1) = & (-3\bar{\phi}_{i,N} - 10\bar{\phi}_{i,N-1} \\ & + 18\bar{\phi}_{i,N-2} - 6\bar{\phi}_{i,N-3} + \bar{\phi}_{i,N-4}) / (12\Delta Z) \end{aligned} \quad (D.9)$$

$$\begin{aligned} \bar{E}_Z(i,N) = \bar{J}_Z(i,N) = & (50\bar{\phi}_{i,N} - 96\bar{\phi}_{i,N-1} + 72\bar{\phi}_{i,N-2} \\ & - 32\bar{\phi}_{i,N-3} + \bar{\phi}_{i,N-4}) / (-24\Delta Z) \end{aligned} \quad (D.10)$$

Knowing \bar{J}_x and \bar{J}_z distribution in the bearing, $(\partial\bar{J}_x/\partial z)$ and $(\partial\bar{J}_z/\partial x)$ may be approximated at each of the grid point by using the same five-point molecule. The formulas may be easily written from the above expressions by replacing ϕ 's with appropriate values of current densities.

APPENDIX E
 CONVERGENCE PARAMETER, MESH SIZE AND
 ERROR INVOLVED IN COMPUTATIONS

E.1 Relaxation Factor For Point Successive-Overrelaxation Method

For point successive overrelaxation method, the optimum values of relaxation factor ω , are discussed in [17,18]. The important relation for linear elliptic type partial differential equations given in [17] are

$$\omega_{\text{optimum}} = 1 + \left[\frac{\lambda}{1+(1-\lambda^2)^{1/2}} \right]^2 \quad (\text{E.1})$$

where $\lambda = \frac{1}{2} \left(\cos \frac{\pi h}{a} + \cos \frac{\pi h}{b} \right)$,

$a/2 = Mh$, $b = Nh$ and $h =$ mesh size. M and N are the number of divisions in x -direction and in z -direction respectively.

In solving the potential equation (5.25) and the pressure equation (5.27), the optimum ω for the grid size employed in computations, was calculated from the above relation.

E.2 Error and Mesh Size

The error is inherent in the numerical solution. The errors due to finite difference approximations of equations (5.25) and (5.27) are of $O(\Delta^2 h)$. These errors can be reduced by increasing the number

of divisions. However, the computing time increases considerably as the mesh size used is further reduced. In the present work, the following mesh size was employed which was in consistence with the tolerance specified in equations (5.36) and (5.38).

For potential equation the mesh size for Region I and II was .0125 and 0.025 respectively, while for pressure equation it was .025.

Since the computations were carried out using the double precision numbers, the round off errors should be insignificant.

APPENDIX F
NUMERICAL EXAMPLE FOR EXTERNALLY
SUPPLIED ELECTRIC POWER

The results of nonuniformly applied electric field are presented for parallel plate slider bearing in Chapter V. To help visualize the load that can be obtained and the electrical power required to maintain this load, a numerical example will be considered. Typical numerical values of the parameter used are (RMKS units):

$$h = 10^{-4} \text{ m}$$

$$L = 0.1 \text{ m}$$

$$D = 0.1 \text{ m}$$

$$U = 10 \text{ m/sec}$$

Using mercury as the lubricant, the following properties of mercury are taken from reference [20].

$$\mu = 1.55 \times 10^{-3} \text{ Newton sec/m}^2$$

$$\sigma = 1.07 \times 10^6 \text{ mho/m}$$

For $S = 0.1$, $M = 0.5$, and $\bar{I} = 2.5$, the bearing load capacity \bar{W} as obtained from Fig. 5.7, is 0.215. From these dimensionless numbers, the important physical quantities are calculated. These are:

$$B_y = 0.19 \text{ Weber/m}^2$$

$$I = 100 \text{ amp}$$

$$W = 334 \text{ Newton}$$

$$(\approx 75 \text{ lbs.})$$

APPENDIX G
COMPUTER PROGRAMS

* IN THE SIXTH COLUMN INDICATES
CONTINUATION FROM PREVIOUS LINE

```

C**** FORTRAN PROGRAM FOR CHAPTER 3
C**** THIS PROGRAM CALCULATES PRESSURE DISTRIBUTION IN
C      MHD BEARING
C**** IN THE ANALYSIS THE INERTIA TERMS ARE RETAINED.THE
C      SOLUTION IS OBTAINED BY SOLVING A SERIES OF 3RD ORDER
C      DIFF. EQUATIONS.IN THIS PROGRAM ONLY SEVEN EQUATIONS
C      ARE SOLVED
C**** SUBROUTINES FROM IBM-SYSTEM/360 SCIENTIFIC SUBROUTINE
C      PACKAGE ARE USED IN THIS PROGRAM
      DOUBLE PRECISION F0(55),F01(55),F02(55),F03(55),F1(55)
      * ,F11(55),
      1F12(55),F13(55),RE,HART,C0,C1,C2,C3,ALPHA(5),B0(5) ,G
      * AMA(5),CB,
      2PRMT(5),Y(3),DERY(3),AUX(8,4),A(55),B(55),C(55),D(55),
      * E(55),
      3 ZZ(55),R(55),CC(55),AF1(5),CF(5),Z(55),B1(5),BB,B2(5)
      * ,F2(55),
      4F21(55),F22(55),F23(55),Z1(55),Z11(55),Z12(55),Z13(55)
      * ,B3(5),
      5F3(55),F31(55),F32(55),F33(55),DEL(21),PGRAD(21),S,ZP(
      * 21) ,B4(5),
      6B5(5),F4(55),F41(55),F42(55),F43(55), F5(55),F51(55),F
      * 52(55),
      7F53(55),CUR ,EE(21) ,B6(5),B7(5),B8(5),F6(55),F61(55),
      * F62(55),
      8F63(55)
      EXTERNAL FCT,OUTP
      COMMON F0,F01,F02,F03,RE,HART,CB,C0,IC
      COMMON /FIRST/IL
C**** CALCULATION FOR 3RD ORDER DIFF. EQNS.
C
C**** SOLUTION FOR EQ. NO. 1 IS OBTAINED USING FOURTH ORDER
C      RUNGE KUTTA METHOD
C ** CALCULATION FOR EQ. NO.1
C**** FILM THICKNESS RATIO = 2.0

```



```

DO 23 MM=1,2
  READ(5,25) ALPHA(MM),B0(MM), GAMA(MM)
25  FORMAT(3F15.9)
  RE=1.0
C**** THE APPLIED MAGNETIC FIELD IS SPECIFIED BY THE VALUES
C      OF C0,C1,C2,C3,..
C      WHEN C0=1.0 AND C1=C2=C3=0.0 ,THE APPLIED MAGNETIC
C      FIELD IS PROPORTIONAL TO (1-X/2)**-1
  C0=1.0
  C1=0.0
  C2=0.0
  C3=0.0
  CB=B0(MM)
  BETA=ALPHA(MM)
  HART= GAMA(MM)
  WRITE(6,27) CB,BETA,HART
27  FORMAT('0',5X, 'CB=',F15.9, 'BETA=',F15.9, 'HART=',F1
* 0.6)
  PRMT(1)=0.0D0
  PRMT(2)=1.0
  PRMT(3)=.025
  PRMT(4)=0.0001
  Y(1)=0.0D0
  Y(2)=0.0D0
  Y(3)= BETA
  DERY(1)=.25D0
  DERY(2)=.25D0
  DERY(3)=0.5D0
  NDIM=3
  IC=0
  CALL DRKGS(PRMT,Y,DERY,NDIM,IHLF,FCT,OUTP,AUX)
C**** EQUATIONS NO. 2 THROUGH 7 ARE PUT IN FINITE DIFF.FORM
C      AND THE RESULTING RECURRENCE RELATION IS THEN SOLVED
C**** CALCULATION FOR EQ. NO. 2
  II=41
  III=II-1
  H=0.025
  READ(5,31) B1(MM)
31  FORMAT(F10.6)
  BB=B1(MM)
  KK=0
  IL=1
45  WRITE(6,32) BB
32  FORMAT('0',5X, 'B1=', F10.6)
  KK=KK+1
  WRITE(6,33)
33  FORMAT('0',9X, 'A',20X,'B', 15X,'C',15X,'D',15X,'E')
DO 34 N=3,III

```

```

A(N)= (1.+0.5*(H**2)*(RE*F01(N)-(HART**2)*(C0**2)))
B(N)= ((H**3)*F02(N)*RE-3.)
C(N)= (3.-0.5*(H**2)*(RE*F01(N)-(HART**2)*(C0**2)))
D(N)=-1.0
E(N)= (H**3)*BB
34 CONTINUE
CALL SOLU(A,B,C,D,E,ZZ)
DO 47 N=2,II
F1(N)=ZZ(N)
47 CONTINUE
F1(1)=0.0
AF1(KK)=F1(II)
CF(KK)= BB
IF(DABS(F1(II)).LT. 1.E-6) GO TO 43
IF(KK.EQ.1) GO TO 44
IF(KK.EQ.3) GO TO 23
DXX= AF1(2)-AF1(1)
DYY=CF(2)-CF(1)
BB=CF(1)-AF1(1)*DYY/DXX
GO TO 45
44 BB=BB+.055
GO TO 45
43 WRITE(6,53 )
53 FORMAT('0'.9X,'F1',15X,'F11',15X,'F12', 10X,'F13')
B1(MM)=BB
NDM=41
CALL DDETS (H,F1 ,Z,NDM,IER)
DO 48 N=1,II
48 F11(N)=Z(N)
CALL DDETS (H,F11,Z,NDM,IER)
DO 49 N=1,II
49 F12(N)= Z(N)
CALL DDETS (H,F12,Z,NDM,IER)
DO 50 N=1,II
50 F13(N)=Z(N)
DO 46 N=1,II
WRITE(6,54)F1(N),F11(N),F12(N),F13(N)
54 FORMAT('0'.5X,4F15.6)
46 CONTINUE
C*** CALCULATION FOR EO. NO. 3
IL=IL+1
READ(5,31) B2(MM)
BB=B2(MM)
KK=0
75 WRITE(6,62) BB
62 FORMAT('0'.5X, 'B2=', F10.6)
KK=KK+1
WRITE(6,33)

```

```

DO 64 N=3,III
A(N)=(1.-.5*(H**2)*(HART**2)*(C0**2))
B(N)=(H**3)*2*RE*F02(N)-3.0
C(N)=(3.+0.5*(H**2)*(HART**2)*(C0**2))
D(N)=-1.0
E(N)=(H**3)*(88-RE*F1(N)*F12(N))
64 CONTINUE
CALL SQLU(A,B,C,D,E,ZZ)
DO 67 N=2,II
F2(N)= ZZ(N)
67 CONTINUE
F2(1)=0.0
AF1(KK)= F2(II)
CF(KK)= BB
IF(DABS(F2(II)).LT. 1.E-6) GO TO 72
IF(KK.EQ.1) GO TO 74
IF(KK.EQ.3) GO TO 23
DXX= AF1(2)-AF1(1)
DYY=CF(2)-CF(1)
BB=CF(1)-AF1(1)*DYY/DXX
GO TO 75
74 BB=BB+.005
GO TO 75
72 WRITE(6,73)
73 FORMAT('0',9X,'F2',15X,'F21',15X,'F22', 10X,'F23')
B2(MM)=BB
CALL DDETS (H,F2 ,Z,NDM,IER)
DO 78 N=1,II
78 F21(N)=Z(N)
CALL DDETS (H,F21,Z,NDM,IER)
DO 79 N=1,II
79 F22(N)=Z(N)
CALL DDETS (H,F22,Z,NDM,IER)
DO 80 N=1,II
80 F23(N)=Z(N)
DO 76 N=1,II
WRITE(6,54)F2(N),F21(N),F22(N),F23(N)
76 CONTINUE
C*** CALCULATION FOR EQ. NO. 4
READ(5,31) B3(MM)
BB=B3(MM)
KK=0
95 WRITE(6,82) BB
82 FORMAT('0',5X, 'B3=', F10.6)
KK=KK+1
WRITE(6,33)
DO 84 N=3,III
A(N)=(1.-0.5*(H**2)*(RE*F01(N)+(HART**2)*(C0**2)))

```

```

      B(N)= ((H**3)*3*RE*F02(N)-3.)
      C(N)= (3.+0.5*(H**2)*(RE*F01(N)+(HART**2)*(C0**2)))
      D(N)=-1.0
      E(N)=(H**3)*(BB-RE*(F1(N)*F22(N)+2*F2(N)*F12(N)-F11(N)
      * *F21(N)))
84  CONTINUE
      CALL SOLU(A,B,C,D,E,ZZ)
      DO 87 N=2,II
      F3(N)=ZZ(N)
87  CONTINUE
      F3(1)=0.0
      AF1(KK)= F3(II)
      CF(KK)= BB
      IF(DABS(F3(II)).LT. 1.E-6) GO TO 92
      IF(KK.EQ.1) GO TO 94
      IF(KK.EQ.3) GO TO 23
      DXX= AF1(2)-AF1(1)
      DYY=CF(2)-CF(1)
      BB=CF(1)-AF1(1)*DYY/DXX
      GO TO 95
94  BB=BB+.005
      GO TO 95
92  WRITE(6,93)
93  FORMAT('0',9X,'F3',15X,'F31',15X,'F32', 10X,'F33')
      B3(MM)=BB
      CALL DDETS (H,F3 ,Z,NDM,IER)
      DO 98 N=1,II
98  F31(N)= Z(N)
      CALL DDETS (H,F31,Z,NDM,IER)
      DO 99 N=1,II
99  F32(N)=Z(N)
      CALL DDETS (H,F32,Z,NDM,IER)
      DO 100 N=1,II
100 F33(N)=Z(N)
      DO 96 N=1,II
      WRITE(6,54)F3(N),F31(N),F32(N),F33(N)
96  CONTINUE
C*** CALCULATION FOR EQ. NO. 5
      READ(5,31) B4(MM)
      BB=B4(MM)
      KK=0
115 WRITE(6,102) BB
102 FORMAT('0',5X,'B4=',F10.6)
      KK=KK+1
      WRITE(6,33)
      DO 104 N=3,II
      A(N)= (1.-0.5*(H**2)*(2*RE*F01(N)+(HART**2)*(C0**2)))
      B(N)= (4*(H**3)*RE*F02(N)-3.0)

```

```

C(N)= (3.+0.5*(H**2)*(2*RE*F01(N)+(HART**2)*(C0**2)))
D(N)= -1.0
E(N)= (H**2)*(BB-RE*(F1(N)*F32(N)+2*F2(N)*F22(N)+3*F3(
* N)*F12(N)-2
1*F11(N)*F31(N)-F21(N)*F21(N)))
104 CONTINUE
CALL SOLU(A,B,C,D,E,ZZ)
DO 107 N=2,II
107 F4(N)= ZZ(N)
F4(1)=0.0
AF1(KK)= F4(II)
CF(KK)=BB
IF(DABS(F4(II)).LT. 1.E-6) GO TO 112
IF(KK.EQ.1) GO TO 114
IF(KK.EQ.3) GO TO 23
DXX= AF1(2)-AF1(1)
DYY=CF(2)-CF(1)
BB=CF(1)-AF1(1)*DYY/DXX
GO TO 115
114 BB=BB+.005
GO TO 115
112 WRITE(6,116)
116 FORMAT('0',9X,'F4',15X,'F41',15X,'F42', 10X,'F43')
B4(MM)= BB
CALL DDETS (H,F4 ,Z,NDM,IER)
DO 117 N=1,II
117 F41(N)= Z(N)
CALL DDETS (H,F41,Z,NDM,IER)
DO 118 N=1,II
118 F42(N)= Z(N)
CALL DDETS (H,F42,Z,NDM,IER)
DO 119 N=1,II
119 F43(N)= Z(N)
DO 120 N=1,II
120 WRITE(6,54) F4(N),F41(N),F42(N),F43(N)
C*** CALCULATION FOR EQ. NO. 6
READ(5,31) B5(MM)
BB=B5(MM)
KK=0
135 WRITE(6,122) BB
122 FORMAT('0',5X, 'B5=',F10.6)
KK=KK+1
WRITE(6,33)
DO 124 N=3,II
A(N)=(1-0.5*(H**2)*(3*RE*F01(N)+(HART**2)*(C0**2)))
B(N)=((H**3)*5*RE*F02(N)-3.)
C(N)=(3.+0.5*(H**2)*(3*RE*F01(N)+(HART**2)*(C0**2)))
D(N)=-1.0

```

```

      E(N)= (H**3)*(BB- RE*(F1(N)*F42(N)+2*F2(N)*F32(N)+3*F3
* (N)*F22(N)+
      1 4*F4(N)*F12(N)-3*F11(N)*F41(N)-3*F21(N)*F31(N))
124 CONTINUE
      CALL SOLU(A,B,C,D,E,ZZ)
      DO 127 N=2,II
127  FS(N)= ZZ(N)
      F5(1)=0.0
      AF1(KK)= F5(II)
      CF(KK)=BB
      IF(DABS(F5(II)). LT. 1.E-6) GO TO 132
      IF(KK.EQ.1) GO TO 134
      IF(KK.EQ.3) GO TO 23
      DXX= AF1(2)-AF1(1)
      DYY=CF(2)-CF(1)
      BB=CF(1)-AF1(1)*DYY/DXX
      GO TO 135
134  BB=BB+.005
      GO TO 135
132  WRITE(6,136)
136  FORMAT('0',9X,'F5',15X,'F51',15X,'F52', 10X,'F53')
      B5(MM)=BB
      CALL DDETS (H,F5 ,Z,NDM,IER)
      DO 137 N=1,II
137  F51(N)=Z(N)
      CALL DDETS (H,F51,Z,NDM,IER)
      DO 138 N=1,II
138  F52(N)= Z(N)
      CALL DDETS (H,F52,Z,NDM,IER)
      DO 139 N=1,II
139  F53(N)= Z(N)
      DO 140 N=1,II
140  WRITE(6,54) F5(N),F51(N),F52(N),F53(N)
C***  CALCULATION FOR EGN. NO. 7
      READ(5,31) B6(MM)
      BB=B6(MM)
      KK=0
201  WRITE(6,202) BB
202  FORMAT('0',5X, 'B6=',F10.6)
      KK=KK+1
      WRITE(6,33)
      DO 204 N=3,II
      A(N)=(1.-0.5*(H**2))*(4*RE*F01(N)+(HART**2)*(C0**2))
      B(N)= (6 *(H**3)*RE*F02(N)-3.0)
      C(N)= (3+0.5*(H**2))*(4*RE*F01(N)+(HART**2)*(C0**2))
      D(N)=-1.
      E(N)= (H**3)*(BB-RE*(F1(N)*F52(N)+2*F2(N)*F42(N)+3*F3(
* N)*F32(N)

```

```

1+4*F4(N)*F22(N)+5*F5(N)*F12(N)-4*F11(N)*F51(N)-4*F21(N
* )*F41(N)-2*
2F31(N)*F31(N))
204 CONTINUE
CALL SOLU(A,B,C,D,E,ZZ)
DO 207 N=2,II
207 F6(N)=ZZ(N)
F6(1)=0.0
AF1(KK)=F6(II)
CF(KK)=BB
IF(DABS(F6(II))).LT. 1.E-6) GO TO 215
IF(KK.EQ.1) GO TO 214
IF(KK.EQ.3) GO TO 23
DXX= AF1(2)-AF1(1)
DYY=CF(2)-CF(1)
BB=CF(1)-AF1(1)*DYY/DXX
GO TO 201
214 BB=BB+.005
GO TO 201
215 WRITE(6,216)
216 FORMAT('0',9X,'F6',15X,'F61',15X,'F62', 10X,'F63')
B6(MM)=BB
CALL DDETS (H,F6 ,Z,NDM,IER)
DO 218 N=1,II
218 F61(N)=Z(N)
CALL DDETS (H,F61,Z,NDM,IER)
DO 219 N=1,II
219 F62(N)=Z(N)
CALL DDETS (H,F62,Z,NDM,IER)
DO 220 N=1,II
220 F63(N)=Z(N)
DO 222 N=1,II
222 WRITE(6,54) F6(N),F61(N),F62(N),F63(N)

C**** CALCULATION FOR PRESSURE DISTRIBUTION
WRITE(6,97) B0(MM),B1(MM),B2(MM),B3(MM) ,B4(MM),B5(MM)
* ,B6(MM)
97 FORMAT('0',5X,'B0=',F10.6/ 'B1=',F10.6/ 'B2=',F10.6/ '
* B3=',F10.6/
15X, 'B4=',F10.6/ 'B5=',F10.6/'B6=',F10.6)
CUR=0.0
DO 800 J=1,21
DEL(J)= (1.0-0.025*(J-1))
EE(J)= {4./3.}*HART*(C0/(DEL(J))+C1+C2*(DEL(J))+C3*((D
* EL(J))**2))
1*(CUR+2*HART*(C0/(DEL(J))+C1+C2*(DEL(J))+C3*((DEL(J))*
* **2))*
2 F0(41)*(C0*1.3863))

```

```

      PGRAD(J)=(-2./(RE*(DEL(J)**3))* (B0(MM)+B1(MM)*DEL(J)
*   +B2(MM)*
1((DEL(J)**2)+B3(MM)*((DEL(J)**3) +B4(MM)*((DEL(J)**
*   4)+ B5(MM)*
2((DEL(J)**5) +B6(MM)*((DEL(J)**6))-(EE(J)/RE)
800 CONTINUE
      S=0.05
      ND=21
      CALL DQSF(S,PGRAD,Z,ND)
      WRITE(6,810)
810  FORMAT('0',12X, 'DEL',20X,'PGRAD',20X,'PRESS')
      DO 840 J=1,21
      WRITE(6,820) DEL(J),PGRAD(J),Z(J)
820  FORMAT('0',5X,F10.6,15X,F10.6,15X,F10.6)
840  CONTINUE
      CALL DQSF(S,Z,ZP,ND)
      WRITE(6,830) ZP(21)
830  FORMAT('0',5X, 'LOAD=',F10.6)
23  CONTINUE
      STOP
      END

```

```

SUBROUTINE FCT (X,Y,DERY)
DOUBLE PRECISION X,Y(3),DERY(3),CB,F0(55),F01(55),F02
* (55),
1 F03(55),RE,HART,CB,C0
COMMON F0,F01,F02,F03,RE,HART,CB,C0,IC
DERY(1)=Y(2)
DERY(2)=Y(3)
DERY(3)= CB-Y(2)*Y(2)*RE+(HART**2)*(C0**2)*Y(2)
RETURN
END

```

```

SUBROUTINE OUTP(X,Y,DERY,IHLF,NDIM,PRMT)
DOUBLE PRECISION X,Y(4),DERY(3), PRMT(5),RE,HART,CB,C0
DOUBLE PRECISION ETAINT(55),F0(55),F01(55),F02(55),F0
* 3(55)
COMMON F0,F01,F02,F03,RE,HART,CB,C0,IC
IC=IC+1
ETAINT (IC) =X
F0(IC)=Y(1)
F01(IC)=Y(2)
F02(IC)=Y(3)
F03(IC)= DERY(3)

```



```

WRITE(6,23) IC,ETAINT(IC),F0(IC),F01(IC),F02(IC),F03(I
* C)
23 FORMAT('0',5X,I2,2X,5F15.6)
RETURN
END

```

```

SUBROUTINE SOLU(A,B,C,D,E,ZZ)
DOUBLE PRECISION A(55),B(55),C(55),D(55),E(55),ZZ(55)
* ,BOT(55)
1TOP(55),R(55),CC(55),ANUME,ADEN
COMMON /FIRST/IL
II=41
III=II-1
IUPPER=II-2
R(1)=0.
R(2)=0.25
CC(1)=0.
IF(IL.EQ.1) GO TO 20
CC(2)=0.0
GO TO 30
20 CC(2)= -0.025/4.
30 DO 300 N=3,III
BOT(N)= B(N)+C(N)*R(N-1)+D(N)*R(N-1)*R(N-2)
R(N)=-A(N)/BOT(N)
TOP(N)= -(C(N)*CC(N-1)+D(N)*R(N-2)*CC(N-1)+D(N)*CC(N-2
* ))+E(N)
CC(N)= TOP(N)/BOT(N)
300 CONTINUE
WRITE(6,36)
36 FORMAT('0',12X,'RN',15X,'CCN')
ANUME=CC(II-1)-CC(II-2)/(4.-R(II-2))
ADEN=3./{4.-R(II-2)}-R(II-1)
ZZ(II)=ANUME/ADEN
DO 39 N=1,IUPPER
I=II-N
ZZ(I)=R(I)*ZZ(I+1)+CC(I)
39 CONTINUE
RETURN
END

```

* IN THE SIXTH COLUMN INDICATES
CONTINUATION FROM PREVIOUS LINE

```

C**** FORTRAN PROGRAM FOR CHAPTER 4
C**** THE PROGRAM CALCULATES PRESSURE DISTRIBUTION,LOAD
C CAPACITY,VELOCITY DISTRIBUTION,FRICITION FACTOR FOR
C MHD SLIDER BEARING
C**** SUBROUTINES FROM IBM-SYSTEM/360 SCIENTIFIC SUBROUTINE
C PACKAGE ARE USED IN THIS PROGRAM
C**** THE APPLIED MAGNETIC FIELD MAY BE UNIFORM OR
C LINEARLY INCREASING TYPE
DOUBLE PRECISION HART(5),FLOW(5),FLO(5),SYB(21),HBAR(
* 21),
1PGRAD(21),PRES(2),Z(21),ZP(21),DELX,DELY,DFLOW,A(21),B
* ,C,D,P,
2ALPHA(21),BY ,RAT(7),DT(7) ,BB,DD(5) ,PL(21),DY,C1(21,
* C2(21),
3 C3(21),U(21,21),DUY(21,21),SY(21,21),DT0(21),ZI(21)
C**** FOR UNIFORM MAGNETIC FIELD LLL.GT.1
C**** FOR LINEARLY INCREASING MAGNETIC FIELD LLL=1
LLL=2
C**** READ HARTMANN NUMBER, MASS FLOW AND FILM THICKNESS
C RATIO AT INLET OF BEARING
DO 10 L=1,3
READ(5,11) HART(L),FLO(L),DD(L)
11 FORMAT(3F10.6)
WRITE(6,12) HART(L)
12 FORMAT('0',5X, 'HARTMANN NUMBER=' ,F10.6)
FLOW(1)=FLO(L)
C**** MESH SIZE
C**** CALCULATE HBAR ALONG THE LENGTH OF BEARING
DELX=.05
DELY=.05
DFLOW=0.02
DO 31 IK=1,4
RAT(IK)=DD(L)+0.010*(IK-1)
DT(IK)= (RAT(IK)-1.0)/20.0
WRITE(6,32) RAT(IK),DT(IK)

```

```

32 FORMAT('0',5X, 'HBAR AT INLET=',F10.6,'0',5X, 'DT=',F1
* 0.6)
C**** CALCULATION ARE CARRIED OUT USING THE ASSUMED MASS
C**** FLOW,LATER REPEATED WITH THE IMPROVED MASS FLOW
KK=0
100 KK=KK+1
DO 33 II=1,2
WRITE(6,15) FLOW(II)
15 FORMAT('0',5X, 'MASS FLOW=',F10.6)
IF (LLL.EQ.1) GO TO 101
C**** CALCULATION IF THE APPLIED MAGNETIC FIELD IS UNIFORM
DO 20 I=1,21
HBAR(I)= (RAT(IK)-DT(IK))*(I-1)
ALPHA(I)=((HBAR(I))**2)*((HART(L))**2)
SYB(I)= FLOW(II)/HBAR(I)
P=(ALPHA(I))**0.5
PL(I)= (ALPHA(I))**0.5
B= (DEXP(-P)+DEXP(P)-2.0)
C= (-SYB(I)*P*( DEXP(-P)-DEXP(P)))/B -1.0)
D= 1.0-DEXP(-P)+(DEXP(-P)-DEXP(P))*((1.-DEXP(P)+P*DEXP(
* P))/((DEXP(P)
1*B)
A(I)=(C/D)*ALPHA(I)
C3(I)= (DEXP(P)/(( P*(DEXP(-P)-DEXP(P)))) *(1.+(A(I)/(P
* **2)))-(A(I)/
I((P**2)*DEXP(P)))
C2(I)= (1./(P*DEXP(P)))*(C3(I)*P*DEXP(-P)+(A(I)/(P**2)
* ))
C1(I)= -C2(I)-C3(I)
BB= (HSAR(1)+1.0)
PGRAD(I)=(2./BB)*HBAR(I)* ((HART(L))**2)*SYB(I) +A(I)
* / ((HBAR(I))
1**2)
20 CONTINUE
GO TO 102
C**** CALCULATION IF THE APPLIED MAGNETIC FIELD IS LINEARLY
C INCRASING
C**** FOR LINEARLY INCREASING CASE,THE MAGNETIC FIELD AT
C OUTLET IS TWICE THAT OF INLET
101 DO 30 I=1,21
BY=(1.+0.05*(I-1))
HBAR(I)= (RAT(IK)-DT(IK))*(I-1)
ALPHA(I)=((HBAR(I))**2)*((HART(L))**2)*(BY**2)
SYB(I)= FLOW(II)/HBAR(I)
P=(ALPHA(I))**0.5
B= (DEXP(-P)+DEXP(P)-2.0)
PL(I)= (ALPHA(I))**0.5
C= (-SYB(I)*P*( DEXP(-P)-DEXP(P)))/B -1.0)

```

```

      D= 1.0-DEXP(-P)+(DEXP(-P)-DEXP(P))*(1.-DEXP(P)+P*DEXP(
      * P))/(DEXP(P)
      1*B)
      A(I)=(C/D)*ALPHA(I)
      C3(I)= (DEXP(P)/(P*(DEXP(-P)-DEXP(P))))*(1.+(A(I)/(P
      * **2))-(A(I)/
      1((P**2)*DEXP(P))))
      C2(I)= (1./(P*DEXP(P)))*(C3(I)*P*DEXP(-P)+(A(I)/(P**2)
      * ))
      C1(I)= -C2(I)-C3(I)
      BB= (HBAR(I)+1.0)
      PGRAD(I)= (2./BB)*HBAR(I)*((HART(L))**2)*SYB(I)*BY*1.5
      * +A(I)/((HBAR
      1(I))**2)
30 CONTINUE
C**** CALCU FOR PRESSURE DISTRIBUTION AND LOAD CAPCITY
102 ND =21
      CALL DQSF(DE LX,PGRAD,Z,ND)
      PRES(II)=Z(21)
      WRITE(6,40)
40 FORMAT('0',10X,'PGRAD ',18X,'PRESS*')
      CALL DQSF (DE LX,Z,ZP,ND)
      WRITE(6,43) ZP(21)
43 FORMAT('0',5X,'LOAD=' ,F10.6)
      IF(DABS(Z(21)).LT..0005) GO TO 39
      FLOW(II+1)= FLOW(II)+DFLOW
33 CONTINUE
      IF (KK.EQ.4) GO TO 39
C**** BETTER APPROXIMATION ON FLOW
      DX=PRES(2)-PRES(1)
      DY=FLOW(2)-FLOW(1)
      YL=FLOW(1)-(PRES(1)*DY/DX)
      FLOW(1)= YL
      GO TO 100
39 DO 41 I=1,21
      WRITE(6,42) PGRAD(I),Z(I) ,HBAR(I)
42 FORMAT('0',5X,F10.6,15X,F10.6,10X,F10.6)
41 CONTINUE
31 CONTINUE
C**** CALCULATE STREAM FUNCTION DISTRIBUTION
      NP=21
      DO 152 I=1,21
      SY(I,1)=0.0
      SY(I,21)=SYB(I)
      DO 154 J=2,20
      DY=DELY*(J-1)
      SY(I,J)= C1(I)+C2(I)*DEXP(PL(I)*DY)+C3(I)*DEXP(-PL(I)*
      * DY) -(A(I)*

```

```

IDY)/((PL(I))**2)
154 CONTINUE
152 CONTINUE
WRITE(6,157)
157 FORMAT(/5X,'STREAM FUNCTION DISTRIBUTION IN THE BEARI
* NG ')
DO 160 I=1,21
WRITE(6,167) (SY(I,J),J=1,21)
167 FORMAT('0',2X,21F6.3)
160 CONTINUE
C**** CALCULATE VELOCITY DISTRIBUTION IN THE BEARING
N=20
C**** CALCULATE 'U' AND 'DUY' AT EACH SECTION OF THE BEARING
DO 170 I=1,21
U(I,1)=1.0
U(I,2)= (SY(I,5)-6*SY(I,4)+18*SY(I,3)-10*SY(I,2)-3*SY(
* I,1))/(12*
1DELY)
U(I,N)= (SY(I,N-3)-6*SY(I,N-2)+18*SY(I,N-1)-10*SY(I,N)
* -3*SY(I,N+1
1))/(-12*DELY)
U(I,N+1)=0.0
DUY(I,1)= (11*SY(I,5)-56*SY(I,4)+114*SY(I,3)-104*SY(I,
* 2)+35*SY(I,
1 1))/(12*(DELY**2))
DUY(I,2)=(-SY(I,5)+4*SY(I,4)+6*SY(I,3)-20*SY(I,2)+11*S
* Y(I,1))/
1(12*(DELY**2))
DUY(I,N)= (11*SY(I,N+1)-20*SY(I,N)+6*SY(I,N-1)+4*SY(I,
* N-2)-SY(I,
1N-3))/(12*(DELY**2))
DUY(I,N+1)=(35*SY(I,N+1)-104*SY(I,N)+114*SY(I,N-1)-56*
* SY(I,N-2)+
1 11*SY(I,N-3))/(12*(DELY**2))
DO 172 J=3,19
U(I,J)= (SY(I,J-2)-8*SY(I,J-1)+8*SY(I,J+1)-SY(I,J+2))/
* (12*DELY)
DUY(I,J)= (-SY(I,J+2)+16*SY(I,J+1)-30*SY(I,J)+16*SY(I,
* J-1)-SY(I,
1 J-2))/(12*(DELY**2))
172 CONTINUE
170 CONTINUE
WRITE(6,177)
177 FORMAT(/5X,'U DISTRBTION IN THE BEARING')
DO 178 I=1,21
WRITE(6,179) (U(I,J),J=1,21)
179 FORMAT('0',2X,21F6.3)
178 CONTINUE

```

```
WRITE(6,180)
180 FORMAT(/5X,'DUY DISTRIBUTION IN THE BEARING')
DO 182 I=1,21
WRITE(6,185) (DUY(I,J),J=1,21)
185 FORMAT('0',2X,21F6.3)
182 CONTINUE
DO 200 I=1,21
  DTO(I) =DUY(I,1)*(1./HBAR(I))
200 CONTINUE
C*** CALCULATE SHEAR FORCE
DO 202 I=1,21
  WRITE(6,203) DTO(I)
203 FORMAT('0',5X,F6.3)
202 CONTINUE
  CALL DQSF(DELX,DTO,ZI,NP)
  WRITE(6,201) ZI(NP)
201 FORMAT('0',5X, 'SHEAR FORCE =' ,F6.3)
10 CONTINUE
STOP
END
```

* IN THE SIXTH COLUMN INDICATES
CONTINUATION FROM PREVIOUS LINE

```

C**** FORTRAN PROGRAM FOR CHAPTER 4
C**** THE PROGRAM CALCULATES PRESSURE DISTRIBUTION,LOAD
C     CAPACITY,VELOCITY DISTRIBUTION,FRICITION FACTOR FOR
C     MHD SLIDER BEARING
C**** SUBROUTINES FROM IBM-SYSTEM/360 SCIENTIFIC SUBROUTINE
C     PACKAGE ARE USED IN THIS PROGRAM
C**** THE APPLIED MAGNETIC FIELD IS STEP TYPE
      DOUBLE PRECISION HART(5),FLOW(5),FLO(5),SYB(41),HBAR(
* 41),
      1PGRAD(41),PRES(2),Z(41),ZP(41),DELX,DELY, A(41),B,C,D,
* P,
      2ALPHA(41),BY ,BB,BETA,DFLOW(5),PGR(41),ZZ(41),RAT(7),D
* T(7),DB(5),
      3 DH(5),PL(41),C1(41),C2(41),C3(41),DY,SY(41,21),U(41,2
* 1),DUY(41,21
      4),DTO(41),ZI(41)
C**** READ HARTMANN NUMBER,MASS FLOW ,INCREANT IN MASS FLOW
C**** STEP LOCATION AND FILM THICKNESS RATIO AT THE INLET
      DO 10 J=1,1
      READ(5,11) HART(J),FLO(J) ,DFLOW(J) ,DB(J),DH(J)
      11 FORMAT(SF10.7)
      WRITE(6,12) HART(J)
      12 FORMAT('0',5X, 'HARTMANN NUMBER=' ,F10.6)
      FLOW(1)=FLO(J)
      NP=41
C**** MESH SIZE
      DELX=0.025
      DELY=.05
C**** BETA DIMENSION IS STEP LOCATION OF APPLIED MAGNECTIC
C     FIELD
      DO 21 IJ=1,3
      BETA=DB(J)+0.025*(IJ-1)
      NI=BETA*40.5
      NN=NI+1
      WRITE(6,17) BETA,NN

```

```

17  FORMAT('0',5X, 'BETA=',F10.6,5X, 'NN=',I2)
C**** CALCULATE HBAR ALONG THE LENGTH OF BEARING
DO 31 IK=1,1
RAT(IK)=DH(J)-0.05*(IK-1)
DT(IK)= (DABS(RAT(IK)-1.0))/40.0
WRITE(6,32) RAT(IK),DT(IK)
32  FORMAT('0',5X, 'HBAR AT INLET=',F10.6,'0',5X, 'DT=', F10
* .6)
C**** CALCULATION ARE CARRIED OUT USING THE ASSUMED MASS
C FLOW,LATER REPEATED WITH THE IMPROVED MASS FLOW
KK=0
100 KK=KK+1
DO 33 II=1,2
WRITE(6,15) FLOW(II)
15  FORMAT('0',5X, 'MASS FLOW=',F10.6)
C**** CALCULATION FOR NO MAGNETIC FIELD PART
DO 13 N=1,NN
HBAR(N)= (RAT(IK)-DT(IK)*(N-1))
SYB(N)= FLOW(II)/HBAR(N)
PGR (N)= (6.-12.*SYB(N))/((HBAR(N))**2)
13  CONTINUE
BB=0.0
ND=NN
CALL DQSF( DELX,PGR,Z,ND)
C**** CALCULATION FOR MAGNETIC FIELD PART
L=0
DO 20 I=NN,NP
HBAR(I)= (RAT(IK)-DT(IK)*(I-1))
ALPHA(I)=((HBAR(I))**2)*((HART(J))**2)
SYB(I)= FLOW(II)/HBAR(I)
P=(ALPHA(I))**0.5
PL(I)= (ALPHA(I))**0.5
B= (DEXP(-P)+DEXP(P)-2.0)
C= (-SYB(I)*P*( DEXP(-P)-DEXP(P))/B -1.0)
D= 1.0-DEXP(-P)+{DEXP(-P)-DEXP(P)}*(1.-DEXP(P)+P*DEXP(
* P))/(DEXP(P)
1*B)
A(I)=(C/D)*ALPHA(I)
C3(I)= (DEXP(P)/{ P*(DEXP(-P)-DEXP(P))}) *(1.+(A(I)/(P
* **2))-(A(I)/
1((P**2)*DEXP(P))))
C2(I)= (1./(P*DEXP(P)))*(C3(I)*P*DEXP(-P)+(A(I)/(P**2)
* ))
C1(I)= -C2(I)-C3(I)
PGR (I)=(2.*BB)*HBAR(I)* ((HART(J))**2)*SYB(I ) +A(I)
* / ((HBAR(I))
1**2)
L=L+1

```



```

PGRAD(L)=PGR(I)
WRITE(6,45) A(I),C3(I),C2(I),C1(I)
45 FORMAT('0',5X,4F10.6)
20 CONTINUE
ND=NP+1-NN
CALL DQSF (DELX,PGRAD,ZZ,ND)
MM=NP-NN
DO 25 IP=1,MM
Z(NN+IP)= Z(NN) +ZZ(IP+1)
25 CONTINUE
PRES(II)=Z(NP)
ND=NP
CALL DQSF (DELX,Z,ZP,ND)
IF(DABS(Z(NP)).LT..00005)GO TO 39
FLOW(II+1)= FLOW(II)+DFLOW(J)
33 CONTINUE
IF (KK.EQ.3) GO TO 39
C**** BETTER APPROXIMATION ON FLOW
DX=PRES(2)-PRES(1)
DY=FLOW(2)-FLOW(1)
YL=FLOW(1)-(PRES(1)*DY/DX)
FLOW(1)= YL
GO TO 100
39 WRITE(6,37) HBAR(NP),Z(NP)
37 FORMAT('0',5X,F10.6,10X,F10.6)
WRITE(6,43) ZP(NP)
43 FORMAT('0',5X, 'LOAD=' ,F10.6)
31 CONTINUE
21 CONTINUE
10 CONTINUE
C**** CALCULATE STREAM FUNCTION DISTRIBUTION

DO 50 I=1,NN
SY(I,1)=0.0
SY(I,21)=SYB(I)
DO 52 J=2,20
DY=DELY*(J-1)
SY(I,J)=(1.-2*SYB(I))*DY**3 -(2.-3*SYB(I))*DY**2 +DY
52 CONTINUE
50 CONTINUE
DO 152 I=NN,41
SY(I,1)=0.0
SY(I,21)=SYB(I)
DO 154 J=2,20
DY=DELY*(J-1)
SY(I,J)= C1(I)+C2(I)*DEXP(PL(I)*DY)+C3(I)*DEXP(-PL(I)*
* DY) -(A(I)*
1DY)/((PL(I))**2)

```

```

154 CONTINUE
152 CONTINUE
    WRITE(6,157)
157 FORMAT(/5X,'STREAM FUNCTION DISTRIBUTION IN THE BEARI
* NG ')
    DO 160 I=1,41,2
        WRITE(6,167) (SY(I,J),J=1,21)
167 FORMAT('0',2X,21F6.3)
160 CONTINUE
C**** CALCULATE VELOCITY DISTRIBUTION IN THE BEARING
    N=20
C**** CALCULATE 'U' AND 'DUY' AT EACH SECTION OF THE BEARING
    DO 170 I=1,41
        U(I,1)=1.0
        U(I,2)= (SY(I,5)-6*SY(I,4)+18*SY(I,3)-10*SY(I,2)-3*SY(
* I,1))/(12*
1DELY)
        U(I,N)= (SY(I,N-3)-6*SY(I,N-2)+18*SY(I,N-1)-10*SY(I,N)
* -3*SY(I,N+1
1)))/(-12*DELY)
        U(I,N+1)=0.0
        DUY(I,1)= (11*SY(I,5)-56*SY(I,4)+114*SY(I,3)-104*SY(I,
* 2)+35*SY(I,
1 1))/(12*(DELY**2))
        DUY(I,2)=(-SY(I,5)+4*SY(I,4)+6*SY(I,3)-20*SY(I,2)+11*S
* Y(I,1))/
1(12*(DELY**2))
        DUY(I,N)= (11*SY(I,N+1)-20*SY(I,N)+6*SY(I,N-1)+4*SY(I,
* N-2)-SY(I,
1N-3))/(12*(DELY**2))
        DUY(I,N+1)=(35*SY(I,N+1)-104*SY(I,N)+114*SY(I,N-1)-56*
* SY(I,N-2)+
1 11*SY(I,N-3))/(12*(DELY**2))
    DO 172 J=3,19
        U(I,J)= (SY(I,J-2)-8*SY(I,J-1)+8*SY(I,J+1)-SY(I,J+2))/
* (12*DELY)
        DUY(I,J)= (-SY(I,J+2)+16*SY(I,J+1)-30*SY(I,J)+16*SY(I,
* J-1)-SY(I,
1 J-2))/(12*(DELY**2))
172 CONTINUE
170 CONTINUE
    WRITE(6,177)
177 FORMAT(/5X,'U DISTRBUTION IN THE BEARING')
    DO 178 I=1,41,2
        WRITE(6,179) (U(I,J),J=1,21)
179 FORMAT('0',2X,21F6.3)
178 CONTINUE
    WRITE(6,180)

```

```
180 FORMAT(//5X, 'DUY DISTRIBUTION IN THE BEARING')
      DO 182 I=1,41,2
      WRITE(6,185) (DUY(I,J),J=1,21)
185  FORMAT('0',2X,21F6.3)
182  CONTINUE
C**** CALCULATE SHEAR FORCE
      DO 200 I=1,41
      DTO(I) =DUY(I,1)*(1./HBAR(I))
200  CONTINUE
      DO 202 I=1,41,2
      WRITE(6,203) DTO(I)
203  FORMAT('0',5X,F6.3)
202  CONTINUE
      CALL DQSF(DELX,DTO,ZI,NP)
      WRITE(6,201) ZI(NP)
201  FORMAT('0',5X, 'SHEAR FORCE =',F6.3)
      STOP
      END
```

* IN THE SIXTH COLUMN INDICATES
CONTINUATION FROM PREVIOUS LINE

```

C**** FORTRAN PROGRAM FOR CHAPTER 5
C**** THIS PROGRAM CALCULATES POTENTIAL DISTRIBUTION FOR
C   FINITE WIDTH PARALLEL PLATE BEARING FROM POTENTIAL
C   DISTRIBUTION ELECTRIC FIELD, CURRENT DENSITY, CURRENT
C   DENSITY GRADIENTS ARE CALCULATED
C**** THE POTENTIAL EQUATION IN FINTE DIFFERENCE FORM IS
C   SOLVED USING POINT SUCCESSIVE-OVERRELAXATION METHOD
C**** SUBROUTINES FROM IBM-SYSTEM/360 SCIENTIFIC SUBROUTINE
C   PACKAGE ARE USED IN THIS PROGRAM
      DOUBLE PRECISION A1,A2,A3,A4,A5,DX,DY, SY,SYN,DIF,DI,
      * OME,ERR,
      1SY(101,101),EX(101,101),EZ(101,101),DX1,DY1,A11,A22,A3
      * 3,A44,A55,
      2 S(101),SJ(101),CU(101),ZZ(101) ,CX(101,101),CZ(101,10
      * 1)
C**** DATA FOR CALCULATION
      M=65
      N=41
      M1=M-1
      N1=N-1
      DX=0.0125
      DY=0.0125
      OME=1.7
      IT=350
      ERR=0.00003
      LL=33
      LP=LL+1
      LK=49
      LO=LK+1
      LKK=LK-1
      LM=LK+1
      NL=21
      NLL=NL-1
      NP=NL-1
C**** SY SYMBOL INDICATES POTENTIAL IN THIS PROGRAM

```

```

C**** STARTING VALUES OF SY AT GRID POINTS
      DO 10 I=1,LK
        SY(I,N)=0.0
      DO 20 J=1,N1
        SY(I,J)=0.3
20 CONTINUE
10 CONTINUE
      DO 13 I=L0,M
        SY(I,NL)=0.0
      DO 14 J=1,NLL
        SY(I,J)=0.1
14 CONTINUE
13 CONTINUE
C**** CALCULATE COEFFICIENTS OF FINITE DIFFERENCE FORM OF
C POTENTIAL EQUATION FOR SMALL STEP SIZE
      A1=1./((DX**2)
      A2=1./((DX**2)
      A3=1./((DY**2)
      A4=1./((DY**2)
      A5= ((DX*DY)**2)/(2*(DX**2+DY**2))
      DX1=0.025
      DY1=0.025
C**** CALCULATE COEFFICIENTS OF FINITE DIFFERENCE FORM OF
C POTENTIAL EQUATION FOR LARGE STEP SIZE
      A11=1./((DX1**2)
      A22=1./((DX1**2)
      A33=1./ (DY1**2)
      A44=1./((DY1**2)
      A55=((DX1*DY1)**2)/ (2*(DX1**2+DY1**2))
      KK=0
70 DI=0.0
C**** STARTING FROM INLET OF BEARING AND MARCHING TOWARDS
C RIGHT SIDE
C**** CALCULATION CONTINUES UP TO THE END OF SIDE ELECTRODE
C USING SMALL STEP SIZE
      DO 45 I=1,LL
        SY(I,1)=2.02
        II=I+1
        III=I-1
      DO 47 J=2,N1
        JJ=J+1
        JJJ=J-1
        IF(I.EQ.1) GO TO 48
        SYY= (A1*SY(II,J)+A2*SY(III,J)+A3*SY(I,JJ)+A4*SY(I,JJJ
* ))*A5
        GO TO 49
48 SYY= (A1*SY(II,J)+A2*SY(III,J)+A3*SY(I,JJ)+A4*SY(I,JJJ
* ))*A5

```

```

49 SYN=OME*(SYY-SY(I,J))+SY(I,J)
   DIF=DABS(SYN-SY(I,J))/SYN
   DI=DMAX1 (DI,DIF)
   SY(I,J)=SYN
47 CONTINUE
45 CONTINUE
C**** CALCULATION FROM END OF ELECTRODE ONWARDS FOR
C INSULATED SIDE PLATE USING SMALL STEP SIZE
DO 35 I=LP,LKK
  II=I+1
  III=I-1
  DO 40 J=1,N1
    JJ=J+1
    JJJ=J-1
    IF(J.GT.1) GO TO 33
    SYY=(A1*SY(II,J)+A2*SY(III,J)+A3*SY(I,JJ)+A4*SY(I,JJJ)
    *   *A5
    GO TO 34
33 SYY=(A1*SY(II,J)+A2*SY(III,J)+A3*SY(I,JJ)+A4*SY(I,JJJ)
    *   *A5
34 SYN=OME*(SYY-SY(I,J))+SY(I,J)
   DIF=DABS(SYN-SY(I,J))/SYN
   DI=DMAX1 (DI,DIF)
   SY(I,J)=SYN
40 CONTINUE
35 CONTINUE
C**** CALCULATION AT THE JUNCTION LK OF SMALL AND LARGE STE
* P SIZE
DO 80 J=1,N,2
  JK=1+(J-1)/2
  S(J)= SY(L0,JK)
80 CONTINUE
DO 85 J=2,N1,2
  S(J)= (S(J+1)+S(J-1))/2.
85 CONTINUE
DO 87 J=1,N1
  SJ(J)=(SY(LK,J)+S(J))/2.
87 CONTINUE
   SJ(N)=0.0
DO 43 J=1,N1
  JJ=J+1
  IF(J.EQ.1) GO TO 44
  JJJ=J-1
  GO TO 42
44 JJJ=JJ
42 SYY =(A1*SJ(J)+A2*SY(LK-1,J)+A3*SY(LK,JJ)+A4*SY(LK,JJJ)
    *   *A5
   SYN=OME*(SYY-SY(LK,J))+SY(LK,J)

```

```

DIF=DABS(SYN-SY(LK,J))/SYN
DI=DMAX1(DI,DIF)
SY(LK,J)=SYN
43 CONTINUE
C**** CALCULATION FOR INSULATED SIDE PLATE USING LARGE STEP
C SIZE
DO 15 I=LO,M
  III=I-1
  IF(I.EQ.M) GO TO 37
  II=I+1
  GO TO 38
37 II=III
38 DO 16 J=1,NP
  JJ=J+1
  IF(J.EQ.1) GO TO 21
  JJJ=J-1
  GO TO 22
21 JJJ=JJ
22 IF(I.EQ.LO) GO TO 17
  J1=J
  GO TO 18
17 J1=1+2*(J-1)
  SY=(A11*SY(II,J)+A22*SY(III,J1)+A33*SY(I,JJ)+A44*SY(
  * I,JJJ)) *A55
  GO TO 19
18 SY=(A11*SY(II,J)+A22*SY(III,J1)+A33*SY(I,JJ)+A44*SY(
  * I,JJJ)) *A55
19 SYN=OME*(SY-SY(I,J))+SY(I,J)
  DIF=DABS(SYN-SY(I,J))/SYN
  DI=DMAX1(DI,DIF)
  SY(I,J)=SYN
16 CONTINUE
15 CONTINUE
  IF(DI.LE.ERR.OR.KK.GE.IT) GO TO 60
  KK=KK+1
  IF(KK.EQ.200) GO TO 61
  GO TO 70
61 DO 63 I=1,LK
  WRITE(6,67) (SY(I,J), J=1,N,2)
63 CONTINUE
  DO 64 I=LO,M
  WRITE(6,67) (SY(I,J),J=1,NL)
64 CONTINUE
  GO TO 70
60 WRITE(6,62) KK,DI
62 FORMAT('0',5X,'NO OF ITERATION=',I3//5X,'MAX DIF =',F1
  * 0.6)
  WRITE(6,52)

```

```

52 FORMAT('0',30X, 'POTENTIAL DISTRIBUTION')
DO 65 I=1,LK
WRITE(6,67) (SY(I,J),J=1,N,2)
65 CONTINUE
DO 68 I=L0,M
WRITE(6,67) (SY(I,J),J=1,NL)
67 FORMAT('0',2X,26F6.3)
68 CONTINUE
N2=N-2
C*** CALCULATE EZ FROM SY VALUES USING 5-POINT MOLECULE
DO 105 I=1,LK
EZ(I,1)=(-6*SY(I,5)+32*SY(I,4)-72*SY(I,3)+96*SY(I,2)-5
* 0*SY(I,1))/
1(-24*DY)
EZ(I,2)=(SY(I,5)-6*SY(I,4)+18*SY(I,3)-10*SY(I,2)-3*SY(
* I,1))/(-12*
1DY)
EZ(I,N1)=(SY(I,N1-3)-6*SY(I,N1-2)+18*SY(I,N1-1)-10*SY(
* I,N1)-3*SY(I
1,N1+1))/( 12*DY)
EZ(I,N)=- (50*SY(I,N)-96*SY(I,N1)+72 *SY(I,N1-1)-32*SY
* (I,N1-2)+
16*SY(I,N1-3))/( 24*DY)
DO 107 J=3,N2
EZ(I,J)= -(SY(I,J-2)-8*SY(I,J-1)+8*SY(I,J+1)-SY(I,J+2)
* )/(12*DY)
107 CONTINUE
105 CONTINUE
WRITE(6,103)
103 FORMAT('0',30X, 'EZ DISTRIBUTION')
DO 110 I=1,LK
WRITE(6,112) (EZ(I,J),J=1,N,2)
112 FORMAT('0',2X,21F8.3)
110 CONTINUE
DO 158 I=1,LK,2
PUNCH 257, (EZ(I,J),J=1,N,2)
158 CONTINUE
NM=NL-2
DO 108 I=L0,M
EZ(I,1)=(-6*SY(I,5)+32*SY(I,4)-72*SY(I,3)+96*SY(I,2)-5
* 0*SY(I,1))/
1(-24*DY1)
EZ(I,2)=(SY(I,5)-6*SY(I,4)+18*SY(I,3)-10*SY(I,2)-3*SY(
* I,1))/(-12*
1DY1)
EZ(I,NP)=(SY(I,NP-3)-6*SY(I,NP-2)+18*SY(I,NP-1)-10*SY(
* I,NP)-3*SY(I
1,NP+1))/( 12*DY1)

```



```

EZ(I,NL)= -(50*SY(I,NL)-96*SY(I,NP)+72*SY(I,NP-1)-32*S
* Y(I,NP-2)+
16*SY(I,NP-3))/(24*DY1)
DO 109 J=3,NM
EZ(I,J)= -(SY(I,J-2)-8*SY(I,J-1)+8*SY(I,J+1)-SY(I,J+2)
* )/(12*DY1)
109 CONTINUE
108 CONTINUE
DO 115 I=LO,M
WRITE(6,116) (EZ(I,J), J=1,NL)
116 FORMAT('0',2X,21F8.3)
115 CONTINUE
DO 159 I=LO,M
PUNCH 257 ,(EZ(I,J),J=1,NL)
159 CONTINUE
C**** CALCULATE EX FROM SY VALUES USING 5-POINT MOLECULE
M2=M-2
LT=LK-2
DO 120 J=1,N
EX(1,J)= (-6*SY(5,J)+32*SY(4,J)-72*SY(3,J)+96*SY(2,J)-
* 50*SY(1,J)
1)/(-24*DX)
EX(2,J)=(SY(5,J)-6*SY(4,J)+18*SY(3,J)-10*SY(2,J)-3*SY(
* 1,J))/(-12*
1*DX)
EX(LKK,J)= (SY(LK-4,J)-6*SY(LK-3,J)+18*SY(LK-2,J)-10*S
* Y(LK-1,J)
1-3*SY(LK,J))/(12*DX)
EX(LK,J)=-(50*SY(LK,J)-96*SY(LK-1,J)+72*SY(LK-2,J)-32*
* SY(LK-3,J)+
1 6*SY(LK-4,J))/(24*DX)
DO 125 I=3,LT
EX(I,J)=-(SY(I-2,J)-8*SY(I-1,J)+8*SY(I+1,J)-SY(I+2,J))
* /(12*DX)
125 CONTINUE
120 CONTINUE
WRITE(6,113)
EX(8,1)=0.0
EX(9,1)=0.0
EX(11,1)= -(SY(9,1)-8*SY(10,1)+8*SY(12,1)-SY(13,1))/(1
* 2*DX)
EX(10,1)= -(SY(8,1)-8*SY(9,1)+8*SY(11,1)-SY(12,1))/(12
* *DX)
113 FORMAT('0',30X, 'EX DISTRIBUTIN')
DO 130 I=1,LK
WRITE(6,114) (EX(I,J),J=1,N ,2)
114 FORMAT('0',2X,21F8.3)
130 CONTINUE

```

```

      LO =LK+1
      L2=L0+1
      L3=L2+1
      DO 150 J=1,NL
      EX(L0,J)=(-6*SY(L0+4,J)+32*SY(L0+3,J)-72*SY(L0+2,J)+96
* *SY(L0+1,J)
1-50*SY(L0,J))/(-24*DX1)
      EX(L2,J)= (SY(L2+3,J)-6*SY(L2+2,J)+18*SY(L2+1,J)-10*SY
* (L2,J)-3*
1SY(L2-1,J))/(-12*DX1)
      EX(M1,J)=(SY(M1 -3,J)-6*SY(M1-2,J)+18*SY(M1-1,J)-10*SY
* (M1,J)-3*SY
1(M1,J))/12*DX1)
      EX(M,J)= -(50*SY(M,J)-96*SY(M-1,J)+72*SY(M -2,J)-32*SY
* (M-3,J)+
1 6*SY(M-4,J))/(24*DX1)
      DO 152 I=L3,M2
      EX(I,J)=- (SY(I-2,J)-8*SY(I-1,J)+8*SY(I+1,J)-SY(I+2,J))
* /(12*DX1)
152 CONTINUE
150 CONTINUE
      DO 154 I=L0,M
      WRITE(6,155) (EX(I,J),J=1,NL)
155 FORMAT('0',2X,21F8.3)
154 CONTINUE
C**** CALCULATE CURRENT FLOW AT THE CENTER
      WRITE(6,191)
191 FORMAT('0',5X, 'CUR IN SMALL STEP SIZE AREA')
      DO 160 J=1,N,2
      DO 163 I=1,LK
      CU(I)=EZ(I,J)
163 CONTINUE
      CALL DQSF (DX,CU,ZZ,LK)
      WRITE(6,168) (ZZ(I),I=1,LK,2)
168 FORMAT( //25F10.6)
160 CONTINUE
      ND=17
      WRITE(6,192)
192 FORMAT('0',5X, 'CUR IN LARGE STEP SIZE AREA')
      JJ=1
      DO 167 J=1,NL
      I=LK
      CU(1)= EZ(LK,JJ)
      DO 169 I=L0,M
      J1=I-L0+2
      CU(J1)= EZ(I,J)
169 CONTINUE
      CALL DQSF (DX1,CU,ZZ,ND)

```

```

WRITE(6,199) (ZZ(I),I=1,ND)
199 FORMAT(//17F10.6)
JJ=JJ+2
167 CONTINUE
C**** CALCULATE GRADIENT OF JX IN Z-DIRECTION)
DO 205 I=1,LK
CX(I,1)=(-6*EX(I,5)+32*EX(I,4)-72*EX(I,3)+96*EX(I,2)-5
* 0*EX(I,1))/
1( 24*DY)
CX(I,2)=(EX(I,5)-6*EX(I,4)+18*EX(I,3)-10*EX(I,2)-3*EX(
* I,1))/( 12*
1DY)
CX(I,N1)=(EX(I,N1-3)-6*EX(I,N1-2)+18*EX(I,N1-1)-10*EX(
* I,N1)-3*EX(I
1,N1+1))/(-12*DY)
CX(I,N)=(50*EX(I,N)-96*EX(I,N1)+72 *EX(I,N1-1)-32*EX
* (I,N1-2)+
16*EX(I,N1-3))/( 24*DY)
DO 207 J=3,N2
CX(I,J)= (EX(I,J-2)-8*EX(I,J-1)+8*EX(I,J+1)-EX(I,J+2)
* )/(12*DY)
207 CONTINUE
205 CONTINUE
CX(8,2)= (-6*EX(8,6)+32*EX(8,5)-72*EX(8,4)+96*EX(8,3)-
* 50*EX(8,2))
1/(24*DY)
CX(9,2)= (-6*EX(9,6)+32*EX(9,5)-72*EX(9,4)+96*EX(9,3)-
* 50*EX(9,2))
1/(24*DY)
WRITE(6,203)
203 FORMAT('0',30X, 'GRAD OF JX IN Z DIRECTION')
DO 210 I=1,LK
WRITE(6,112) (CX(I,J),J=1,N,2)
210 CONTINUE
DO 256 I=1,LK,2
PUNCH 257,(CX(I,J),J=1,N,2)
257 FORMAT(3(8F10.5/))
256 CONTINUE
DO 208 I=LO,M
CX(I,1)=(-6*EX(I,5)+32*EX(I,4)-72*EX(I,3)+96*EX(I,2)-5
* 0*EX(I,1))/
1( 24*DY1)
CX(I,2)=(EX(I,5)-6*EX(I,4)+18*EX(I,3)-10*EX(I,2)-3*EX(
* I,1))/( 12*
1DY1)
CX(I,NP)=(EX(I,NP-3)-6*EX(I,NP-2)+18*EX(I,NP-1)-10*EX(
* I,NP)-3*EX(I
1,NP+1))/(-12*DY1)

```

```

CX(I,NL)= (50*EX(I,NL)-96*EX(I,NP)+72*EX(I,NP-1)-32*E
* X(I,NP-2)+
16*EX(I,NP-3))/( 24*DY1)
DO 209 J=3,NM
CX(I,J)= (EX(I,J-2)-8*EX(I,J-1)+8*EX(I,J+1)-EX(I,J+2)
* )/(12*DY1)
209 CONTINUE
208 CONTINUE
DO 215 I=LO,M
WRITE(6,116) (CX(I,J), J=1,NL)
215 CONTINUE
DO 260 I=LO,M
PUNCH 258,(CX(I,J),J=1,NL)
258 FORMAT(3(8F10.5/))
260 CONTINUE
C**** CALCULATE GRADIENT OF JZ IN X -DIRECTION)
DO 220 J=1,N
CZ(1,J)= (-6*EZ(5,J)+32*EZ(4,J)-72*EZ(3,J)+96*EZ(2,J)-
* 50*EZ(1,J)
1)/( 24*DX)
CZ(2,J)=(EZ(5,J)-6*EZ(4,J)+18*EZ(3,J)-10*EZ(2,J)-3*EZ(
* 1,J))/( 12*
1*DX)
CZ(LK,J)=-(EZ(LK-4,J)-6*EZ(LK-3,J)+18*EZ(LK-2,J)-10*E
* Z(LK-1,J)
1-3*EZ(LK,J))/(12*DX)
CZ(LK,J)= (50*EZ(LK,J)-96*EZ(LK-1,J)+72*EZ(LK-2,J)-32*
* EZ(LK-3,J)+
1 6*EZ(LK-4,J))/(24*DX)
DO 225 I=3,LT
CZ(I,J)= (EZ(I-2,J)-8*EZ(I-1,J)+8*EZ(I+1,J)-EZ(I+2,J))
* /(12*DX)
225 CONTINUE
220 CONTINUE
WRITE(6,213)
213 FORMAT('0',30X, 'GRAD OF JZ IN X DIRECTION')
DO 230 I=1,LK
WRITE(6,114) (CZ(I,J), J=1,N,2)
230 CONTINUE
DO 270 I=1,LK,2
PUNCH 257, (CZ(I,J),J=1,N,2)
270 CONTINUE
DO 250 J=1,NL
CZ(LO,J)=(-6*EZ(LO+4,J)+32*EZ(LO+3,J)-72*EZ(LO+2,J)+96
* *EZ(LO+1,J)
1-50*EZ(LO,J))/( 24*DX1)
CZ(L2,J)= (EZ(L2+3,J)-6*EZ(L2+2,J)+18*EZ(L2+1,J)-10*EZ
* (L2,J)-3*

```

```
1EZ(L2-1,J))/( 12*DX1)
  CZ(M1,J)=(EZ(M1 -3,J)-6*EZ(M1-2,J)+18*EZ(M1-1,J)-10*EZ
* (M1,J)-3*SY
1(M,J))/(-12*DX1)
  CZ(M,J)= (50*EZ(M,J)-96*EZ(M-1,J)+72*EZ(M -2,J)-32*EZ
* (M-3,J)+
1 6*EZ(M-4,J))/(24*DX1)
  DO 252 I=L3,M2
  CZ(I,J)= (EZ(I-2,J)-8*EZ(I-1,J)+8*EZ(I+1,J)-EZ(I+2,J))
* /(12*DX1)
252 CONTINUE
250 CONTINUE
  DO 254 I=L0,M
  WRITE(6,155) (CZ(I,J),J=1,NL)
254 CONTINUE
  DO 265 I=L0,M
  PUNCH 258, (CZ(I,J),J=1,NL)
265 CONTINUE

  STOP
  END
```

* IN THE SIXTH COLUMN INDICATES
CONTINUATION FROM PREVIOUS LINE

```

C**** FORTRAN PROGRAM FOR CHAPTER 5
C**** THIS PROGRAM CALCULATE PRESSURE DISTRIBUTION FOR
C    FINITE WIDTH PARALLEL PLATE SLIDER BEARING
C**** THE PRESSURE EQUATION IN FINITE DIFFERENCE FORM IS
C    SOLVED USING POINT SUCCESSIVE OVERRELAXTION METHOD
C**** SUBROUTINES FROM IBM-SYSTEM/360 SCIENTIFIC SUBROUTINE
C    PACKAGE ARE USED IN THIS PROGRAM
C    DOUBLE PRECISION A0(41,41),A1,A2,A3,A4,A5,HART(5),DX,D
*    Z,SLOP,
    IP(41,41),PP,PN,OME,ERR,DI,DIFF,Z(41),ZZ(41),Z1(41),CX(4
*    1,41),
    2CZ(41,41),EZ(41,41),QX1(41),QX2(41),PGR(41,41)
C**** DATA FOR CALCULATION
    M=41
    N=41
    NN=21
    M1=M-1
    N1=N-1
    DX=0.025
    DZ=0.025
    OME=1.5
    ERR=0.00005
    IT=300
C**** STARTING VALUES OF PRESSURE AT GRID POINTS
    DO 22 I=1,M
    DO 32 J=1,NN
    P(I,J)=0.0
    32 CONTINUE
    22 CONTINUE
C**** READ HARTMANN NUMBER
    DO 15 L=1,1
    READ(5,11) HART(L)
    11 FORMAT( F10.6)
    WRITE(6,12) HART(L)
    12 FORMAT('0',5X, 'HARTMANN NUMBER=',F10.6)

```

```

C**** READ CURRENT DENSITY GRADIENTS AS OBTAINED FROM THE
C SOLUTION OF POTENTIAL EQUATION
DO 10 I=1,41
  READ(5,110) (CX(I,J),J=1,21)
110 FORMAT(3( 8F10.5/))
10 CONTINUE
DO 20 I=1,41
  READ(5,110) (CZ(I,J),J=1,21)
20 CONTINUE
DO 120 I=1,41
  WRITE(6,118) (CX(I,J),J=1,21)
118 FORMAT(2X/21F10.5)
120 CONTINUE
DO 122 I=1,41
  WRITE(6,118) (CZ(I,J),J=1,21)
122 CONTINUE
C**** CALCULATE COEFFICIENTS OF FINITE DIFFERENCEFORM EQ.
A1=1./(DX**2)
A2=1./(DX**2)
A3=1./(DZ**2)
A4=1./(DZ**2)
A5= ((DX*DZ)**2)/(2*(DX**2+DZ**2))
DO 25 I=2,M1
DO 27 J=2,NN
  A0 (I,J)=-HART(L)*(CX(I,J)+CZ(I,J))
27 CONTINUE
25 CONTINUE
C**** START ITERATING
KK=0
45 DI=0.0
DO 35 I=2,M1
  II=I+1
  III=I-1
DO 40 J=2,NN
  JJ=J+1
  JJJ=J-1
  IF(J.EQ.21) GO TO 47
  PP=(A0(I,J)+A1*P(II,J)+A2*P(III,J)+A3*P(I,JJ)+A4*P(I,J
* JJ))*A5
  GO TO 49
47 PP=(A0(I,J)+A1*P(II,J)+A2*P(III,J)+A3*P(I,JJJ)+A4*P(I,
* JJJ))*A5
49 PN=ONE*(PP-P(I,J))+P(I,J)
  DIF= DABS(PN-P(I,J))/PN
  DI=DMAX1 (DI,DIF)
40 P(I,J)=PN
35 CONTINUE
  IF (DI.LE.ERR.OR.KK.GE.IT) GO TO 50

```

```
      KK=KK+1
      GO TO 45
50  WRITE(6,55)
55  FORMAT('0',25X, 'PRESSURE DISTRIBUTION')
      WRITE(6,56) KK,DI
56  FORMAT('0',5X, 'NO OF ITERATION=',I3//5X,'MAX DIFF',F1
* 0.6)
      DO 60 J=1,NN
      WRITE(6,58) (P(I,J),I=1,M,2)
58  FORMAT('0',2X,21F10.3)
60  CONTINUE
C*** CALCULATE LOAD CAPACITY
      ND=41
      DO 70 J=2,NN
      DO 75 I=1,M
      Z(I)=P(I,J)
75  CONTINUE
      CALL DQSF(DX,Z,ZZ,ND)
      WRITE(6,80) (ZZ(I),I=1,M,2)
80  FORMAT(/2X,21F6.3)
      ZI(J)=ZZ(ND)
70  CONTINUE
      Z1(1)=0.0
      CALL DQSF(DZ,Z1,ZZ,NN)
      WRITE(6,85) ZZ(NN)
85  FORMAT(/5X, 'LOAD=',F10.6)
15  CONTINUE
      STOP
      END
```